1986

Optical measurement of etched grid contrast and surface roughness.

George Tsz Wun. Ng
University of Windsor

CANADIAN THESES

THÈSES CANADIENNES

NOTICE

The quality of this microfiche is heavily dependent upon the quality of the original thesis submitted for microfilming. Every effort has been made to ensure the highest quality of reproduction possible.

If pages are missing, contact the university which granted the degree.

Some pages may have indistinct print especially if the original pages were typed with a poor typewriter ribbon or if the university sent us an inferior photocopy.

Previously copyrighted materials (journal articles, published tests, etc.) are not filmed.

Reproduction in full or in part of this film is governed by the Canadian Copyright Act, R.S.C. 1970, c. C-30.

AVIS

La qualité de cette microfiche dépend grandement de la qualité de la thèse soumise au microfilmage. Nous avons tout fait pour assurer une qualité supérieure de reproduction.

S'il manque des pages, veuillez communiquer avec l'université qui a conféré le grade.

La qualité d'impression de certaines pages peut laisser à désirer, surtout si les pages originales ont été dactylographiées à l'aide d'un ruban usé ou si l'université nous a fait parvenir une photocopie de qualité inférieure.

Les documents qui font déjà l'objet d'un droit d'auteur (articles de revue, examens publiés, etc.) ne sont pas microfilmés.

La reproduction, même partielle, de ce microfilm est soumise à la Loi canadienne sur le droit d'auteur, SRC 1970, c. C-30.

THIS DISSERTATION
HAS BEEN MICROFILMED
EXACTLY AS RECEIVED

LA THÈSE A ÉTÉ
MICROFILMÉE TELLE QUE
NOUS L'AVONS REÇUE

Canada

NL-339 (r 86/06)

OPTICAL MEASUREMENT OF ETCHED GRID CONTRAST AND SURFACE ROUGHNESS

by

© George Tsz Wun Ng

A Thesis
Submitted to the
Faculty of Graduate Studies and Research
Through the Department of
Mechanical Engineering in Partial Fulfillment
of the Requirements for the Degree
of Master of Applied Science at
the University of Windsor

Windsor, Ontario, Canada

1986

ISBN 0-315-32017-6

ABSTRACT

The primary purpose of this study was to establish a method to measure contrast level for lines etched on steel surfaces that are used for qualifying a die. This contrast level would serve as a guideline for line detection by electro-optical detectors.

An electro-optical scanning unit was designed, built and interfaced with an Apple computer to evaluate the output data obtained by scanning the etched lines on steel surfaces.

For practical and feasible reasons, a contrast ratio of 0.6 is recommended. The establishment of the recommended contrast level was based on a study of contrast as it was affected by strain level, magnification, illumination, wavelength, polarization, etching duration, surface finish, surface coating etc.. If the contrast ratio of the grid on the etched steel plate should be less than the recommended value, it should not be put through the die qualifying process.

The secondary purpose of this study was to develop a white light optical technique to measure the surface roughness of ground metal surfaces.

A pair of photo detectors was used to detect the specular and scattered reflected light and subsequently yielded the Intensity Ratio. The experiment results showed that this ratio

had good correlation with surface roughness. The applicable roughness range of this method can be extended to 3 microns (120 micro inches) or more by increasing the incident light angle. The correlation curves were unique for each material.

ACKNOWLEDGEMENTS

The author would like to express his sincere gratitude to Dr. W.P.T. North for his supervision and encouragement throughout the course of this study, and to Dr. D.F. Watt and Dr. V.M. Huynh for their valuable guidance.

The author is grateful to Mr. M. Donoghue of GM Technical Center in Warren Michigan, and to Mr. W. Beck and Mr. R. Tattersall of the ME Department, and Mr. D. Liebsch of the Central Research Shop for their technical assistance in this project. A special thanks is extended to Miss C.E. Mac Neil for proof-reading this manuscript.

This project was financially supported by the National Science and Engineering Research Council of Canada (NSERC) through Grant No. 9067.

CONTENTS

LIST OF TABLES

LIST OF FIGURES

NOMENCLATURE

AA	arithmetic average roughness
A/D	analog to digital
C	contrast
CCD	charged coupled device
CLA	center line average roughness
D1	output voltage of detector 1, V.
D2	output voltage of detector 2, V.
D/A	digital to analog
DS	dual-slope
He-Ne	helium-neon
IL	major diameter of illumination field, mm
IR	intensity ratio, optical surface roughness
Lb	luminance of the background
Lt	luminance of the object or task
MC	mean contrast
N	number of lines scanned
θ	incident light angle
Pb	reflectance of the background
Pt	reflectance of the object or task
Ra	average roughness, CLA or AA
Rt	peak-to-peak maximum roughness, height of the roughness curve
S	standard deviation
SA	successive approximation
T	etching duration, seconds

Chapter I

INTRODUCTION

Today, metal forming by stamping is still more of an art than a science. Reducing the weight of the car is a trend pursued by the Auto industry in order to achieve higher fuel economy. However, with the use of thinner materials, more complex shaped and contoured body panels must be employed to off-set the decreased rigidity and increased vibration potential of the thinner sections. In order to maintain cost efficiency, industry engineers must optimize the use of materials and decrease the time to design and test the dies, improve stamping methods, and quality control procedures.

The need to reduce the costs incurred by inefficient stamping and the production of excessive scrap material is shared by all sheet metal manufacturers and users. Fisher Body and Oldsmobile Divisions alone introduce an average, one new die every day. Before it goes to the production floor, each die must be put through a testing procedure designed to ensure that the parts which it produces will meet all the required specifications. One of the testing techniques used is called "grid method".

The grid method is one of the oldest experimental stress analysis methods. Lines or circles are marked on the surface of

the flat steel stock. By measuring the distance between the lines before and after the deformation, the average Lagrangian strains can be determined by dividing the change of distance by the original distance between points. When a circular grid is used, an ellipse is formed after the deformation. The major and minor diameters of the ellipse indicate the magnitude and direction of the principal strains, however information on the strain path - how it reached its final value - is unfortunately lost.

To qualify a die, a blank sheet of steel is etched with square and/or circular grids before being stamped with the die being tested. Strains can be determined by comparing the grid sizes before and after the stamping. The principal strains are then compared with the forming limit curve in order to determine the reliability of the die to produce parts without tears or folds.

The measurement procedure may involve manually measuring hundreds of thousands of points on the stamped grid surface -- a long, tedious task subject to the production of inaccurate data and costly turnaround time. For example, a quarter panel, i.e., rear fender and part of the rear door opening, may have 100,000 data points and require several weeks to analyze. If the contrast between the surface and the lines is high enough, the procedure of determing the location of the points could be replaced by light sensors. However, lines that are very clear to the naked eye may be undetectable by light sensors. What contrast level then is acceptable by light sensors? In order to automate the

line reading process, the threshold of line contrast must be determined.

The GM Technical Center goals are to correlate finite element strain models with actual testing information from a given die. They hope to be able to automate the experimental data-gathering such that a die and material can be qualified in less than eight hours. When they are confident that the theoretical model is accurate, then they will be able to qualify a new die totally by computer with only the die geometry and material information.

1.1 Concept of Contrast [1,2]

In any visual task - whether performed by machine or human vision - the object considered must appear different from its background or surrounding objects. Figure 1.1 shows black lines on a black and white background. In that illustration black lines cannot be seen as distinct from the black background, since the lines and background have no difference. However, the same black lines stand out clearly from the white background and can be distinguished very easily.

Numbers appearing in the square brackets designate references at the end of this thesis.

1.1.1 Calculation of Contrast

Contrast (C) is the difference between the luminance of the object or task (Lt) and the luminance of the adjacent background (Lb). It is defined by the following equation:

$$C = \frac{Lb - Lt}{Lb} \quad - - - - - (1)$$

Some authors prefer to take the absolute value of the numerator, in order to always yield a positive contrast. If the object and its adjacent background are lighted to the same illuminance level, contrast becomes a function of only the reflectances of the two surfaces. The equation (1) can then be rewritten as

$$C = \frac{Pb - Pt}{Pb} \quad - - - - - (2)$$

where Pb is the reflectance of the background and Pt is the reflectance of the object or task. From equation (2), the contrast range is from zero to one. In the case of black lines on a black background, the contrast is rendered as zero, or approaching zero, which means that it is difficult or even impossible to see. In the case of black lines on a white background, the contrast would approach, or would be, one. The higher the contrast then, the easier the visual task.

1.2 Surface Roughness

Besides considering contrast, this study was also involved with the measurement of surface roughness in as much as surface roughness will also affect contrast. Surface roughness has been known for years as a critical factor in machine life. If a rough surface finish on a part such as the crank shaft or bearing ring was used in the machine, it could reduce the endurance limit of that equipment significantly. Other problems such as paintability, corrosion resistance, wear resistance and absorption characteristics are all associated with surface roughness.

1.2.1 Concept of Surface Finish [3,4,5]

In general, a surface consists of LAY, FLAWS, WAVINESS AND ROUGHNESS (Figure 1.2).

LAY is the machine marks left on the material surface by the machine which was used to process the work surface. It is the predominant direction of surface pattern.

FLAWS are irregularities that do not appear in a consistent pattern.

WAVINESS is an irregular surface condition of greater spacing than roughness. It is usually caused by deflections or vibrations - not by the cutting edge.

ROUGHNESS is defined as finely spaced surface irregularities, in a consistent pattern, produced by machining or processing.

These properties of a surface are shown in Figure 1.3. In

most cases, only roughness is considered because it is the most important factor in surface finish.

1.2.2 Surface Roughness Measurement [3,4,5]

There are many ways to represent the roughness of a surface, but the calculation has now been standardized by using Ra or Rt. Ra is Center Line Average (CLA), or Arithmetic Average (AA). The mathematical model of the roughness curve can be written as,

$$y = f(x)$$

and the Ra value is determined by

$$Ra = 1/L \int_0^L |f(x)| \, dx \qquad \text{(see Fig. 1.4)}$$

Rt is the Height of the Roughness Curve. In another words, Ra is the average roughness, and Rt is a peak-to-peak maximum roughness. The most popular method - and the only method recognized internationally - for roughness measurement, is by using a profilometer. The profilometer works like a record player. It has a typical 10 microns (400 micro-inches) radius diamond stylus which moves up and down with the surface profile of a work piece. The other end of the stylus is linked with a coil that moves in a magnetic field inside the cartridge. These actions generate voltages proportional to the surface profile. The electronics then convert the movements of the stylus and produce the Ra or Rt reading. The cartridge of the profilometer must travel in a direction perpendicular to the lay. The travelling speed is either 2 or 6 mm per

second (0.079 or 0.236 inches per second). The travel itself can be done manually or mechanically. With a mechanical power drive, the cartridge travels at a reliable speed and achieves much higher accuracy and produces repeatable readings. If the cartridge is driven by hand, a significant amount of set-up time can be saved.

1.2.2 Disadvantages of Profilometers

A renewed emphasis on quality is demanded in industry today. An on-line, one hundred percent successful inspection rate is now the goal to ensure quality. Profilometers are not designed for on-line inspection, therefore, they have several significant limitations in achieving this goal.

a) The stylus of the profilometer must trace the surface in order to make a measurement. The physical contact is unavoidable. The diamond stylus itself is very delicate, and any unexpected movement may result in damage to the stylus. Therefore, the set-up is very precise, and measurements should be carried out with great care. In fact, the set-up must be so precise that the process resembles more a laboratory experiment and an on-line inspection procedure is impractical.

b) The frequency response of the profilometer is relatively low which also makes it difficult to use with on-line inspection equipment.

c) Profilometers have some problems of their own. It has

difficulty in measuring some odd shaped parts like crank shafts, tapered bearings, or just some hard to reach corners. These measurements are never easy even in the laboratory.

Since profilometers have many disadvantages, several efforts have been made to invent new methods to measure surface roughness. One of the most promising recently discovered methods of measuring surface roughness is by the use of light. These fall into two basic procedures, ones which measure distance and those which respond to the light scattering effect.

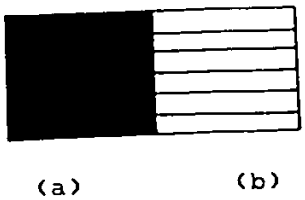

Fig. 1.1 Contrast Difference Between
a) Black lines on a Black Background, and
b) Black lines on a White Background.

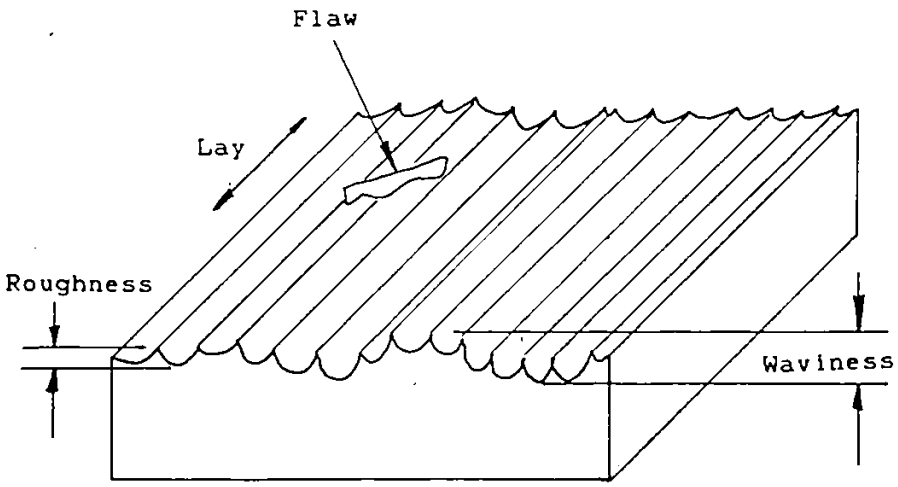

Fig. 1.2 Surface Roughness on a Machined Surface

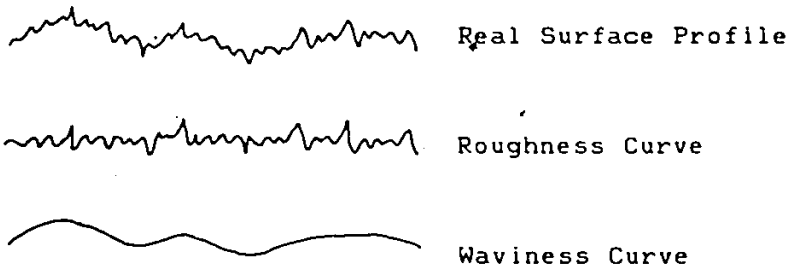

Fig 1.3 Real surface Profile,
Roughness and Waviness Curves

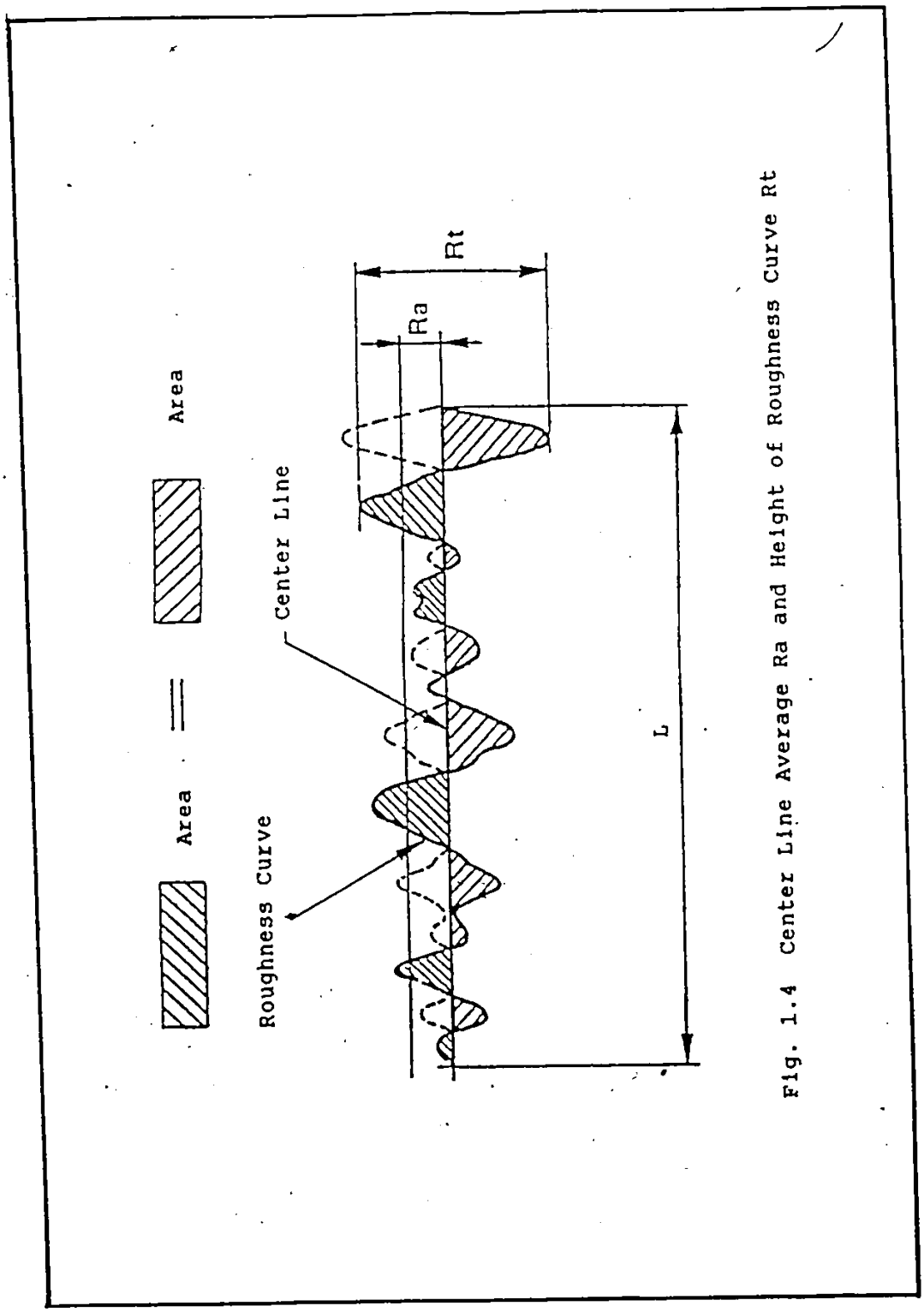

Fig. 1.4 Center Line Average Ra and Height of Roughness Curve Rt

Chapter II

LITERATURE SURVEY

2.1 Making and Marking Grids on Specimens

In the early days, marking a surface with grid lines took great effort. Most of the grids were scribed on by hand. There was hardly any uniformity and each grid had its own unique size. Later, a ruling engine [6] was introduced to scribe flat or cylindrical surfaces, which gave better tolerances, greater uniformity and improved accuracy. The University of Southern California developed a similar method [7] to scribe surfaces. A phonogragh needle was first honed to a fine point. The needle was then placed in a spring-loaded jig such that the pressure between the needle and the specimen could be easily controlled. By experimentation, a pressure setting was obtained that produced a satisfactory line. In this manner, lines which were approximately three to five ten-thousandths of an inch in width were scribed on the specimens.

In the late 1930's and early 40's, when photographic printing techniques became available, the above methods were used to scribe the master grids only. The grids were applied photographically by printing sensitive emulsions on the surface, covering the surface with a master grid negative, exposing it to light, and then developing the resultant print. There were many

papers published that report trying different chemical compounds as the emulsions.

In 1943 Brewer [8] reported the emulsion prepared by mixing 4 parts of photo-engraving glue, 28 parts of water, 1 part of ammonium bichromate and a 1/4 part of ammonia water. Exposure time was 5 to 7 minutes at a distance of 36 inches from a 35 ampere arc light. After exposure, the specimen was dipped in cold water to remove the unexposed portions of the emulsion. It was then placed in a hot solution of Diamond dye of the desired color. An air blast would be used to hasten drying.

One year later, O'Haven and Harding [9] developed a dichromated polyvinyl alcohol (PVA) solution for applying photo grids to test specimens. The PVA solution was prepared by mixing 660g of distilled water, 70g of PVA-RH428 (type A), 3.5g of potassium dichromate, 30g of finely powdered Nigrosine WSJ dye (0.6% aqueous solution) and 3.0g of Duponole L144WD. The printing and developing method was similar to Brewer's.

In 1948 MacLaren [10] reported that both Brewer and O'Haven's emulsion solutions were impractical when a large or vertical surface was used. In the meantime, several emulsions were commercially available. Among them were Defender Emulsion, Martin Multi-Mulsion and Eastman Kodak Transfax Spray and Primer. MacLaren's test concluded that the Transfax solution was the most reliable for irregular surfaces.

In 1952 Miller [11] reported that using a photo-engraving glue known as "cold top enamel" and its developer, produced a

purple-colored grid which gave a better result. He further suggested an alternative black "Dyrite" contact emulsion which gave an even higher contrast but less strainability.

In 1981 Sevenhuijsen [12] reported that a strippable photographic paper grid method gave the best contrast. In that method, a photographic paper with a polyethylene (PE) coated paper base was used. After printing, the picture layer (with one of the PE layers as backing) was peeled from the rest and bonded on a metallic sheet by means of a cyanoacrylate type cement. Sevenhuijsen demonstrated that this method can sustain up to a 45% strain if it is bonded on a polished surface.

The above grid methods have a common weakness; the grids would be too fragile for the die press. The strain level for die qualifications may reach up to 100% or more. A marking method called Electro-chemical etching would be more appropiate for this type of work. A more detailed discussion of this grid method is given in the next chapter.

2.2 Surface Roughness Measurement by Optical Methods

For surface roughness measurement, the profilometer has dominated the field for years. It was the first method that provided satisfatory measurement and was relatively easy to use. As pointed out in the previous chapter, it has many shortcomings, especially when its use was attempted in co-operation with on-line inspections. In recent years, optical methods have gained much attention as a promising new replacement for profilometers.

They offer the advantages listed below:

a) Non-contact: For on-line inspection, the stylus used in the profilometer will wear out quickly, even though it is made of diamond. Also, it scratches the sample surfaces, especially those of soft materials. In optical methods, neither the light source nor the detectors make contact with the work piece, avoiding stylus wear and scratch marks on the sample surfaces. Perhaps even more important, the non-contact method provids more freedom for on-line inspection assembly.

b) Resolution: For optical methods, the effective size of the stylus is the wavelength of the light, which is in the range of 400 to 700 nanometers, and is 20 to 30 times smaller then the common size diamond stylus used in profilometers. Therefore, optical methods can measure narrow valleys that the stylus is unable to enter.

c) High speed: The typical response time for a light detector is one megahertz, and the amplifiers are in terms of kilohertz. There is no comparitive in speed in any machine that depends on mechanical movements, such as a profilometer.

When light energy is directed onto a surface, three phenomena occur. They are TRANSMISSION, ABSORPTION and REFLECTION [2]. Transmission can be observed by viewing an object through a piece of glass or by observing sunlight shining through a window. Absorption can be seen indoors by turning off the lights at night. The whole place becomes dark because all the light energy

is absorbed by the walls, carpet and furniture. Reflection is an everyday experience illustrated when one sees one's own face in the mirror. When an incident light wave reflects off a very smooth surface, such as a mirror, the angle of reflection equals the incident angle. This is the well known Snell's Law. If the surface is not so smooth, the incident light scatters, with a portion still reflecting specularly.

In 1954 Davies [13] proposed the theory of electromagnetic waves reflected from rough surface and Beckmann [14] proposed the theory of the scattering of electromagnetic waves from rough srfaces.

These theories were developed in connection with the scattering of radar waves from rough water surfaces, they are equally valid in the optical region.

Davies derived the reflectance of the specular component for the case of normal incidence is given by:

$$\exp[-(4\pi\sigma/\lambda)^2]$$

Where σ is RMS deviation of the surface heights; and

λ is the wavelength of the illumination.

For the diffusely reflected component, the reflectance is given by:

$$(2^5\pi^4/m^2)\,(\sigma/\lambda)^4\,(\Delta\theta)^2$$

Where m is the RMS surface slope; and

$\Delta\theta$ is the instrument's acceptance angle.

In the case of the surface is perfectly conducting and hence would have a specular reflectance of unity if it were

perfectly smooth. Since no material is perfectly conducting, in order to apply Davies' theory to an actual metal surface it is necessary to modify this expression slightly and the complete expression for the measured reflectance R is:

$$R = Ro \exp[-(4\pi\sigma/\lambda)^2] + (Ro\, 2^5 \pi^4/m^2)\,(\sigma/\lambda)^4\,(\Delta\theta)^2$$

Where Ro is the reflectance of a perfectly smooth surface of the same material.

If the root mean square roughness σ is small compare with the wavelength λ , the expression of the equation can be reduced to

$$R = Ro \exp[-(4\pi\sigma/\lambda)^2]$$

Beckmann's theory was also simplified into a useful form in the similar way and for specular reflection

$$Rs = Ro \exp[-(4\pi\sigma \cos\theta/\lambda)^2]$$

Where Rs is the specular reflectance of the rough surface;

Ro is the reflectance of a perfectly smooth surface of the same material;

σ is a measure of average vertical roughness height;

λ is wavelength of illumination; and

θ is angle of incidence.

In 1961 Bennett and Porteus [15] were the first to experimentally verify Davies' theory by using ground glass and steel surfaces. Others, like Houchens and Hering [16]; Depew and Weir [17], and Birkebak [18] also reported similar findings. However, they agreed that the theory proposed by Beckmann is more satisfactory than that by Davies regarding the incoherent

reflected component of radiation. Therefore, the most comprehensive development of this work is given by Beckmann, who formulated the theory that light scattered into the specular direction gives information about the variance of surface height, while light scattered away from the specular direction depends on the function of surface slopes.

More recently, North and Agarwal [19] used a pair of fiber-optics to transmit He-Ne laser light back and forth to a ground surface. The ratio of the reflected laser light from the sample surface to the incident light was found to have a linear correlation with the mechanical roughness Ra in the log-log scale. The similar method was used two years later by Inasaki [23] to monitor the surface roughness of surfaces finished by the cylindrical grinding process.

Stout [20] experimented by shining infared light onto ground specimens (Rubert blocks), and measured the specular reflection. The intensity of the reflected light indicated the relative surface roughness.

Jansson, Rourke and Bell [21] used a 64-element linear lead selenide array to scan the reflection from a modified 3.39 microns wavelength helium-neon laser. The scans covered the area of 23 degrees from each side of the specular angle. A linear correlation was found from a plot of the logarithm ratio of the specular reflection and the total reflection versus the roughness measured by a stylus machine. The modification of the He-Ne laser to the wavelength of 3.39 microns was to maximize the deviation

of the specular intensity for the surface roughness of 2 to 20 micro-inches (0.05 to 0.5 microns).

Tsukada and Yanagi [22] reported using a charged coupled device (CCD) to measure the reflected He-Ne laser light from the specimens. A frosted glass was placed in front of the CCD to serve as speckle-pattern filter. The reflected light received from the CCD at the specular angle plus 5 degrees was taken as scattered light. The intensity ratio was calculated by the reflection of scattered light divided the specular light. Beckmann's theory expressed the intensity ratio as a function of standard deviation of roughness height (H), wavelength of the incident light, and the correlation length of surface roughness (T). By substituting T for the empirical formula

$$T = 27 (1-\exp(-H))$$

45 degrees for the incident angle, and 0.6328 microns for the wavelength of the incident light, for a relatively smooth surface (0.25 microns or 10 micro inches), the measured results are in fairly strong agreement with the calculated values.

2.3 Objectives of the Present Research

Although the theory of contrast has long existed and has been well defined, there have been no previous attempts to find the minimum required contrast for a line measurement. The work contained here tries to establish a guideline for an optical sensor contrast ratio for use with line measurements.

For optical roughness measurement, a considerable amount of work has been done. However, all of the investigators had some notable shortcomings. Some did not normalize their output from the transducers before correlating it with the surface roughness. This would cause concern about the transducer output being affected by factors other than surface roughness, subsequently resulting errors of unknown origin. Also, it was difficult to compare the results of different studies. All authors admitted that the proposed methods only worked in a small range of surface roughness (within 0.5 microns or 20 micro-inches), and that the pattern of light scattered beyond that range remained either unknown or was not mentioned by the authors. Most of the methods were very complex to perform, or required complicated and expensive apparatus.

The objectives of this study were:

A1. to develop an electro-optical sensor capable of measuring etched grid line contrast before and after the surface is deformed.

A2. to examine the parameters (magnification, illuminatin size

polarization, configuration, surface finish, strain level, etching duration) which may affect the contrast reading.

A3. to build a hand-held unit able to scan a rectangular etched grid-pattern measuring the contrast level, and indicating to what degree it is acceptable.

A4. to interface this hand-held unit with an Apple computer to analyze the output data.

B1. develop a simple technique to measure the specular and scattered reflected light from a metal surface which is illuminated by a focussed white light source.

B2. determine the best way to calculate the Intensity Ratio (IR) in order to report an optical surface roughness number.

B3. determine optical surface roughness IR vs roughness Ra curves for aluminum, brass, copper, stainless steel and tool steel samples, with the illumination incidence angle varied from 60 to 85 degrees. These flat samples were prepared on the same surface grinding machine using either aluminum oxide or silicon carbide wheels.

B4. compare the resulting IR ratios with the mechanical properties of the material.

B5. determine the effect that light oil on a sample surface has on the optical surface roughness measurement.

CHAPTER III

Analog to Digital Conversion and Electrochemical Etching

3.1 Analog to Digital Conversion [23,24,25]

At the preliminary stage of this study, a digital multimeter was connected to the amplifier of an optical sensor scanning over an etched line. The output of the amplifier was then read and recorded manually. A single contrast measurement took an hour to scan and record using this method. Later, a storage oscilloscope was connected to the amplifier. The analog signals of each scan were stored in the memory of the oscilloscope and an X-Y plotter was used to retrieve these analog signals from the storage-scope, plotting these signals on plain paper. Each desirable value was then measured from the paper and was used to calculate the contrast. The speed of obtaining contrast was improved slightly by the second method. By using the analog to digital (A/D) converter, the analog signals were converted into digital values. Through the micro-computer, the contrast was obtained directly.

In the later stage of this study, the analog output of System 7A [30] was linked directly to the Apple computer through an Adalab interface card. One of the many functions of this card is analog to digital (A/D) signal conversion. The converted signals were stored in the computer memory for further data

processing.

Voltage to frequency converters, voltage to time converters, and discrete voltage comparison converters are three major type of A/D converters.

Currently, there are two common types of A/D converters on the market. One is called dual-slope (or integrating) A/D converter and the other is called the successive approximation A/D converter. The dual-slope is one of the voltage-to-time converters, and the successive approximation A/D converter is one of the discrete voltage comparison converters which are based on the use of the D/A converters.

The successive approximation (SA) A/D converter contains a digital to analog converter, a comparator and/or a sample-and-hold amplifier. When an analog signal comes in, the SA A/D converter turns on the most significant bit of the digital to analog (D/A) converter. The comparator compares the input analog signal to the internal analog signal from the D/A converter. If the input analog signal is higher than the internal analog signal, the most significant bit of the D/A converter remains "on", otherwise it will be turned off. The first bit A/D conversion is completed. The second most significant bit of the D/A converter will be turned on and compared in the same manner to the most significant bit. The process will continue turning on and off the bits of the D/A converter until the least significant bit is completed. The end product is the binary number in the D/A converter, which is equivalent to the input analog signal. An

n-bit successive approximation converter requires only n clock periods to complete the A/D conversion, regardless of the magnitude of the converting voltage.

The output signals of most laboratory equipment contain noise. Suppose that the output "signal" (true signal plus noise) is momentarily higher than the true signal. Then one or more bits of the D/A converter will be left on when they should have been turned off. When the subsequent bits are tested, the noise in the signal may vanish or even change sign. The remaining bits in the D/A converter will be turned off, since the internal analog signal is higher than the output analog signal from the instrument. Therefore, the digital value equals neither the "signal" nor the true signal. This situation is also true when the "signal" is momentarily lower than the true signal. For this reason some SA A/D converter contain a sample-and-hold amplifier. The function of the sample-and-hold amplifier is to sample the output analog signal from the equipment for a very short period of time and hold on to that signal. The typical sampling, or aperture, time is less than one micro-second. The A/D converter samples the locked signal in the sample-and-hold amplifier instead of the fluctuating output signal from the equipment.

The dual-slope (DS) A/D converter contains a capacitor and a timer. The capacitor is allowed to charge by the output voltage of the equipment for a predetermined precise period. Because of the high impedance of the A/D input circuit, very little current is drawn from the external equipment. The capacitor is then

allowed to discharge, and the discharge time is monitored by the timer. The discharge time is a digital signal which can be read by the computer and is proportional to the external voltage. The name "dual-slope" came from the charging and discharging slope. During the charge period, the positive noise increases the charging rate of the capacitor, but this is off-set by the negative noise, which reduces the charging rate. The DS A/D converter converts the true signal and filters the noise automatically.

The A/D conversion of the Adalab was done in the dual-slope manner. Although it had a relatively slower conversion speed (Table 3.1 and Figure 3.1) when compared with the SA A/D converters, the variable conversion speed was utilized through the programming (Appendix D). The surface of the steel specimens was very bright and shiny, and it rendered a high output voltage. On the other hand, the grid lines were much darker than the surface, and they rendered a much lower output voltage. In the Data Collection Program, the conversion speed was set at maximum. Therefore, the data were taken in much higher frequency at the line than at the surface.

3.2 Electrochemical Etching [26,27,28]

The phenomenon of electrolysis was first studied scientifically more than 180 years ago. In 1929, a Russian, W. Gusseff, filed a patent for an electrochemical machining process with many features almost identical to the process as it is now practised. In 1941, an American named Burgess, demonstrated the

possibilities of the process and pointed out the striking differences between the traditional mechanical and the new electrolytic methods. In 1935, before Burgess's demonstration, Jacquet developed a method of controlled electrolytic removal of the actual metal of a workpiece to produce a polished surface. During the second World War, the U.S. Army Air Corps experienced failure of aircraft engine components at the points where the metal parts were stamped with identification numbers. A new marking method was required. Electrochemical etching was developed by A. R. Lindsay in 1943 as a promising solution to the problem.

Electrochemical etching removes metallic material atom-by-atom. Both the anode and the cathode are immersed in a solution called electrolyte which is acid based or a solution of salt in a suitable solvent, usually water. The workpiece is connected to the anode of the power supply. When the direct current starts to flow from the power supply, the workpiece begins to dissolve into ions which carry positive charges attracted by the cathode. Therefore, a thin layer of the workpiece is etched away and deposited on the cathode. If a mask made from non-conductive material is placed on the surface of the workpiece, only the exposed area can be etched. If the workpiece is connected with the cathode, the process is called electroplating. If a direct current is replaced by an alternating current, the workpiece is etched in the first half of the cycle, and a stable compound of the base metal is redeposited into the etch during the other half

of the cycle.

In this study, the grid lines were etched on the specimen's surface by an electrochemical marking process using an AC power supply (Figure 5.4). No material was removed from the surface and the lines can withstand the strain level up to the point of failure of the specimen. The lines did not appear to influence the failure process.

Table 3.1 Results of the Adalab analog to digital conversion speed:

Voltage (V.)	Samples per second
0.096	48
0.51	44
1.1	40
1.5	35
2.1	33
2.6	30
3.0	27
3.6	26
4.0	25

Regression analysis of the data:

Sampling rate = $4.8.8 - 9.92\ V + 0.982\ V^2$

Coefficient correlation = 0.997

Standard error of estimate = 0.727

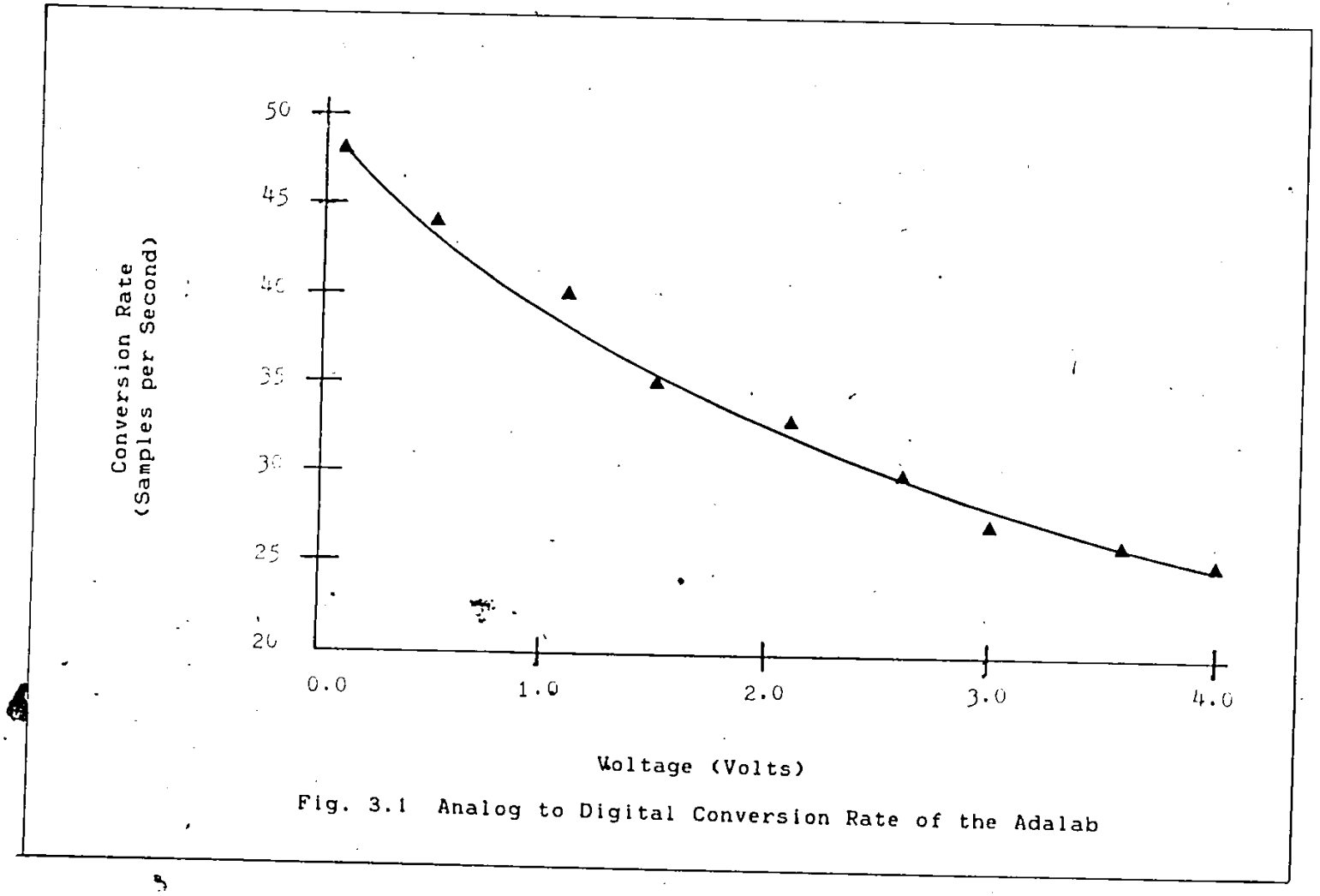

Fig. 3.1 Analog to Digital Conversion Rate of the Adalab

Chapter IV

EXPERIMENTAL APPARATUS

In this experimental study, the contrast of etched lines on sheet metal and light scattered from the roughness samples were measured by two entirely different sets of apparatus. These apparatus are described below.

The experimental apparatus of contrast measurement consists the following main components:

a) Hand-held Unit I: This is one of the two hand-held units which were specially designed and built for this experiment. Each of the units consists of a light source, imaging lens and a light detector. The light source illuminates the sample surface. The imaging lens then collects the reflected light from the sample surface and focusses it onto the detector.

This unit is depicted in Figure 4.1.

Specifications:

Dimensions:	102mm X 74mm X 43mm 4.0" X 2.9" X 1.7"
Magnification:	3X
Light source:	Carley Lamp No.628 (white light)
	Voltage: 5.0 V
	Current: 0.5 A

	Luminance: 1.0 Candela
	Temperature: 400 K
	Lifetime: 5000 Hours
Illumination Dia.:	0.82mm (1/32") minimum
Imaging lens:	Focal length: 7.6mm (0.3")
	Diameter: 5.1mm (0.2")
Detector:	Active diameter: 1.02mm (0.040")
	(See also Section c: Amplifier)

This detector is part of the DiffractoGage System 7A. The linearity response curves of System 7A under white, red, green and blue light are shown in Figures A1 and A2 (Appendix A). The response curves were obtained by using a Photodye Model 66XLA Optical Power/energy Meter with Model 250 Photodetector.

b) Hand-held Unit II: This unit is essentially identical in all respects to Hand-held Unit I except that it is slightly larger and has a sharp single contact point instead of a flat contact surface (Figures 4.1 and 4.2). This Unit allows an angle sensitivity test and can also scan a curved surface.

Specifications:

Dimensions:	127mm X 102mm X 43mm 5" X 4" X 1.7"
Magnification:	2.5X
Light source:	Same as Unit I
Illumination Dia.:	2.4mm (3/32") minimum

Imaging lens:	Focal length: 14.5mm (0.57")
	Diameter: 7.6mm (0.3")
Detector:	Same as Unit I

c) Amplifier: The detector in the hand-held unit received the light energy, which was reflected from the sample surface, and rendered an equivalent analog signal. This analog signal was amplified in order to be read by other equipment. A specially modified DiffractoGage System 7A amplifier was used in this study.

Specifications [29]:

Frequency response:	DC to 100 KHZ
Non-linearity:	<1%
Output voltage:	Variable gain
Long term stability:	<3% deviation at constant temperature

d) Analog to digital signal converter: The function of an A/D converter is described in Section 3.1. An Adalab interface card was used in this experimental work.

Specifications (A/D converter) [25]:

Integrated circuit:	Intersil 7109 dual-slope A/D converter
Resolution:	12 bits plus sign bit and over-range bit
Full scale voltage:	0.5V, 1.0V, 2.0V, 4.0V jumper selectable
Max. conversion time:	50 milliseconds

Min. conversion rate:	20 samples per second
Max. input voltage:	+/- 12V without damage
Input impedance:	min. 8 megohms
Input current:	max. 0.5 micro amperes
Temperature coeft.:	100 ppm/degree C
Overall accuracy:	better than 0.1% of full range

The experimental apparatus to measure "ground" metal surface roughness consists of the following main components:

e) Profilometer [5]: A surftest III profilometer was used in this study.

Specifications:

Detecting system:	moving magnet system
Material of stylus:	diamond
Tip radius:	10 +/-2.5 microns
Tip angle:	90 +/-10 degrees
Measuring force:	1.5gf (14.7 N)

f) Light source: A white light, which was the same as in the hand-held-units, was used in this experiment to cast light energy on the surface of roughness samples.

g) Lens: A lens was used to focus the light energy from the light source on the sample surfaces. Since this work did not use a laser as the light source, a lens must be used to concentrate the light energy onto the sample

surfaces.

Specifications:

Focal length:	152mm (6.0")
Diameter:	38mm (1.5")

h) Detector: In this part of the experimental study, two United Detector Technology model PIN-10DP detectors were used. The specularly reflected light from the sample surface was monitored by one detector. The second detector was always located at 45 degrees from the normal line of the sample surface regardless of the angle of the incident light.

Specifications [30]:

Active area:	100 square mm (0.155 square inches)
Maximum incident light power:	10 mW
Response time:	1 microsecond
Responsivity:	0.35 A/W
Linearity:	DC light level changes of up to 10 decades
Operating temperature:	0 - 71 degree C

i) Amplifier: The matching United Detector Technology amplifiers model 101A were used to convert the output current from the silicon photodetectors to voltages. These amplifiers were set in the hi-sensitivity mode.

Specifications [31]:

Transimpedance:	1E7 volts/amp
Frequency response:	DC to 1.6 KHZ
Output noise:	0.10 millivolts RMS
Output impedance:	75 ohms
Output current:	10 milliamps
Zero offset drift (after 5 minutes):	0.2 millivolt/hour
Output voltage range:	+/- 10 volts
Temperature range:	0 to 40 degree C

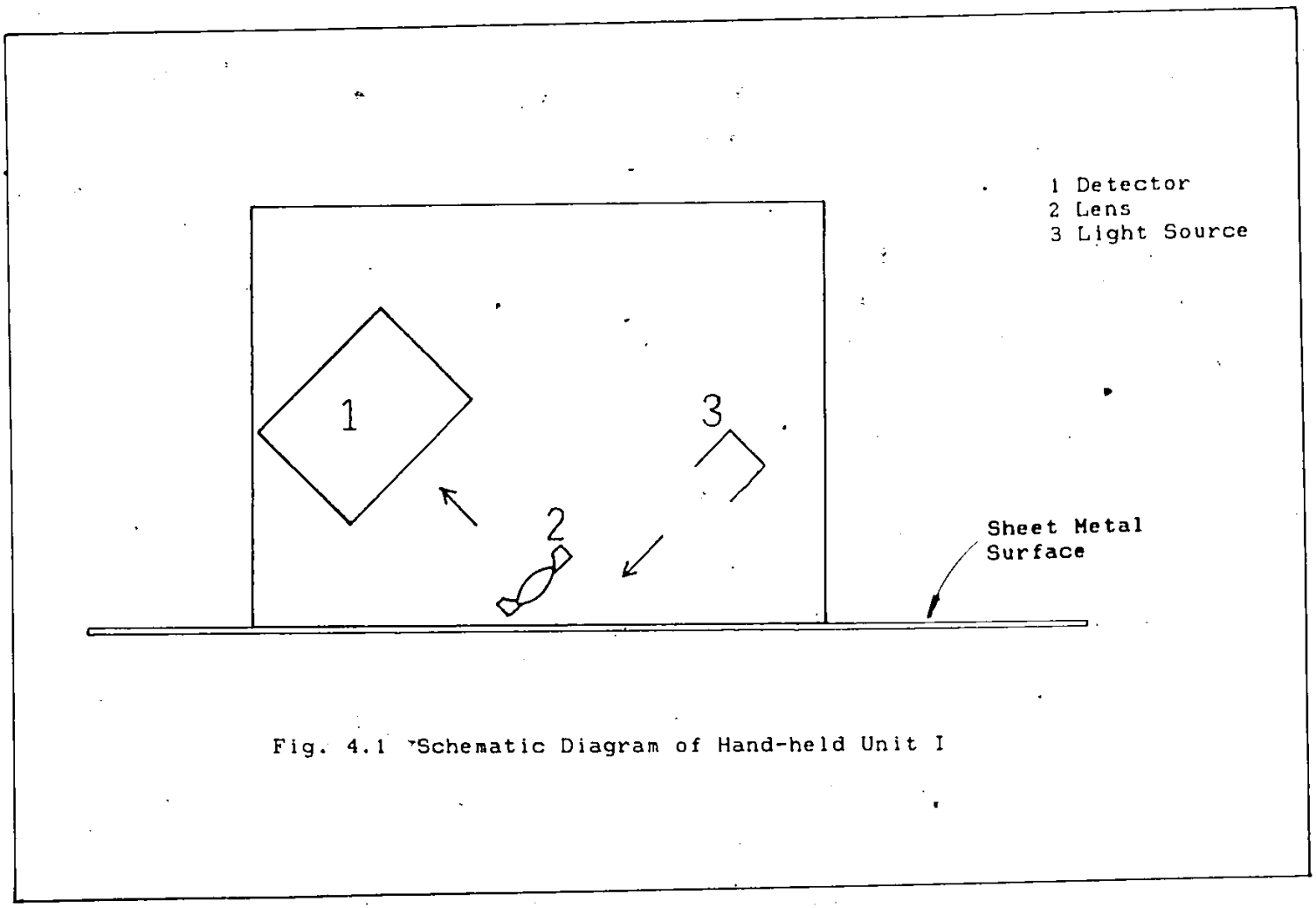

Fig. 4.1 Schematic Diagram of Hand-held Unit I

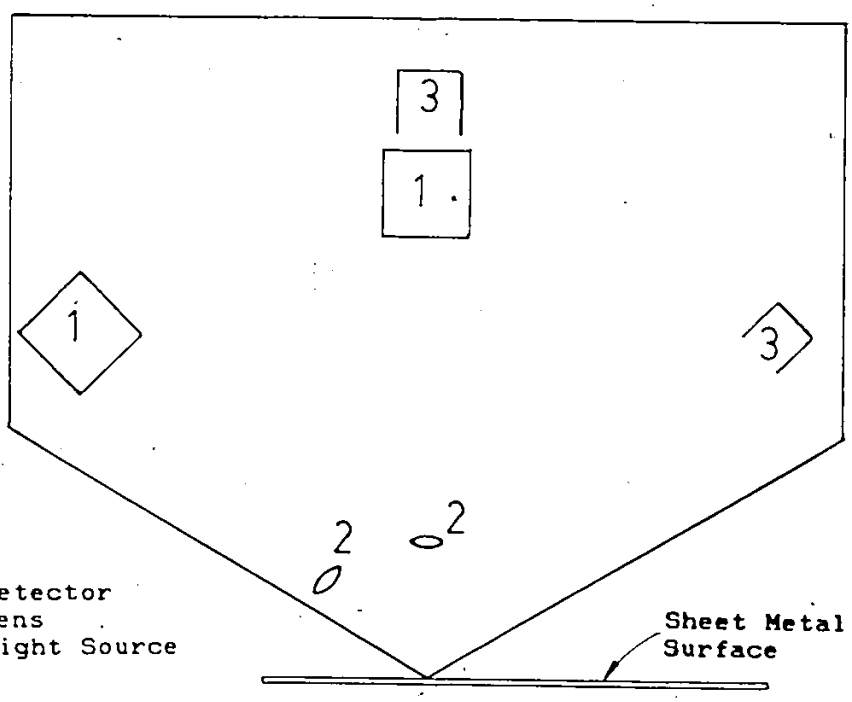

Configuration I
Incident Light Angle 45 Degrees
Detector Angle 0 Degrees
Illumination Diameter 9.5mm

Configuration II
Incident Light Angle 45 Degrees
Detector Angle 45 Degrees
Illumination Diameter 9.5mm

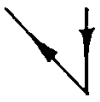

Configuration III
Incident Light Angle 0 Degrees
Detector Angle 45 Degrees
Illumination Diameter 7.1mm

Fig. 4.2 Schematic Diagram of Hand-held Unit II

CHAPTER V

EXPERIMENTAL PROCEDURES, RESULTS AND DISCUSSION OF CONTRAST MEASUREMENT

The System 7A had a linear response with white, red, green, blue and polarized white light. The test results are depicted in Figures A1 to A4 (Appendix A). Since this system exhibited such a characteristic, it was an ideal tool for this study.

A detector in the optical system, such as the Hand-held Unit only "sees" a very small part of the sample surface at one time. The size of the sample surface which is seen by the detector is determined by the active area of the detector and the magnification of the optical system. In order for a detector to scan a surface, the optical system must move relative to the sample surface.

All the scans in this study were achieved by holding the optical system or the Hand-held Unit in a stationary position, and the sample was moved against the system during the scan.

5.1 Magnification Test

The detector itself can not "see" a sharp image unless an image lens was used. The second function of the lens was

magnification. The objective of this test was to determine the affects of the magnification on contrast measurement, and also to determine the optimal magnification.

In this test, the sample was a piece of 51mm X 51mm (2" X 2") well polished tool steel. Several coats of flat black paint were sprayed onto the center of the steel sample to form a line of width 2.5mm (0.10"). The detector used in this test had an active (light sensing) diameter of 3.8mm (0.150").

The incident light and the detector were located at the incident and angle of reflection of 45 degrees. The experimental procedures are listed below.

1. Set the incident light angle at 45 degrees from the normal line of the sample surface.
2. Set the focal lens and the detector at the specular reflection angle of the light source.
3. Adjust the imaging lens and the detector until the image of the sample appears clearly on the detector.
4. Measure the size of the line's image.
5. Move the sample forward 0.5mm.
6. Record the output voltages from the System 7A.
7. Repeat procedures 5 & 6 until the scan passes the line on the sample surface.
8. Repeat procedures 3 to 7 for another magnification.

The results of this test is listed and shown in Table 5.1 and Figure 5.1. From the illustration the best contrast appeared at the magnification between 1.5 to 4.5. This corresponds to the

Ratio (image size of the line / active diameter of the detector) between 1 to 3.

Recall that contrast is determined by the outputs of the system when it sees only the line or only the unmarked surface. Any other data, included when the system sees part of the line and part of the surface, should be disregarded.

When the Ratio is less than one, the line image was not wide enough to cover the active area of the detector. i.e. the detector did not image the line by itself. In order to obtain a valid contrast, the Ratio must be larger than one. However, a large Ratio did not improve contrast. The curve saturates as shown in Figure 5.1.

When the magnification increased, the distance between the sample surface and the detector also increased. When the magnification was larger than 4.5, the image became ambiguous. Therefore, further increasing magnification rendered decreasing contrast, see Figure 5.1.

5.2 Size of the Illumination Footprint

The optical set-up was the same as the last test. The magnification was set at 1.2 X. A 1mm (0.040") diameter drill was used to form a pinhole in a thin piece of aluminum to form an aperture. The pinhole was placed in the path of the incident light to control the size of illumination field. The size of the illumination field became smaller when the pinhole was moved closer to the sample surface. The output of the System 7A was

hooked up to the Adalab, and the Apple computer computed the contrast. With the automation of data taking, the sample was driven by an electric motor in this test.

The objective of this test was to determine the effect of the size of illumination on the contrast. The experimental procedures are listed below.

1. Measure the size of illumination field on the sample surface.
2. Scan the surface and obtain the contrast.
3. Move the pinhole to the new location and repeat procedures 1 and 2.

The result of this test is listed in Table 5.2 and shown in Figure 5.2. Regression analysis produced the following equation:

$$C = -4.015E-4\ IL^3 + 4.536E-3\ IL^2 - 1.895E-2\ IL + 1.024$$

Correlation Coefficient = 0.9999

Standard error of estimate = 3.596E-3

Where C is contrast and IL is the major diameter of illumination field in millimeters.

Note that the contrast can be greatly improved by reducing the size of the illumination field. This is explained by the fact that when the detector was looking at the image of the black line, stray light would bounced into the active area of the detector if the illumination field size was large. If the illumination field was small, the problem of stray light was decreased.

These results show that in order to obtain a proper

contrast, the image of the line should be large enough to cover the active area of the detector. However, reduction of the illumination field size is equivalent to reducing the active diameter of the detector in the contrast measurement (Figure 5.3).

5.3 Etching Duration Test I

Four types of steel were available for this test. The first was traditional plain carbon steel, which is currently used in the production line. The second was conventional hot dipped galvanized steel, which had large grains and shiny surfaces. The third one was a relatively new hot dipped galvanized steel, which had a smaller grain size and a dull surface. The last was electro-galvanized steel. According to the GM technical center, the electro-galvanized steel has better paintability and weldability.

Based on the above facts, the plain carbon and electro-galvanized steel were selected for this test. The size of the specimens was 178mm X 51mm X 0.9mm (7" X 2" X 0.035"). The specimens were etched by the electro-chemical marking process and then scanned by Hand-held Unit I. The metal marking processes were performed by GM Technical Center staff in Warren, Michigan using their standard procedures as listed below.

1. Clean the specimen with Chlorothene and then place it on the etching table.
2. Place the master grid (mask) on top of the specimen.

3. Set the etching duration on the clock of the Lectroetch power supply.
4. Wet the master grid and the sample with Lectroetch electrolyte No.353.
5. Roll the roller on the master grid a few times to observe if there is enough electrolyte to cover the master grid surface completely. If not, add more electrolyte.
6. Start the power supply and roll the roller gently on the master grid, until the etching process is completed.
7. Clean the specimen with Lectroetch Cleaner Formula 2.
8. Oil the specimen to prevent rust.

The marking apparatus is shown in Figure 5.4. The test results are listed in Table 5.3 and also shown in Figure 5.5. The equations of the correlation curves from the test results are listed below.

For plain carbon steel:

$C = -1.814E-6\ T^2 + 1.417E-3\ T + 0.4515$

Correlation Coefficient = 0.9593

Standard Error of Estimate = 3.231E-2

For electro galvanized steel:

$C = 1.012E-8\ T^3 - 6.534E-6\ T^2 + 1.914E-3\ T + 0.3133$

Correlation Coefficient = 0.9475

Stand Error of Estimate = 6.483E-2

where C is contrast and T is etching time in seconds.

For plain carbon steel, the optimal etching time was between 6 to 7 minutes. For electro-galvanized steel, the

contrast increased with increasing etching time. In general, the lines looked darker when viewed by the naked eye. Microscopic inspection on the electro-galvanized steel surfaces showed that the galvanized coating was etched away particularly for the specimens which had extensive etching.

5.4 Effect of Surface Roughness on Line Contrast

As mentioned in a previous chapter, a very smooth surface reflects light specularly, as described by Snell's law, and a rough surface scatters light. Also recall that contrast increases with increasing Pb (Reflectance of the background surface).

This test was designed to determine the effect of surface roughness on the measured contrast. The specimens for this test were 89mm X 25mm (3.5" X 1") plain carbon steel and were ground on a surface grinder at different combinations of feed rates and grinding wheels and then polished by hand. The roughnesses of the specimen surfaces were then measured by the Surftest III in Ra and Rt with 3 different cut-off values. These results are listed in Tables 5.4 and 5.5. The lines were etched on the specimens by the electrochemical marking process which was described in Section 5.3. The etching duration of the specimens was 1 minute.

The resulting contrast from these specimens are listed in Table 5.6 and also depicted in Figures 5.6 and 5.7. The results coincide with the equation (2) (page 4) indicating that smoother surfaces yield higher contrast in both Ra and Rt measurements. A smaller cut-off value shifted the resulting curve to the left.

5.5 Configuration Test

One of the capabilities of the specially developed Hand-held Unit II was used in this test. This unit had three configurations (Figure 4.2) and each one was used to scan one plain carbon and two electro-galvanized steel specimens. The scans were done in a specified 51mm X 6mm (2" X 0.25") area of the specimen in order to produce better comparison data.

The results are listed in Table 5.7 and the comparisons between configurations by the student t test are listed in Table 5.8. The video sighals of the configuration are depicted in Figures 5.8 to 5.14. From the results, Configuration II was the best and configuration I came second with a 99% level of confidence (Table 5.8). Therefore, the specular reflection angle is the best location for the detector in contrast measurement.

Both Units, Unit II with configuration II and Unit I, failed to determine the contrast of specimen G1. (Figure 5.8). By changing the configuration, Unit II was capable of determining the contrast on G1 with configuration I or III (Figures 5.9 & 5.10). In some cases, an uneven coating, dirt, and rust created the variations in surface signal confusing the etched line signal. In this case it would be beneficial to move the detector away from the specular reflection angle. Configuration I and III was used with the Unit to filter out the variations of the surface signals (Figures 5.8 to 5.14).

5.6 Etching Duration Test II

Based on the results of the Configuration test, the electro-galvanized steel specimens were retested for contrast to determine the optimal etching time using the Hand-held-unit II with configuration I. The test was done by scanning 60 lines on each of the electro-galvanized steel specimens.

The results are listed in Table 5.9 and also shown in Figure 5.15. The results indicated that the optimal etching period was 20 seconds. Unit II obtained higher contrast than Unit I in the Etching Duration Test I provided that the specimens' etching durations were less than 30 seconds. For longer etching duration, the higher contrast measured by Unit I was caused by the fact that the galvanized coating on the specimens were etched away as mentioned in the discussion of Section 5.3.

5.7 Tensile Test

During the die qualifing process, the lines are measured before and after the deformation. Therefore, the contrast is equally important in both cases. To simulate the deformation in the actual process, five 89mm X 25mm (3.5" X 1") specimens were selected and stretched to failure by tensile force. The T numbers were the rank of their Ra values. The surface condition of specimen T4 was as received, and it did not go though any grinding or polishing process. Therefore, T4 represent the production surface condition. The experimental procedures are listed below.

1. Record the grid pattern of the specimen's surface and number each intersection of the etched lines.
2. Measure the distance of each intersection from their related referance point by a modified Mitutoyo height gage which has a pin pointer and a magnifying glass to facilitate the measurement.
3. Scan the four corners of each intersection (Figure 5.16) by the Hand-held Unit I.
4. Slowly stretch the specimen to failure in a Tinius Olsen Universal Testing Machine.
5. Repeat procedure 2 to determine strain levels by Fischer's Method [35] (Figures 5.17 to 5.21).
6. Repeat procedure 3 to determine the change of contrast.

The test results, which are listed in Table 5.10, indicated that the strain had positive and negative affects on contrast. In general, lines perpendicular and parallel to the axis of stretch increased and decreased their contrast respectively (Figures 5.22 to 5.26). The width of the lines showing decreased contrast were checked (Table 5.11), and it was found that there was no correlation between the % decrease of contrast and the line width. Also the surface roughness did not affect these results. In some specimens, the maximum decrease in contrast did not appear at the maximum strain level (Figures 5.24 & 5.25).

Another interesting observation of this test was that after the stretch, the surface changed from shiny to dull. It was more noticeable on a smooth surface such as specimen T1. For a rough

surface, such as specimen T5, the change only occurred in the immediate area of failure.

The summary of the measurement of the grid size from all T specimens are as follows:

Mean Size = 6.35mm (0.2499")

Coefficient of Variation = 1.766

The maximum strain level was over 100%.

5.8 Dome Test

In this test, biaxial strain was applied to the specimens instead of tensile stress forming the specimens into a dome shape. The experimental procedures of this test are described below. Again the mechanical deformation was carried out at the GM Technical Center.

1. Record the grid pattern of the specimens' surface and number each intersection of the etched lines.
2. Scan the specimen between two intersection points (Figure 5.16) by Hand-held Unit II. Use configuration II for plain carbon steel specimens and configuration I for electro-galvanized steel specimens.
3. Oil the specimen with light oil on both sides and place it into the MTS testing machine with the circular grid facing the ram.
4. The MTS machine forms the specimen into a dome shape with the ram speed of 25.4mm (1") per minute. The machine stops itself when the first crack appears.

5. Measure the deformed grids to obtain strain levels.

6. Repeat procedure 2 to obtain the change of contrast.

The uniformity of the grid size was established from the results of the Tensile Test (Section 5.7, The summary of the measurement of the grid size from all T specimens). For this test, therefore, it was assumed that the grid size before deformation was 6.35mm (0.2499") at the risk of less than 2% error. The specimens used in this test were etched on both sides, one side with a square grid and the other with a circular grid.

After the deformation, the strain levels were determine by a 6X Edscorp comparator on the square grid side of the surface. The strain level of four specimens (C10, C11, G1 and G3) were also measured with an Optical Grid Analyzer on the circular grid side of the surface. This optical sensor images etched circular grids using a 2D CCD camera. A software algorithm fits the best ellipse to the resulting image which is then used to determine both the direction and magnitude of the strains. This automated strain measurement was also performed at the GM Technical Center by their operators. The comparison of these two measurements are shown in Figures 5.27 & 5.28. The results from these two methods correlated well, except for the region close to the failure.

Due to the physical size of the circular grids (2.5mm or 0.1" diameter), they were able to get closer to the failure zone. Therefore, the peak values measured by circular grids should be more accurate than the square grids.

Hand-held Unit II was used to scan the specimen surface. The major concern here was the decreasing contrast as a result of the strain. Therefore, only the lines parallel to the strain direction were rescanned to determine the percent change of contrast due to the strain level. The test results are listed in Tables 5.12 & 5.13 and also shown in Figures 5.29 & 5.30. It reinforced the results of the Tensile Test. All plain carbon steel specimens' contrasts decreased for lines parallel to the axis of stretch and the magnitude did not correlate with the strain level. Again, the maximum decrease in contrast did not appear at the maximum strain level (Figures 5.29 & 5.30) for both types of steel. Electro-galvanized steel reacted differently under the strain, as the contrast actually increased in some cases. The increased contrast might be caused by the applied strain separating the coating from the surface, revealing part of the shiny bare metal surface. This speculation was also supported by observation as it was noticed that the black compound of the etched line comes away from the surface with the lubrication oil. It was also more noticable with the specimens which had an etching time of 2 minutes or more.

5.9 Alignment Sensitivity Test

The Hand-held Unit I was designed to check the line contrast before the qualifying test, hence before the deformation of the sheet metal. Unit I works with flat surfaces and the box shape of the Unit eliminates the error of alignment. Let it be

thought that the surface may not be flat, or the Unit may not be set on the surface properly, in which case an alignment error results. Unit II was designed to test this error. Its localized contact surface allows the Unit to misalign with the specimen surface. The specimen was the same one used in magnification test. The Unit was then misaligned by +/- 1, 3 and 5 degrees, taking counter clockwise rotation of the unit as positive when viewing the unit and the specimen from the top. All three configurations of the Unit II were tested. The test procedures are listed below.

1. Set up the Hand-held Unit II with proper alignment with the specimen's surface.
2. Scan the line five times and average the readings.
3. Rotate the Unit to a new angle as stated above.
4. Repeat procedure 2.
5. Repeat procedures 3 and 4 until all proposed angles are completed.
6. Repeat all procedures for each configuration.

The percent change of contrast due to the misalignment angles are shown in Figure 5.31. The results indicate that all the configurations had less than 10% error, when the angular error was less than 5 degrees. Configuration I, which was used in the dome tests for galvanized steel, increased the contrast when rotated in counter clockwise direction and decreased the contrast when rotated in opposite direction. Configuration II, which was used in the dome test for plain carbon steel, decreased the

contrast regardless of the rotation direction. This may partly account for the fact that some of the contrast measurements increased on the galvanized steel and all contrast measurements decreased in carbon steel after the plates were deformed.

TABLE 5.1 Results of Magnification Test

Image (in.)	V High (V.)	V Low (V.)	* Ratio	M	C
0.045	2.8	1.6	0.3	0.45	0.43
0.078	4.1	1.8	0.52	0.78	0.56
0.129	3.0	0.9	0.86	1.29	0.70
0.153	4.4	1.1	1.02	1.53	0.75
0.175	5.2	1.3	1.17	1.75	0.75
0.247	5.1	1.2	1.65	2.47	0.76
0.270	5.0	1.2	1.80	2.70	0.76
0.308	5.3	1.3	2.05	3.08	0.75
0.346	5.1	1.2	2.31	3.46	0.76
0.360	5.1	1.2	2.40	3.46	0.76
0.444	5.3	1.4	2.96	4.44	0.74
0.816	5.0	2.0	5.44	8.16	0.60

* $\text{Ratio} = \dfrac{\text{Image size of the line}}{\text{active diameter of the detector}}$

M Magnification

C Contrast

TABLE 5.2 Results of the Illumination Size Test

Illumination Footprint (Major Diameter) (mm)	Illumination Footprint (Major Diameter) (inches)	Contrast
2.4	0.094	0.998
4.0	0.156	0.997
6.4	0.250	0.981
8.7	0.344	0.938
12.7	0.500	0.692

TABLE 5.3 Results of Etching Duration Test I

Specimen #	Etching Time (Sec.)	Mean Contrast (MC)	Standard Deviation (S)	Number of Lines Scanned (N)
C1	5	0.424	7.31E-2	17
C2	8	0.440	4.97E-2	30
C3	13	0.446	4.30E-2	29
C4	20	0.490	3.57E-2	30
C5	32	0.501	4.68E-2	29
C6	50	0.575	2.80E-2	30
C7	80	0.577	4.16E-2	29
C8	120	0.616	3.24E-2	30
C9	180	0.632	3.03E-2	29
C10	300	0.678	4.07E-2	30
C11	480	0.727	2.80E-2	30
G1	5	Cannot be determined		
G2	8	0.415	5.60E-2	30
G3	15	0.263	6.25E-2	27
G4	20	0.281	5.19E-2	30
G5	30	0.372	3.58E-2	30
G6	50	0.474	6.23E-2	28
G7	80	0.415	4.11E-2	29
G8	120	0.448	7.02E-2	30
G9	180	0.509	6.05E-2	30
G10	300	0.574	4.91E-2	30
G11	480	0.845	2.95E-2	30

Table 5.4 Ra Surface Finish of Specimens, microns (micro-inches)

Cut-Off Value	0.8mm 0.03"		0.25mm 0.01"		0.08mm 0.003"	
Specimen #	Range	Ave.	Range	Ave.	Range	Ave.
1	0.18/0.22	0.20	0.15/0.18	0.17	0.12/0.13	0.13
1	(7/8.5)	(8)	(6/7)	(7)	(4.8/5.3)	(5)
2	0.28/0.33	0.31	0.23/0.28	0.26	0.20/0.24	0.22
2	(11/13)	(12)	(9/11)	(10)	(8/9.5)	(9)
3	0.30/0.36	0.33	0.30/0.33	0.32	0.25/0.28	0.27
3	(12/14)	(13)	(12/13)	(13)	(10/11)	(11)
4	0.46/0.56	0.51	0.41/0.51	0.46	0.33/0.41	0.38
4	(18/22)	(20)	(16/20)	(18)	(13/16)	(15)

Table 5.5 Rt Surface Finish of Specimens, microns (micro-inches)

Cut-Off Value	0.8mm 0.03"	0.25mm 0.01"	0.08mm 0.003"
1 1	2.54 (100)	2.29 (90)	1.70 (67)
2 2	3.30 (130)	3.0 (118)	2.54 (100)
3 3	4.95 (195)	4.52 (178)	4.52 (178)
4 4	6.86 (270)	6.86 (270)	6.05 (238)

Table 5.6 Contrast of Roughness Specimens

Sample #	Surface roughness Ra (microns)	(micro inches)	MC	S	N
1	0.20	8	0.723	175E-2	20
2	0.30	12	0.638	4.45E-2	20
3	0.30	13	0.530	2.69E-2	20
4	0.51	20	0.455	3.10E-2	20

N Number of Lines Scanned
MC Mean Contrast
S Standard Deviation of Contrast

Table 5.7 Results of Configuration Test

Configuration	Galvanized Steel G8	Plain Carbon Steel C8	Galvanized Steel G1
I (45/0)	N=35 MC=0.442 S=7.34E-2	N=35 MC=0.513 S=3.93E-2	N=35 MC=0.440 S=6.93E-2
II (45/45)	N=36 MC=0.636 S=4.08E-2	N=35 MC=0.651 S=2.92E-2	Indeterminable
III (0/45)	N=35 MC=0.359 S=7.28E-2	N=35 MC=0.408 S=3.14E-2	N=35 MC=0.401 S=3.42E-2

Table 5.8 The Comparison of Configurations

Specimen #	Comparison Between Configuration	Resulting Student - t Value
Galvanized Steel G8	II & I	13.8
	II & III	19.85
	I & III	4.75
Plain Carbon Steel C8	II & I	16.68
	II & III	33.5
	I & III	12.35
Galvanized Steel G1	I & III	2.986

Table 5.9 Results of the Etching Duration Test II

Specimen #	Mean Contrast	Standard Deviation	Coefficient Variation	Number of Lines Scanned
G1	0.505	7.02E-2	14.7	60
G2	0.555	4.74E-2	8.54	60
G3	0.610	3.17E-2	5.20	60
G4	0.670	2.81E-2	4.20	60
G5	0.534	5.34E-2	10.0	60
G6	0.452	7.25E-2	16.0	60
G7	0.387	4.70E-2	12.2	60
G8	0.414	0.110	26.5	60
G9	0.458	7.14E-2	15.6	60
G10	0.361	5.04E-2	14.0	60
G11	0.413	6.31E-2	15.3	60

Table 5.10 Results of Tensile Test

Specimen	Ra Microns (Micro-inches)	Point #	% Strain	Average Percentage Contrast Change * a&c	b&d
T1	0.18 (7)	16	42.4	12.9	-9.81
		17	55.4	9.37	-14.0
		18	128	13.4	-25.5
		19	81.0	13.1	-20.2
T2	0.33 (13)	16	52.1	23.5	-8.22
		17	119	46.3	-27.8
		18	72.7	13.2	-17.8
		19	34.4	15.2	-12.2
T3	0.51 (20)	16	36.4	24.6	-4.32
		17	45.6	28.5	2.79
		18	57.7	31.7	-14.2
		19	96.6	30.7	-15.5
		20	115	19.0	-10.5
		21	53.2	28.7	-8.60
T4	0.64 (25)	28	64.9	30.2	-0.24
		29	100	34.6	-21.3
		30	78.1	9.44	-23.6
		31	36.4	9.00	-11.9
		32	2..8	8.16	-5.08
T5	1.22 (48)	15	42.4	12.8	-8.81
		16	90.0	7.06	-35.1
		17	90.0	18.7	-28.7
		18	54.3	18.2	-11.9
		19	34.4	12.9	-9.86

* See Figure 5.16

Table 5.11 Line Thickness of Tensile Specimen After Stretch

Specimen #	Point #	Average Percentage Contrast Change * b&d	Line Width After Stretch	
T1	18	-25.5	0.483mm	0.019"
T1	19	-20.2	0.533mm	0.021"
T2	17	-27.8	0.432mm	0.017"
T2	18	-17.8	0.508mm	0.020"
T3	18	-14.2	0.559mm	0.022"
T3	19	-15.5	0.559mm	0.022"
T4	29	-21.3	0.508mm	0.020"
T4	30	-23.6	0.635mm	0.025"
T5	16	-35.1	0.533mm	0.021"
T5	17	-28.7	0.508mm	0.020"

* See Figure 5.16

Table 5.12 Plain Carbon Steel Dome Test Results

Specimen #	Line between Points	% Strain	Contrast % Change
C1	38 / 39	76	-39
	39 / 40	38	-29
	40 / 41	30	-31
C2	36 / 37	72	-41
	37 / 38	50	-55
	38 / 39	25	-38
C3	36 / 37	54	-5.3
	37 / 38	68	-4.2
	38 / 39	34	-44
C4	37 / 38	66	-33
	38 / 39	54	-56
	39 / 40	32	-43
C5	36 / 37	50	-37
	37 / 38	66	-48
	38 / 39	36	-39
C6	38 / 39	76	-20
	39 / 40	54	-28
	40 / 41	36	-11
C7	38 / 39	74	-47
	39 / 40	52	-39
	40 / 41	34	-18
C8	38 / 39	36	-4.2
	39 / 40	72	-35
	40 / 41	42	-37
C9	38 / 39	68	-24
	39 / 40	58	-39
	40 / 41	36	-20

Table 5.13 Electro-galvanized Steel Dome Test Results

Specimen #	Line between Points	% Strain	Contrast % Change
G2	37 / 38	28	3.8
	38 / 39	82	-42
	39 / 40	46	-5.8
G4	38 / 39	72	-25
	39 / 40	56	-47
	40 / 41	32	-40
G5	38 / 39	38	25
	39 / 40	76	-25
	40 / 41	40	-22
G6	38 / 39	36	28
	39 / 40	80	7.1
	40 / 41	36	-21
G7	38 / 39	76	-1.2
	39 / 40	50	-15
	40 / 41	28	-15
G8	20 / 21	44	25
	21 / 22	62	6.6
	22 / 23	38	13
G9	37 / 38	36	1.4
	38 / 39	84	-14
	39 / 40	42	-7.0
G10	38 / 39	76	-18
	39 / 40	50	-36
	40 / 41	52	22
G11	38 / 39	86	-26
	39 / 40	56	-28
	40 / 41	30	-16

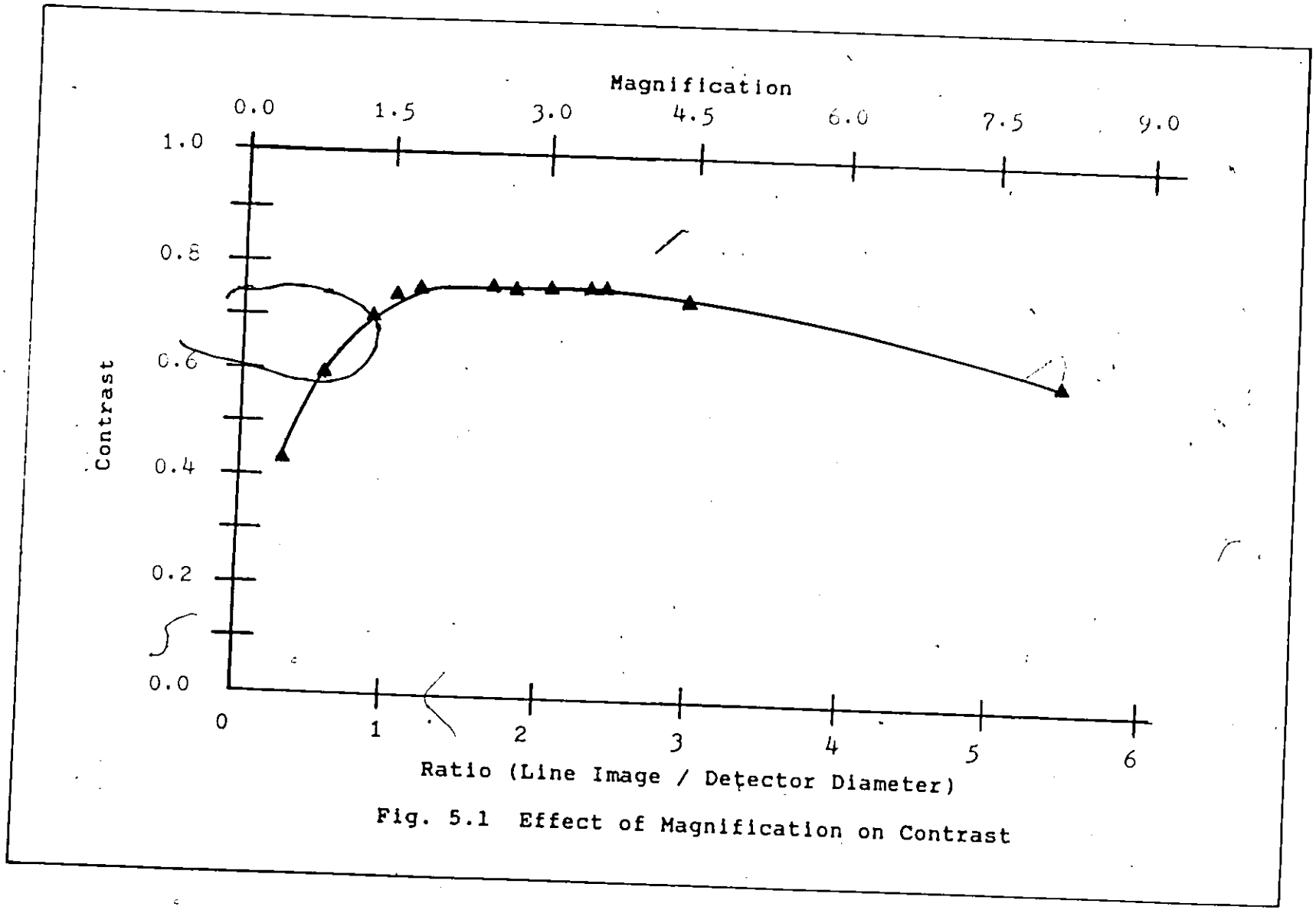

Fig. 5.1 Effect of Magnification on Contrast

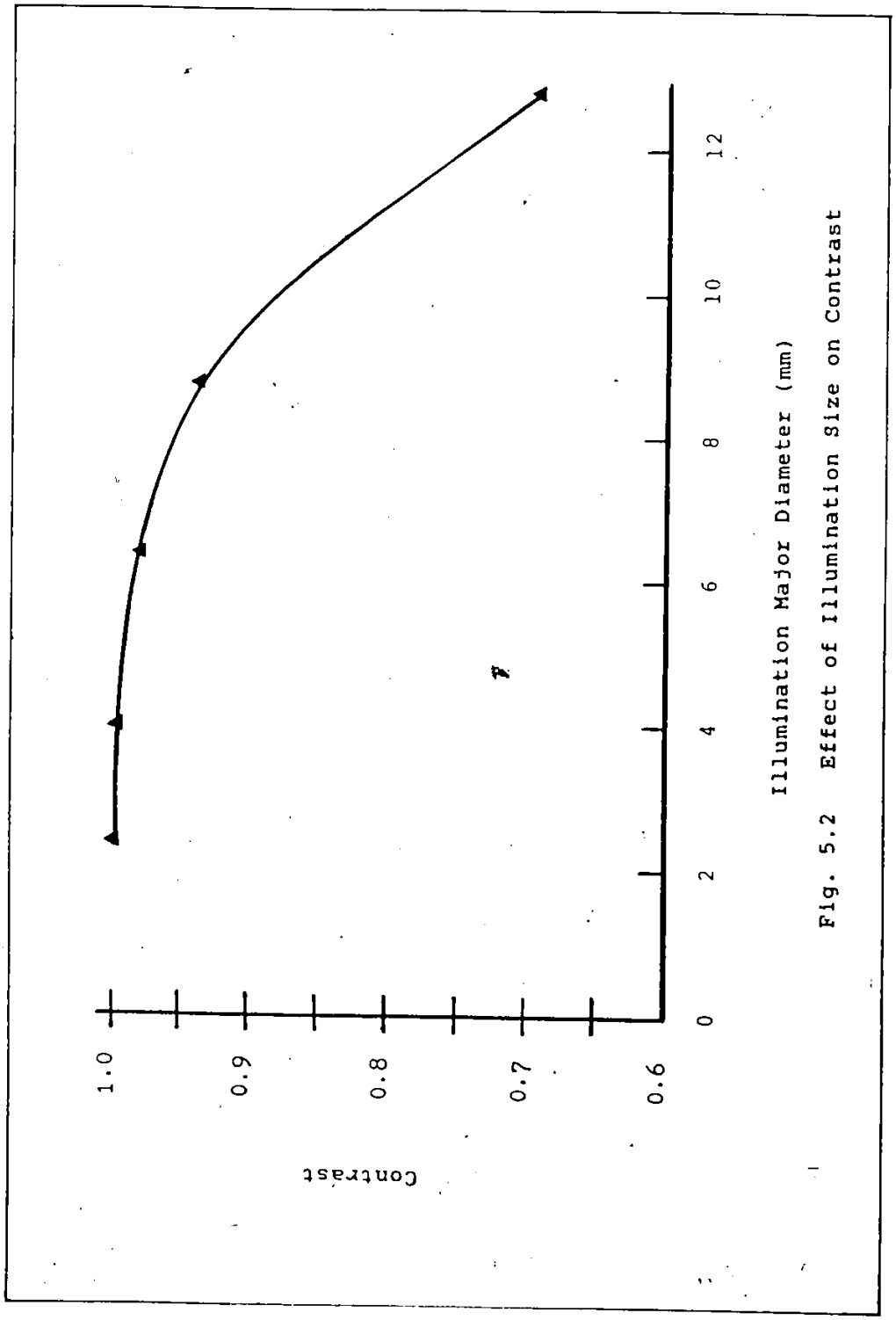

Fig. 5.2 Effect of Illumination Size on Contrast

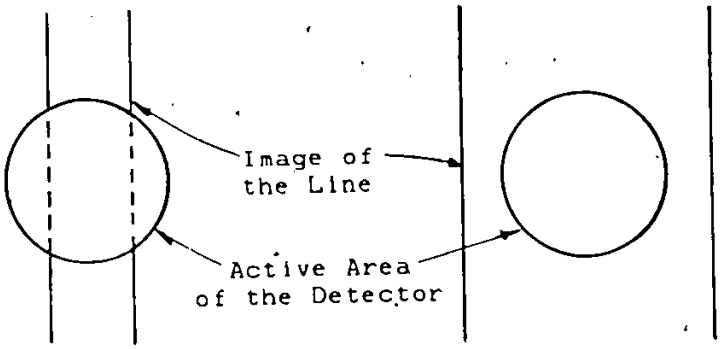

a) Poor Contrast Caused by Improper Magnification

b) Contrast Improved by Adequate Magnification

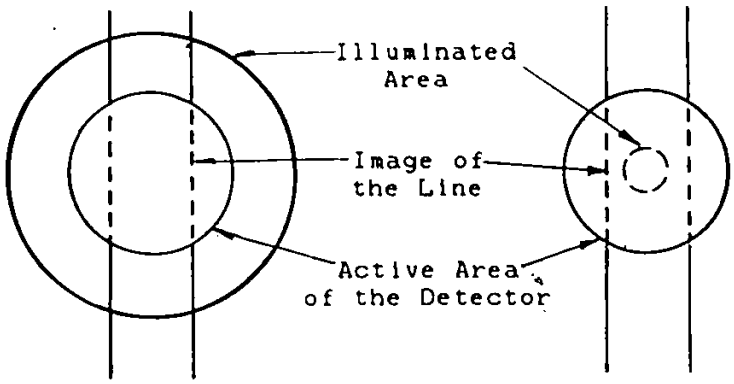

c) Poor Contrast Caused by Over Illumination

d) Contrast Improved by Proper Illumination

Fig. 5.3 Interrelationship of Magnification, Illumination size and Contrast

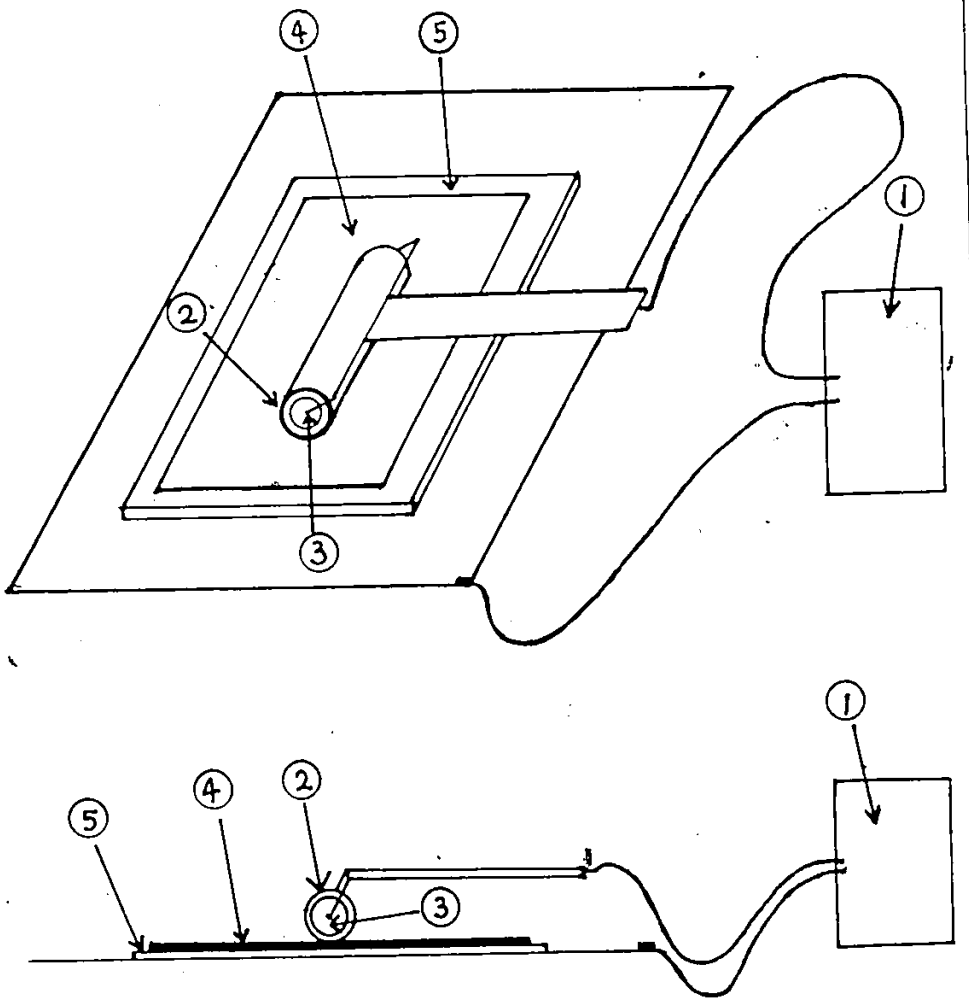

1	Power Supply
2	Thin Felt
3	Carbon Roller
4	Vinyl Mask
5	Steel Specimen

Fig. 5.4 Schematic Diagram of Electro-chemical Etching

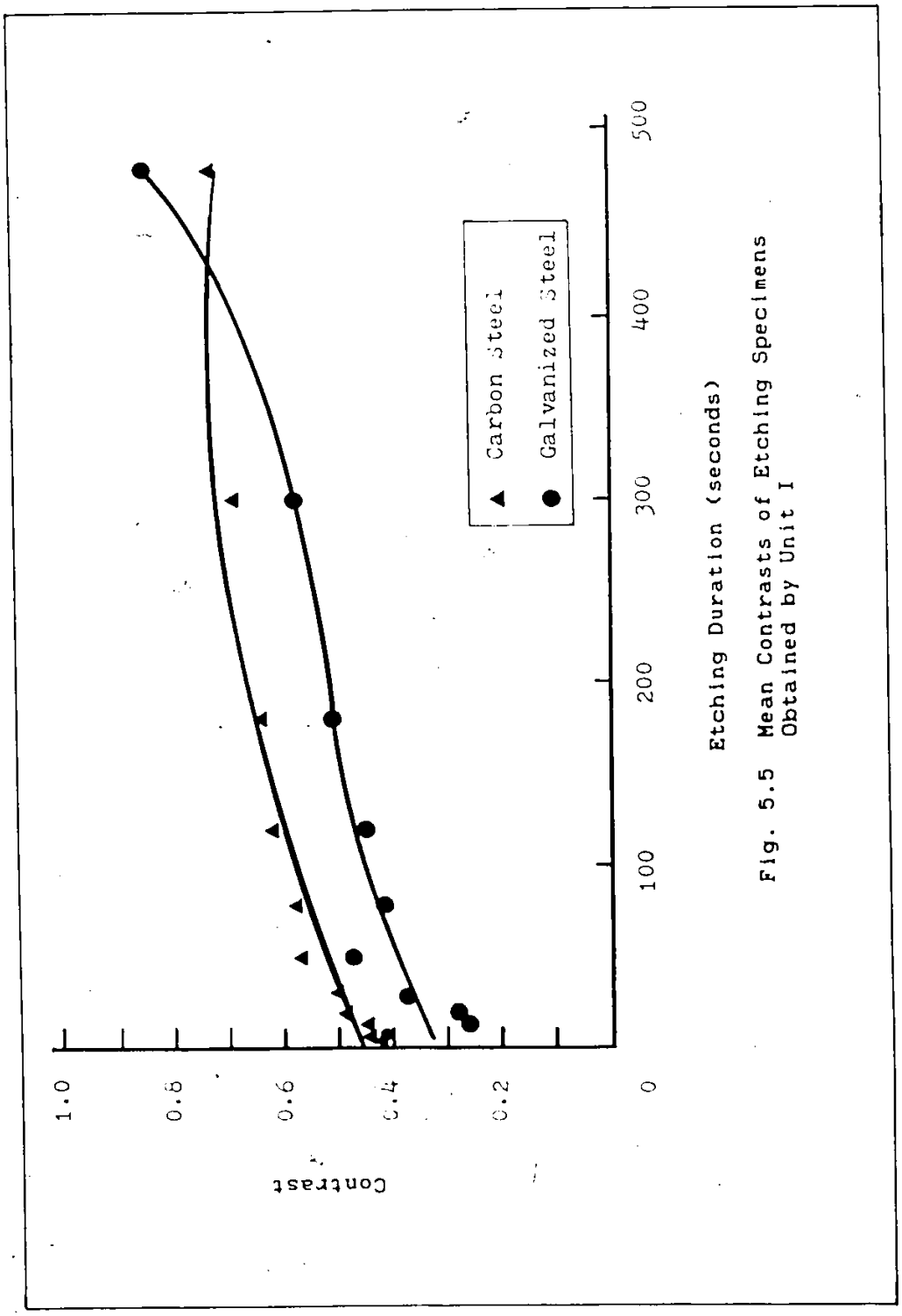

Fig. 5.5 Mean Contrasts of Etching Specimens Obtained by Unit I

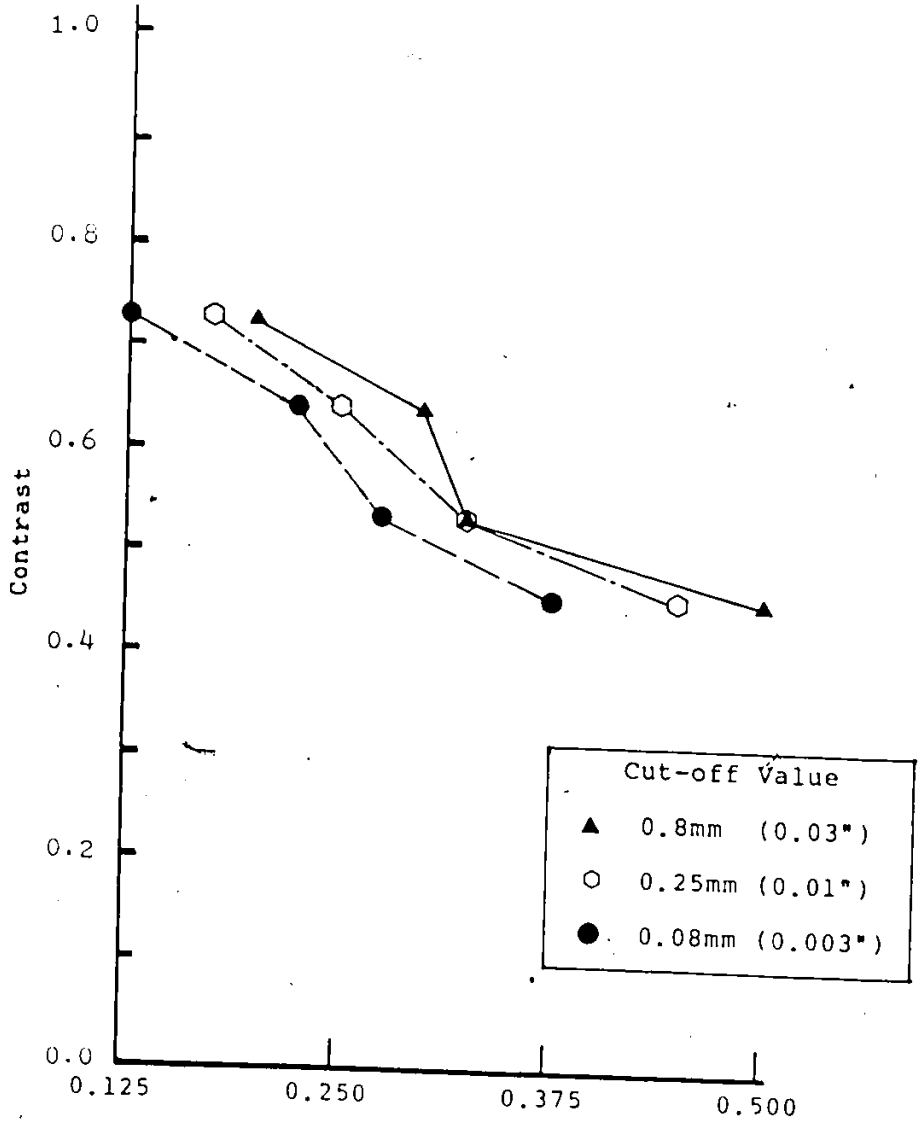

Fig. 5.6 Contrast of Surface Roughness Specimens

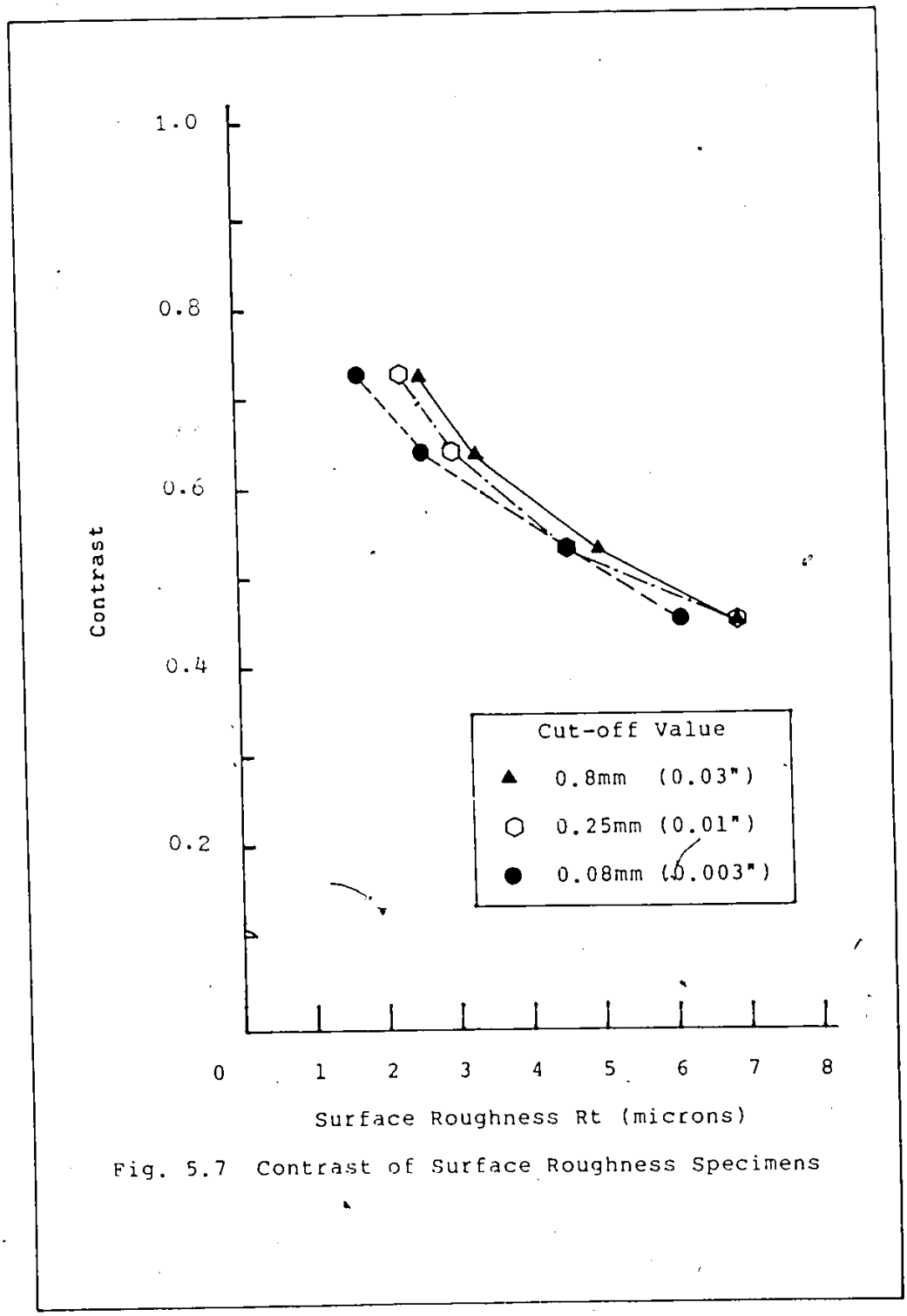

Fig. 5.7 Contrast of Surface Roughness Specimens

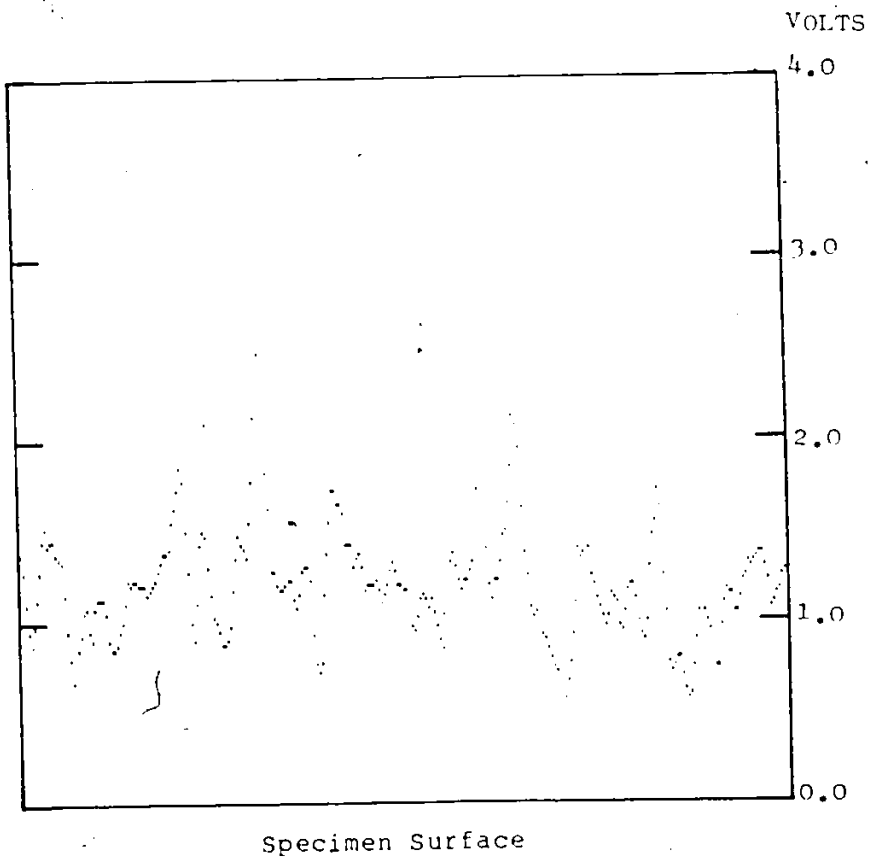

Fig. 5.8 Video Signals of Specimen G1
Obtained by Unit II
with Configuration II

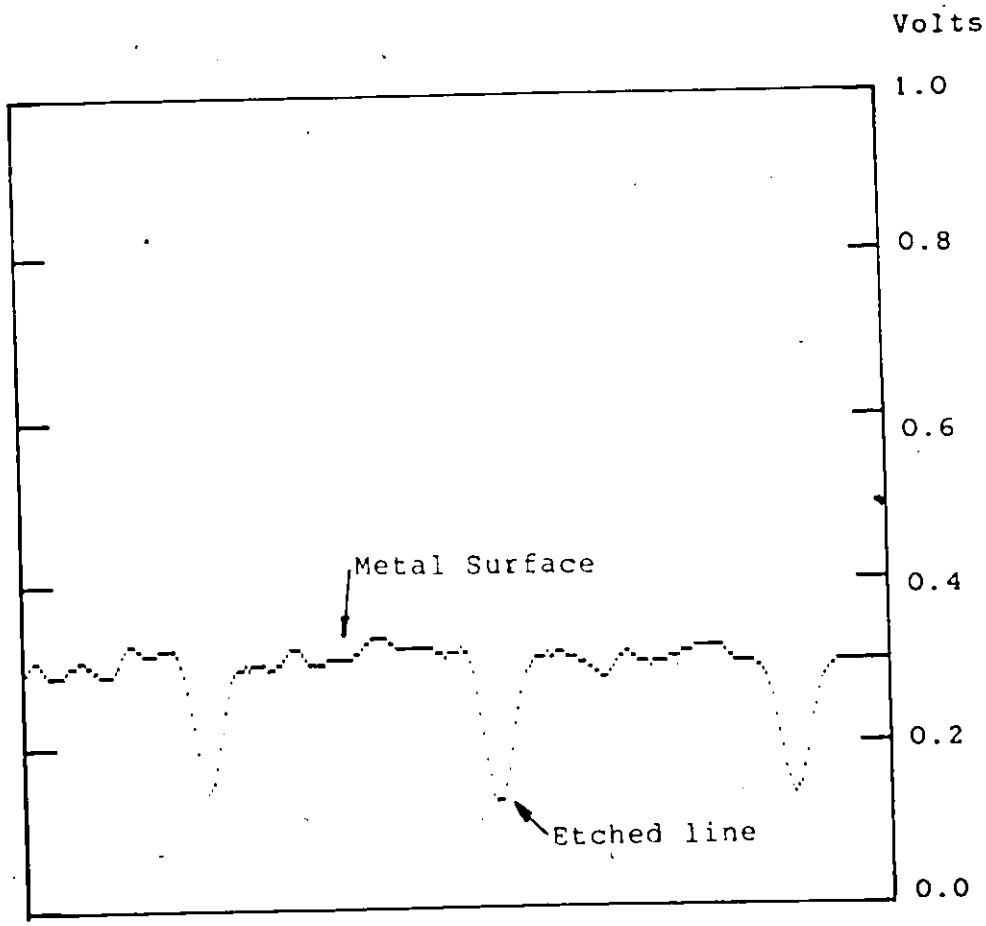

Fig. 5.9 Video Signals of Specimen G1 Obtained by Unit II. with Configuration I

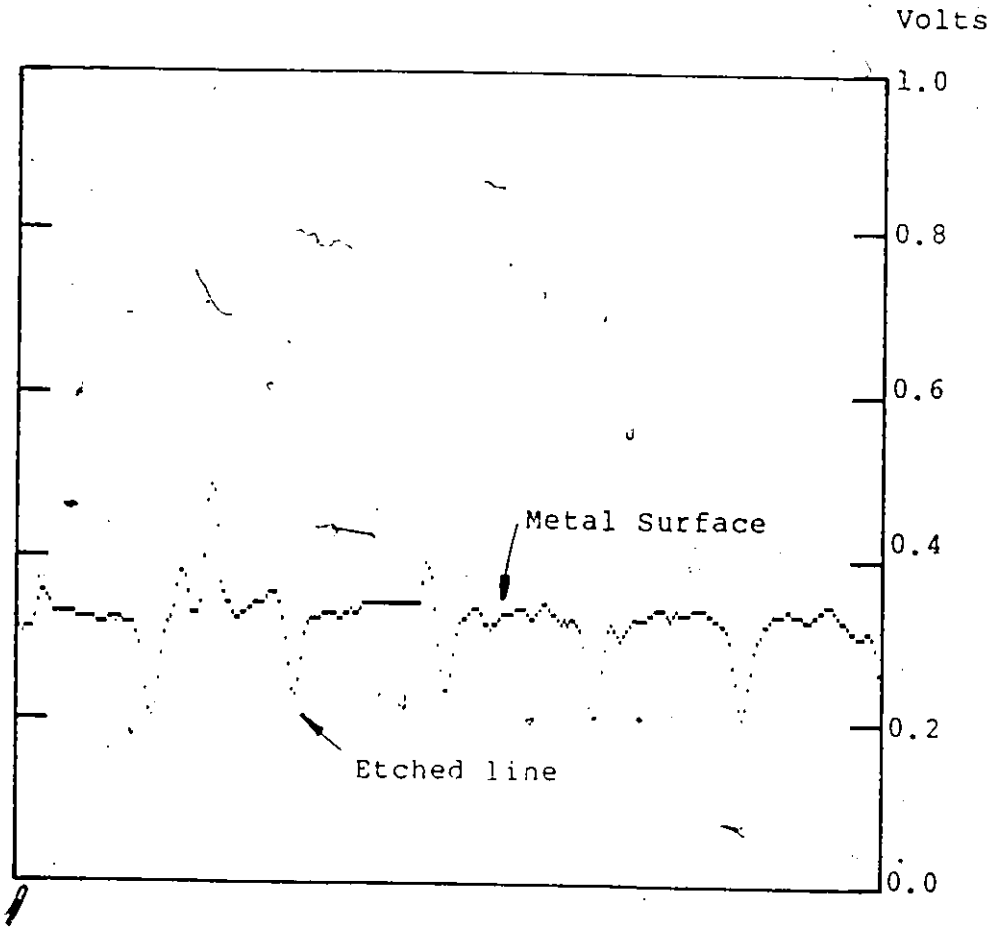

Fig. 5.10 Video Signals of Specimen G1
Obtained by Unit II
with Configuration III

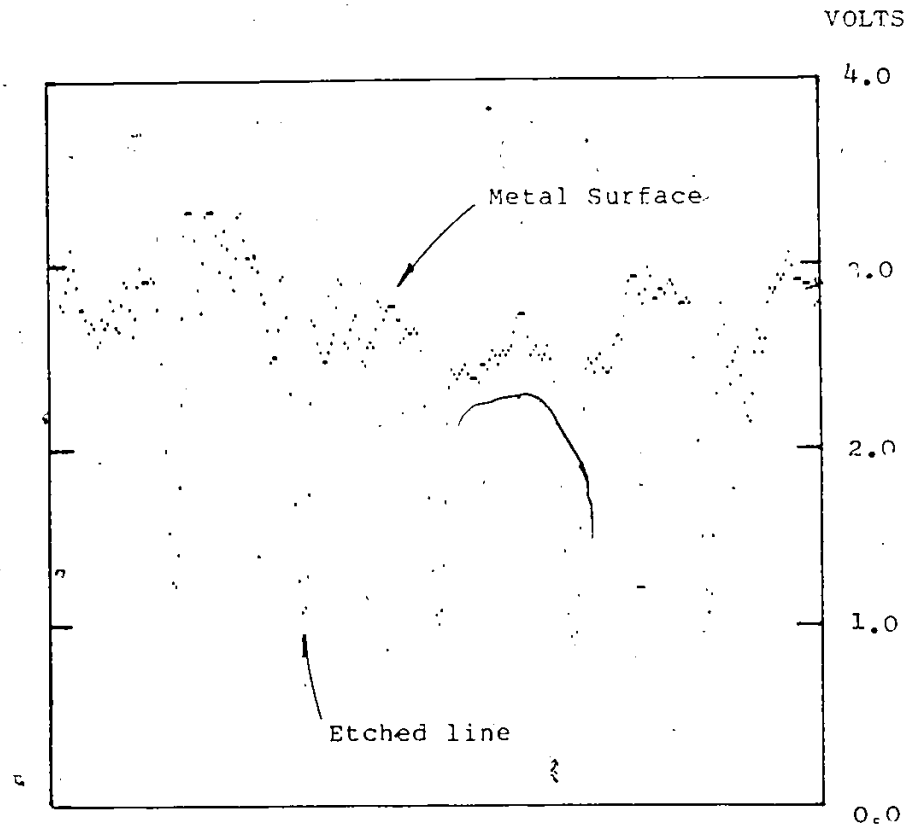

Fig. 5.11 Video Signals of Specimen C8
Obtained by Unit II
with Configuration II

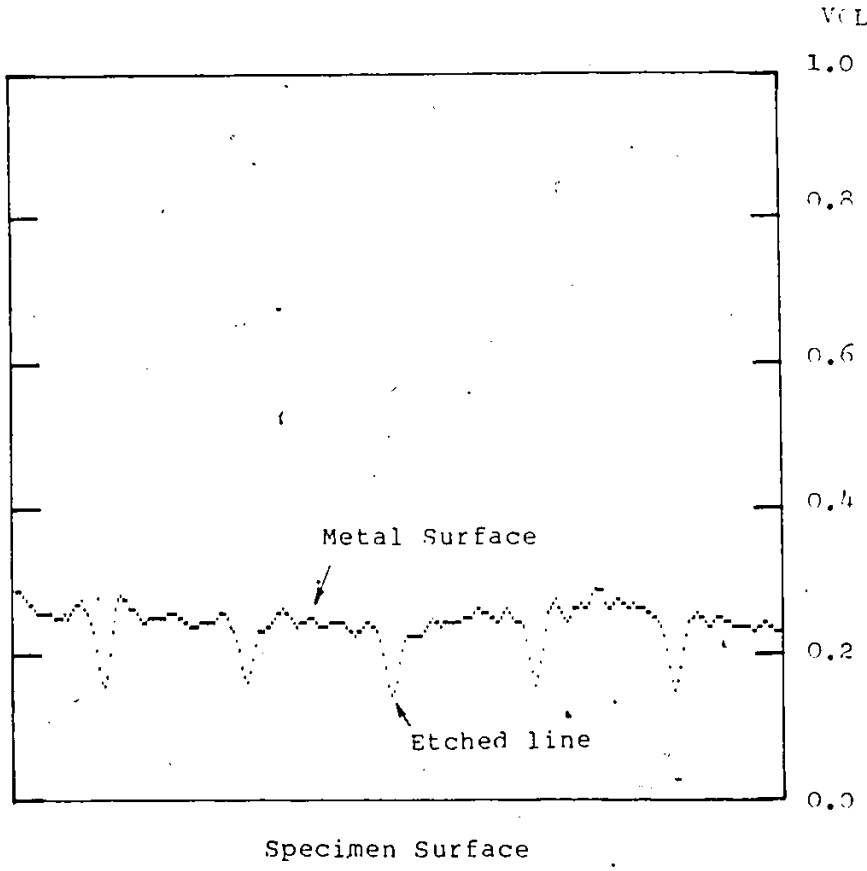

Fig. 5.12 Video Signals of Specimen C8 Obtained by Unit II with Configuration III

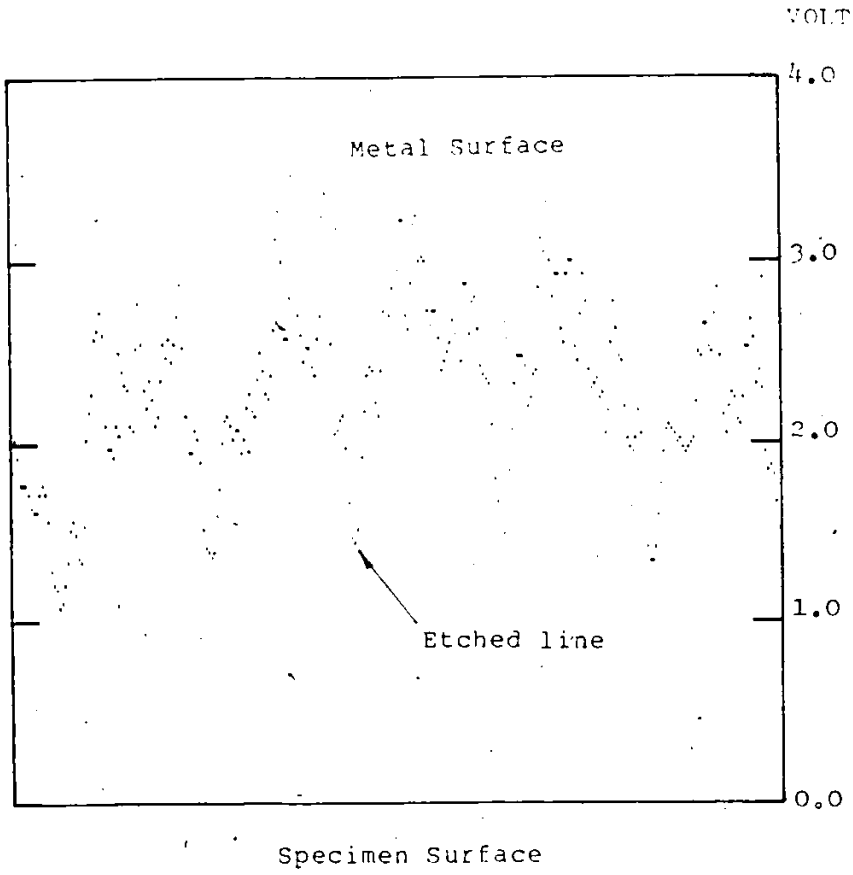

Fig. 5.13 Video Signals of Specimen G8
Obtained by Unit II
with Configuration II

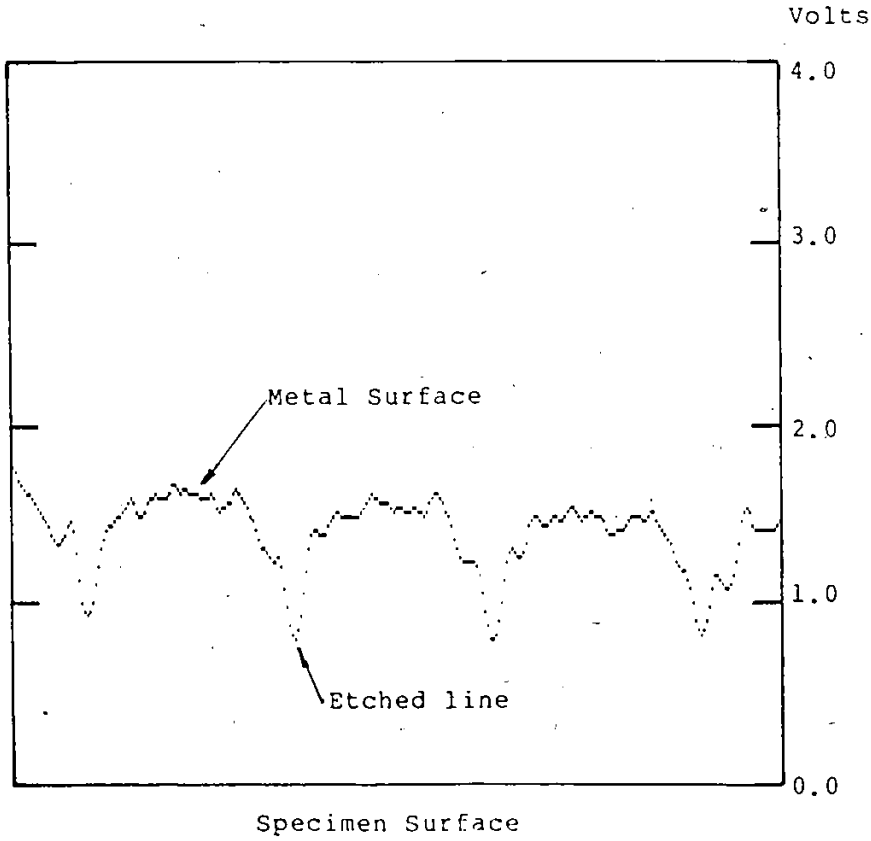

Fig. 5.14 Video Signals of Specimen G8
Obtained by Unit II
with Configuration I

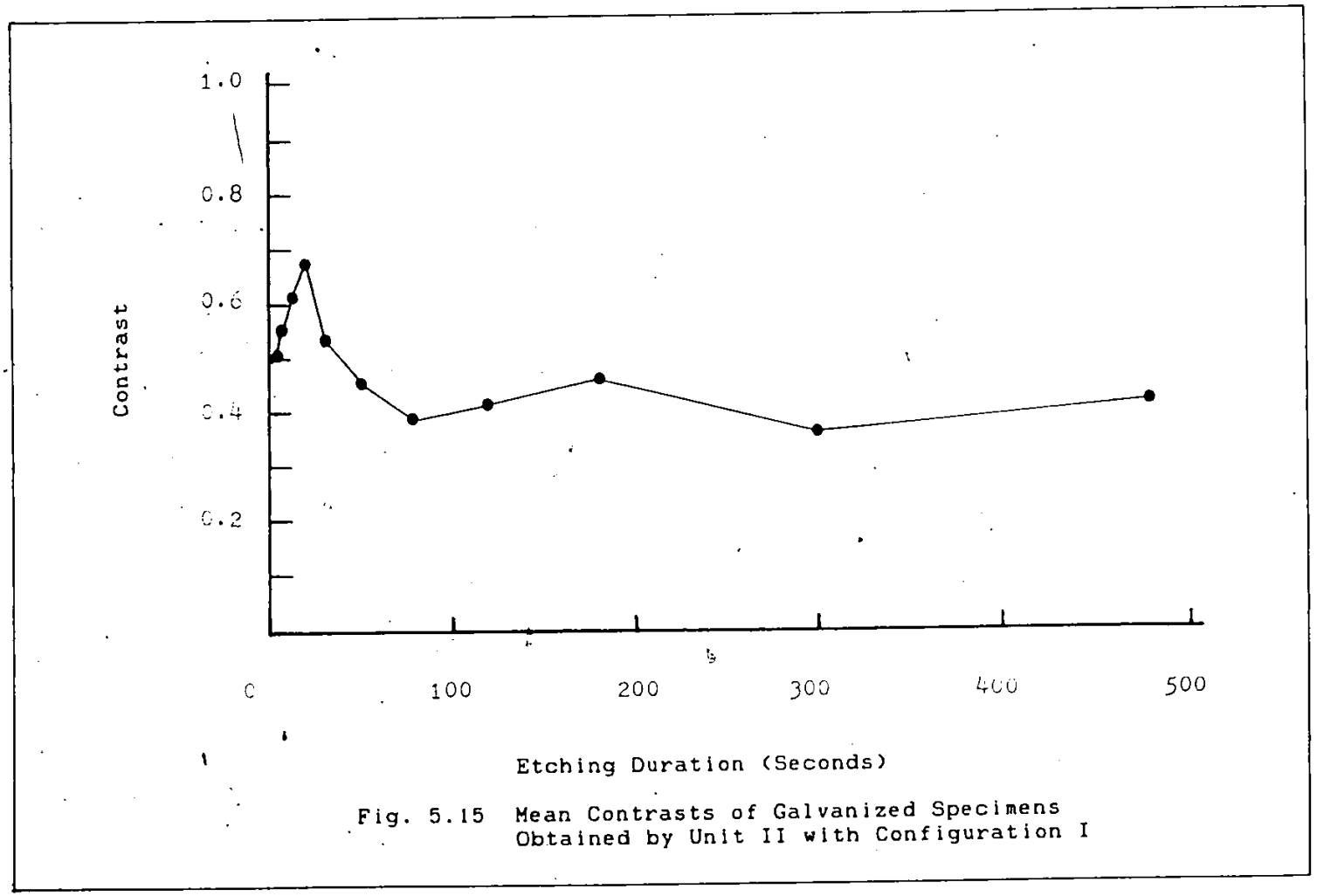

Fig. 5.15 Mean Contrasts of Galvanized Specimens Obtained by Unit II with Configuration I

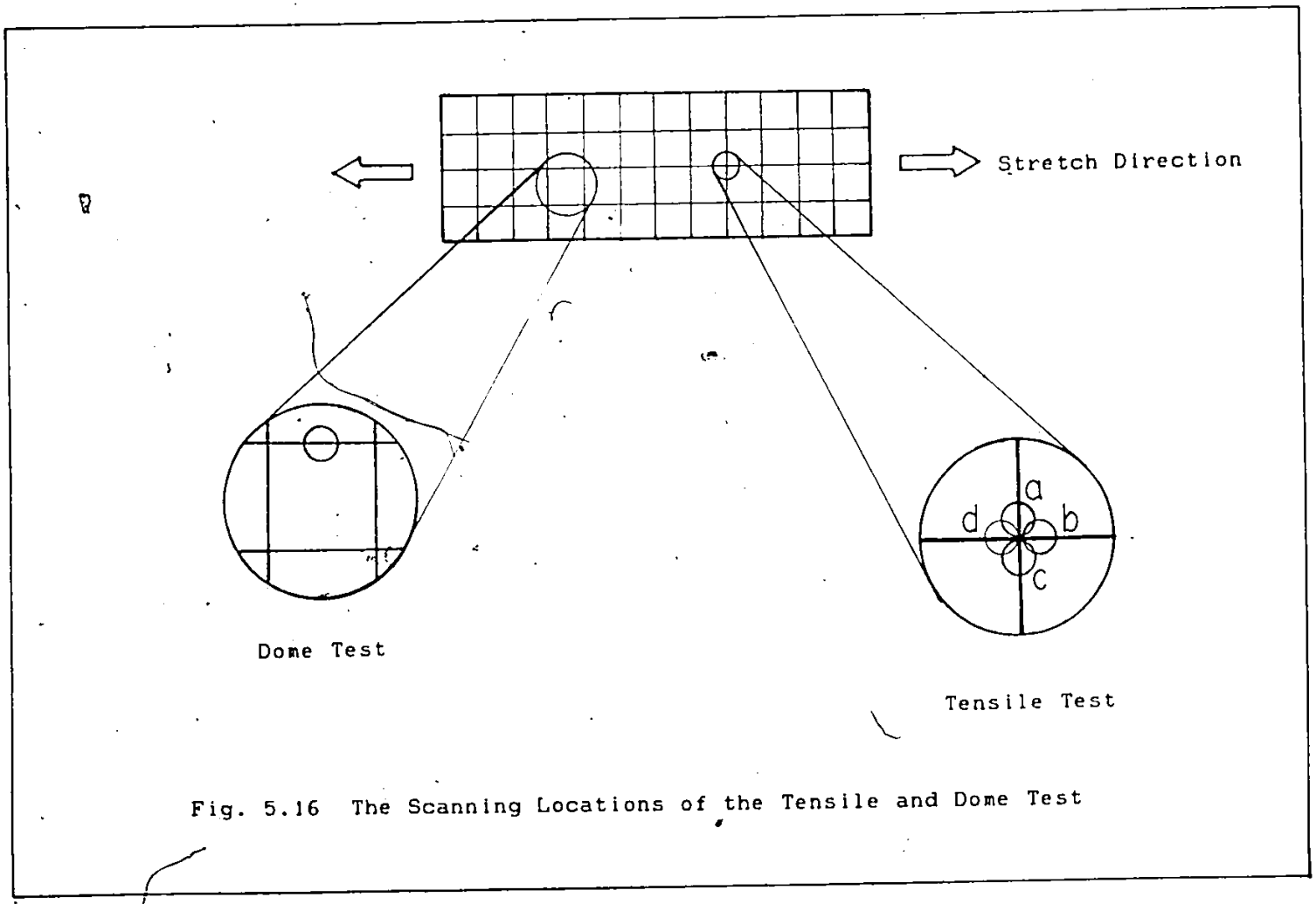

Fig. 5.16 The Scanning Locations of the Tensile and Dome Test

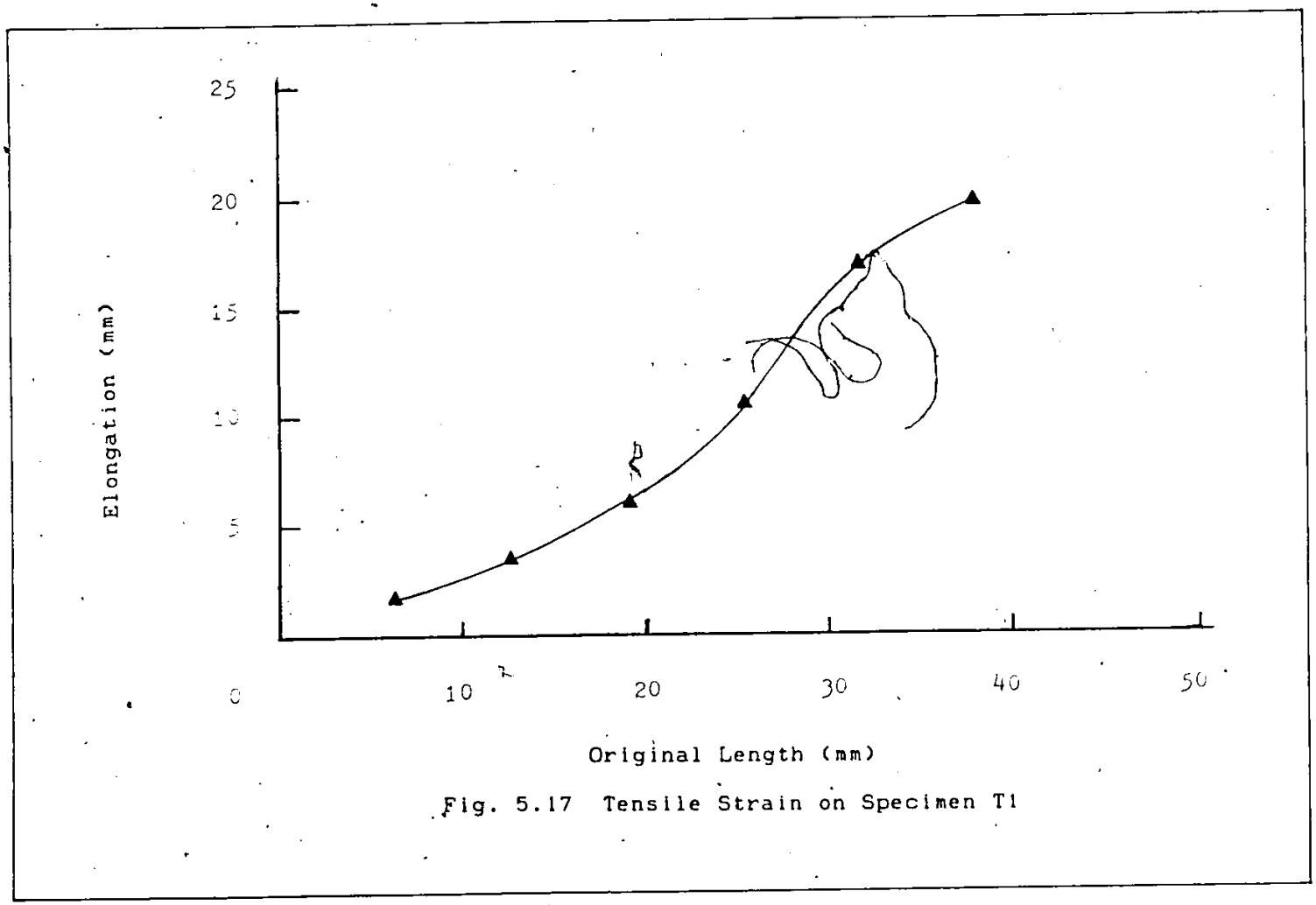

Fig. 5.17 Tensile Strain on Specimen T1

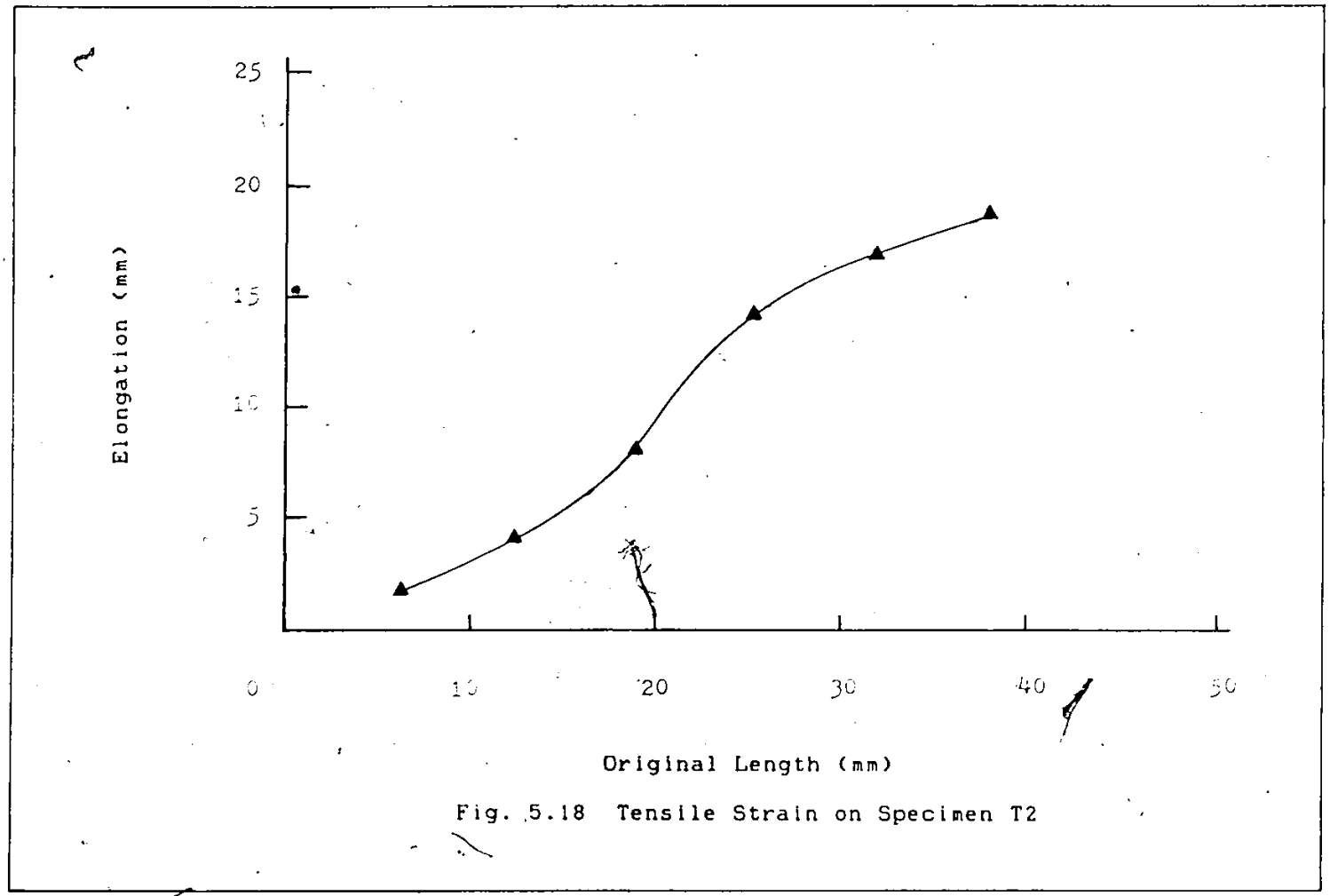

Fig. 5.18 Tensile Strain on Specimen T2

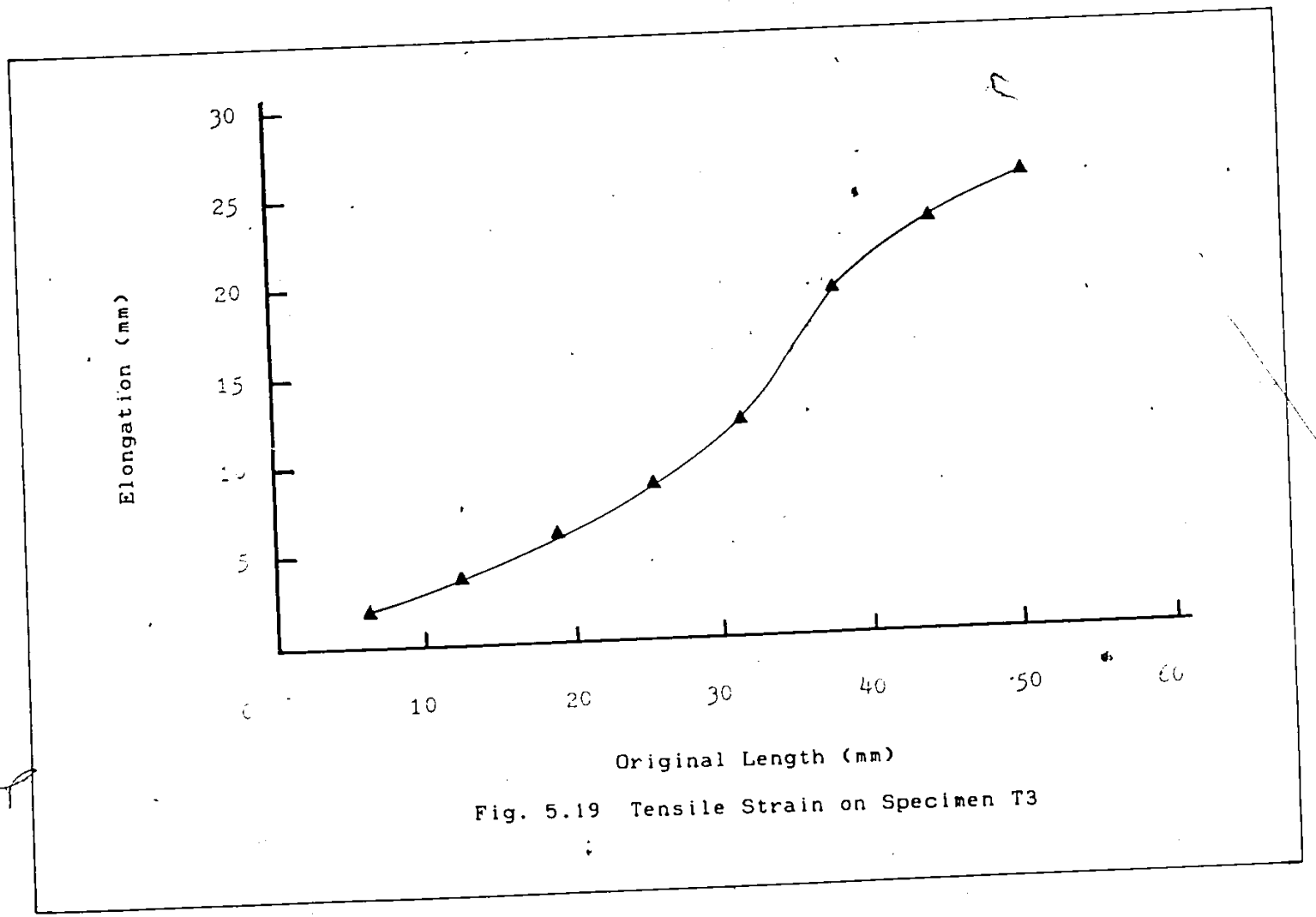

Fig. 5.19 Tensile Strain on Specimen T3

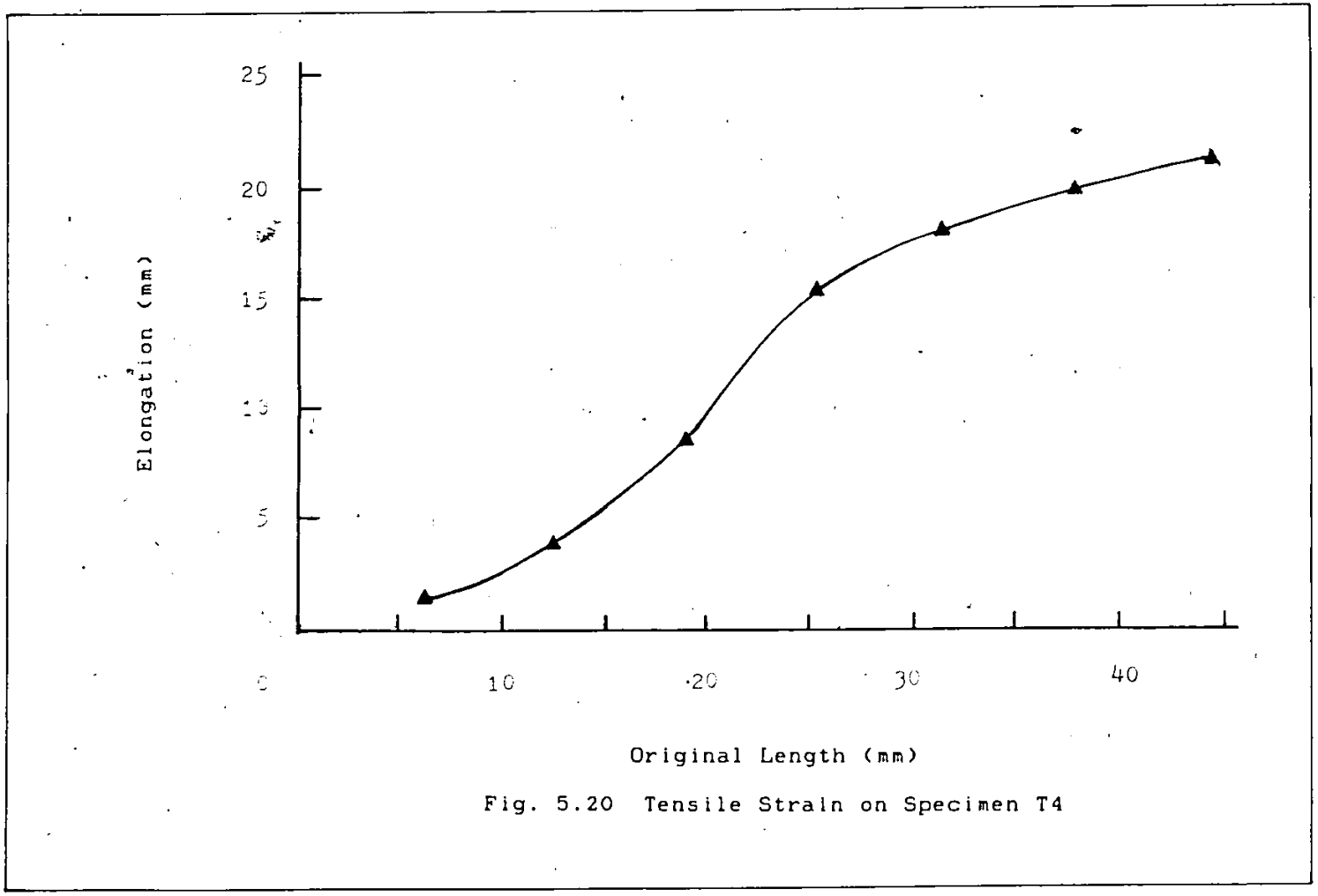

Fig. 5.20 Tensile Strain on Specimen T4

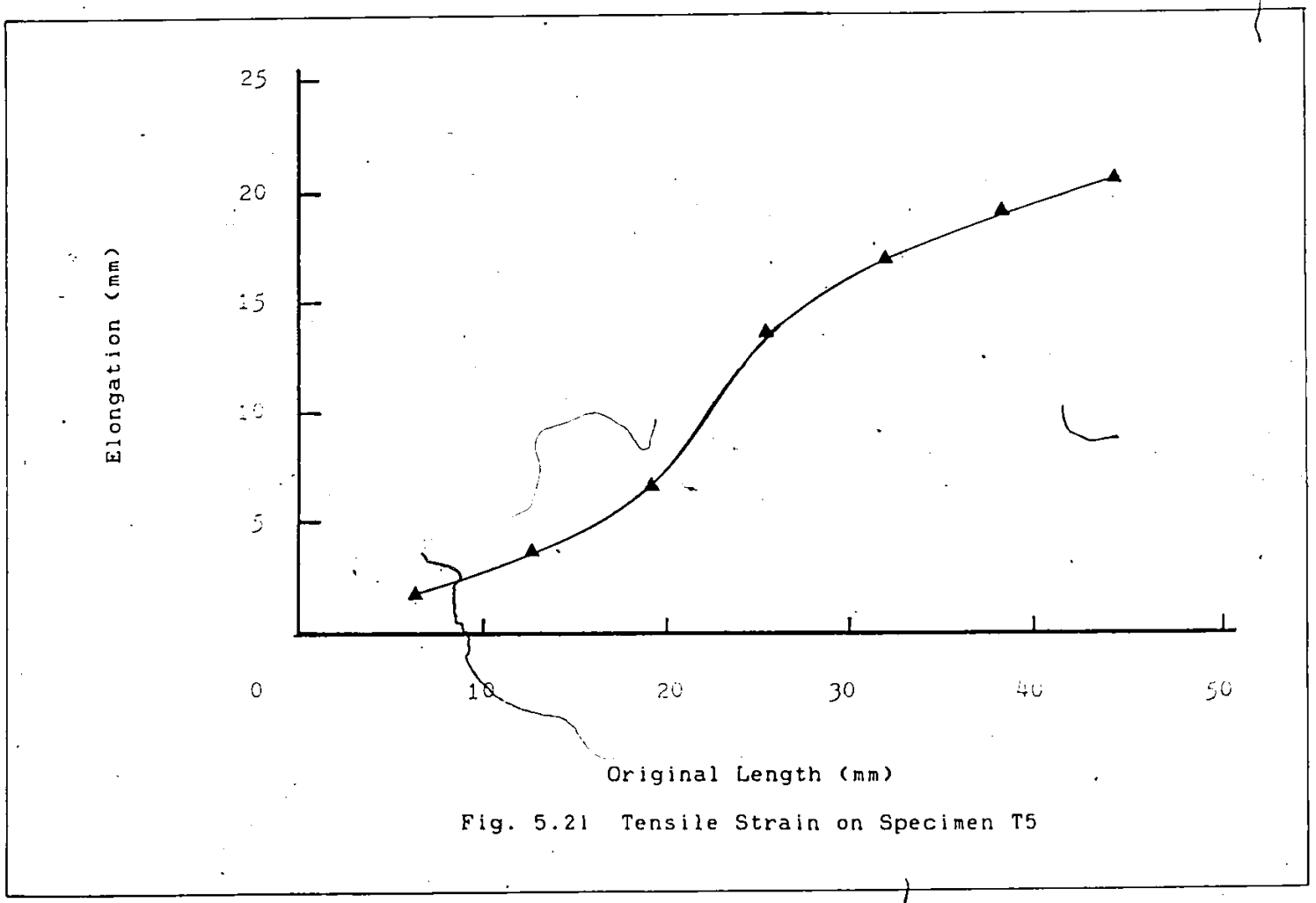

Fig. 5.21 Tensile Strain on Specimen T5

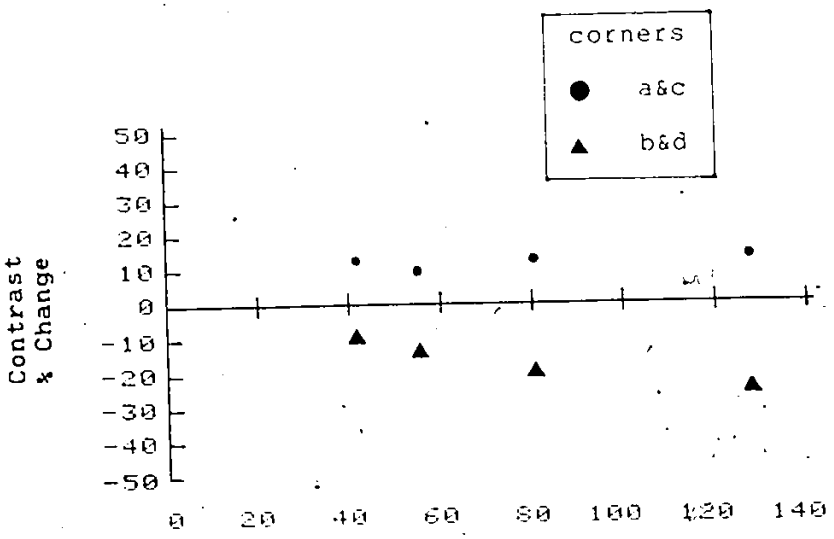

Fig. 5.22 T1 Contrast Changes Under Tensile Strain

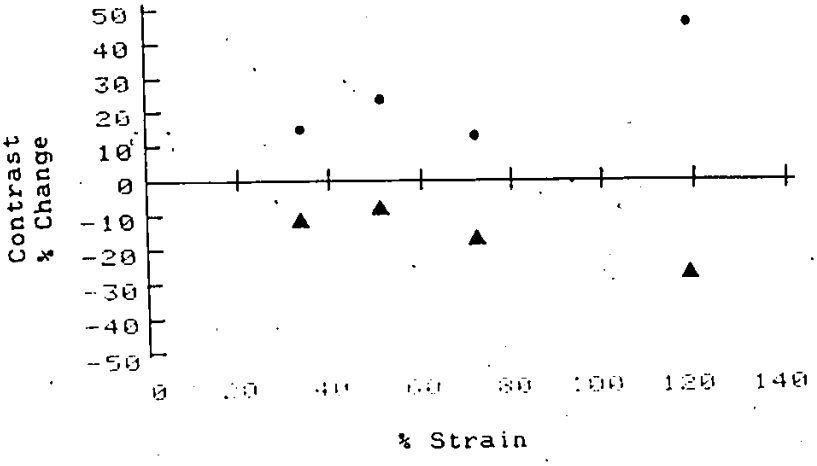

Fig. 5.23 T2 Contrast Changes Under Tensile Strain

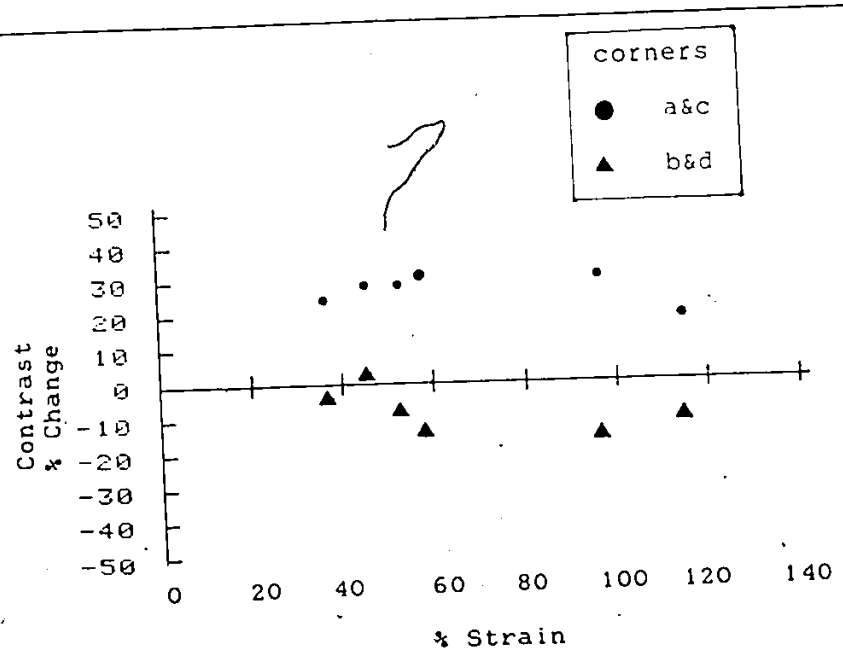

Fig. 5.24 T3 Contrast Changes Under Tensile Strain

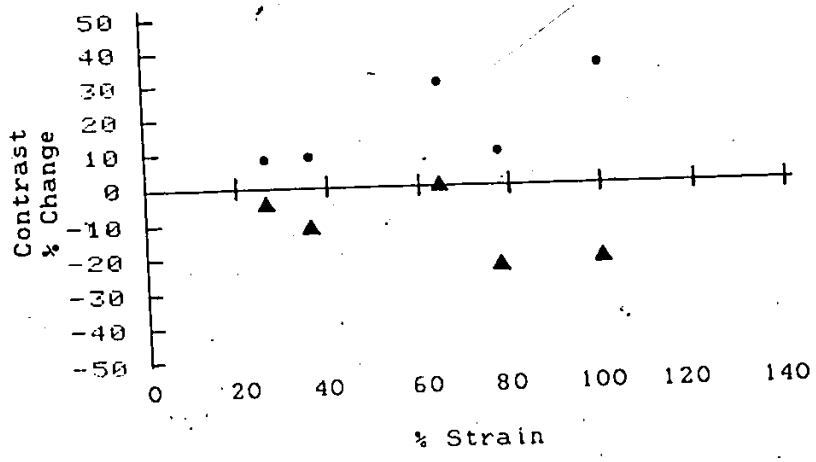

Fig. 5.25 T4 Contrast Changes Under Tensile Strain

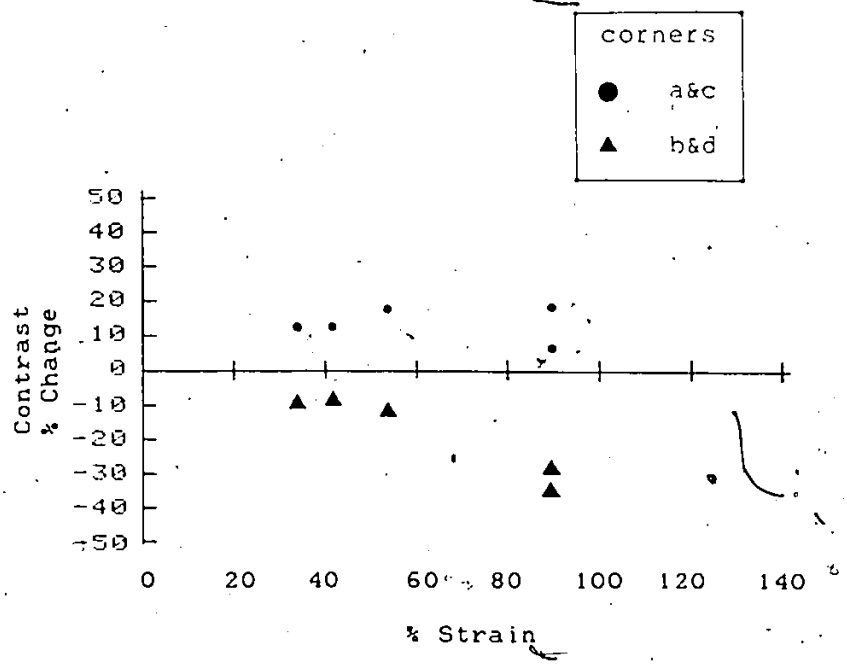

Fig. 5.26 T5 Contrast Changes Under Tensile Strain

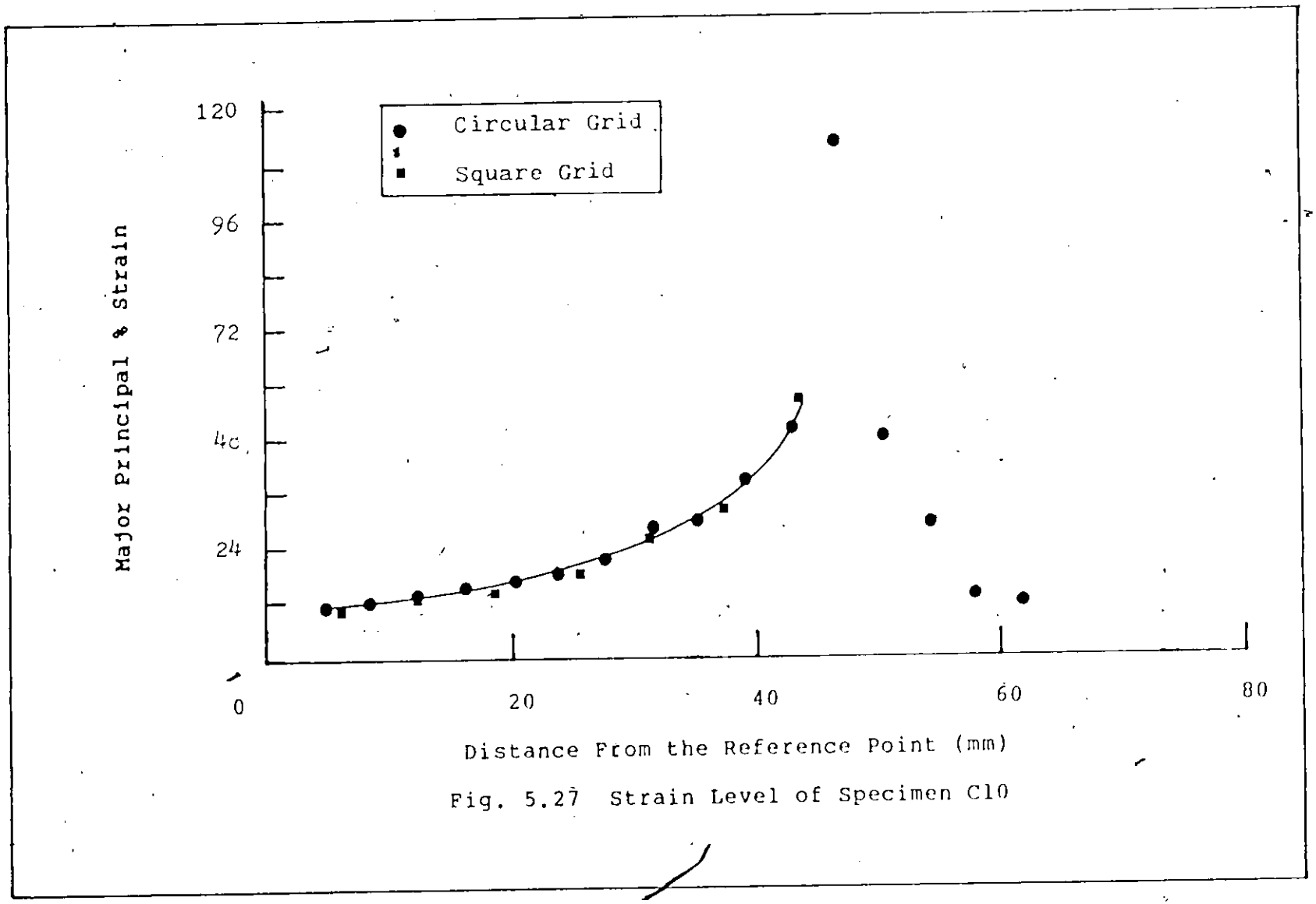

Fig. 5.27 Strain Level of Specimen C10

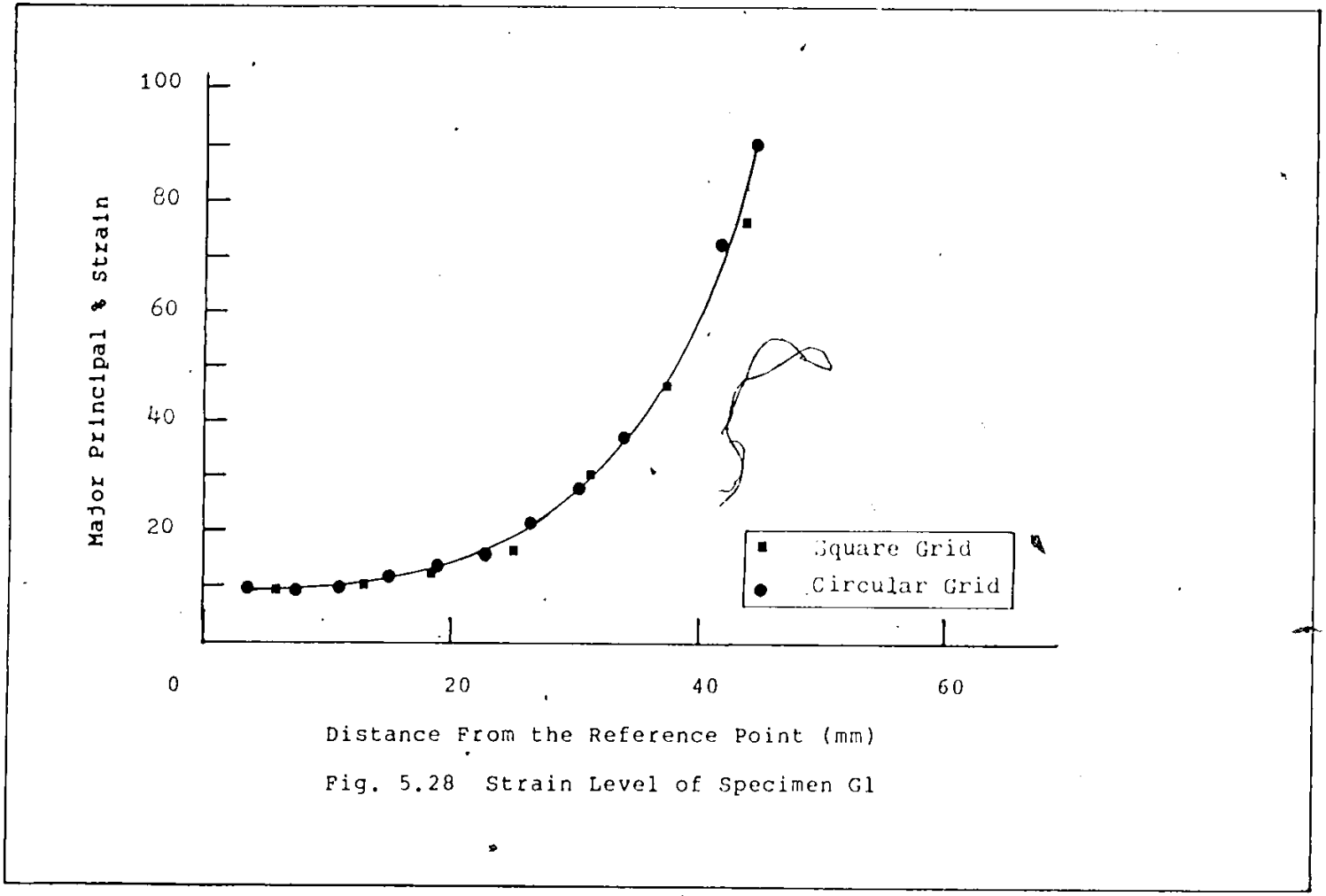

Fig. 5.28 Strain Level of Specimen G1

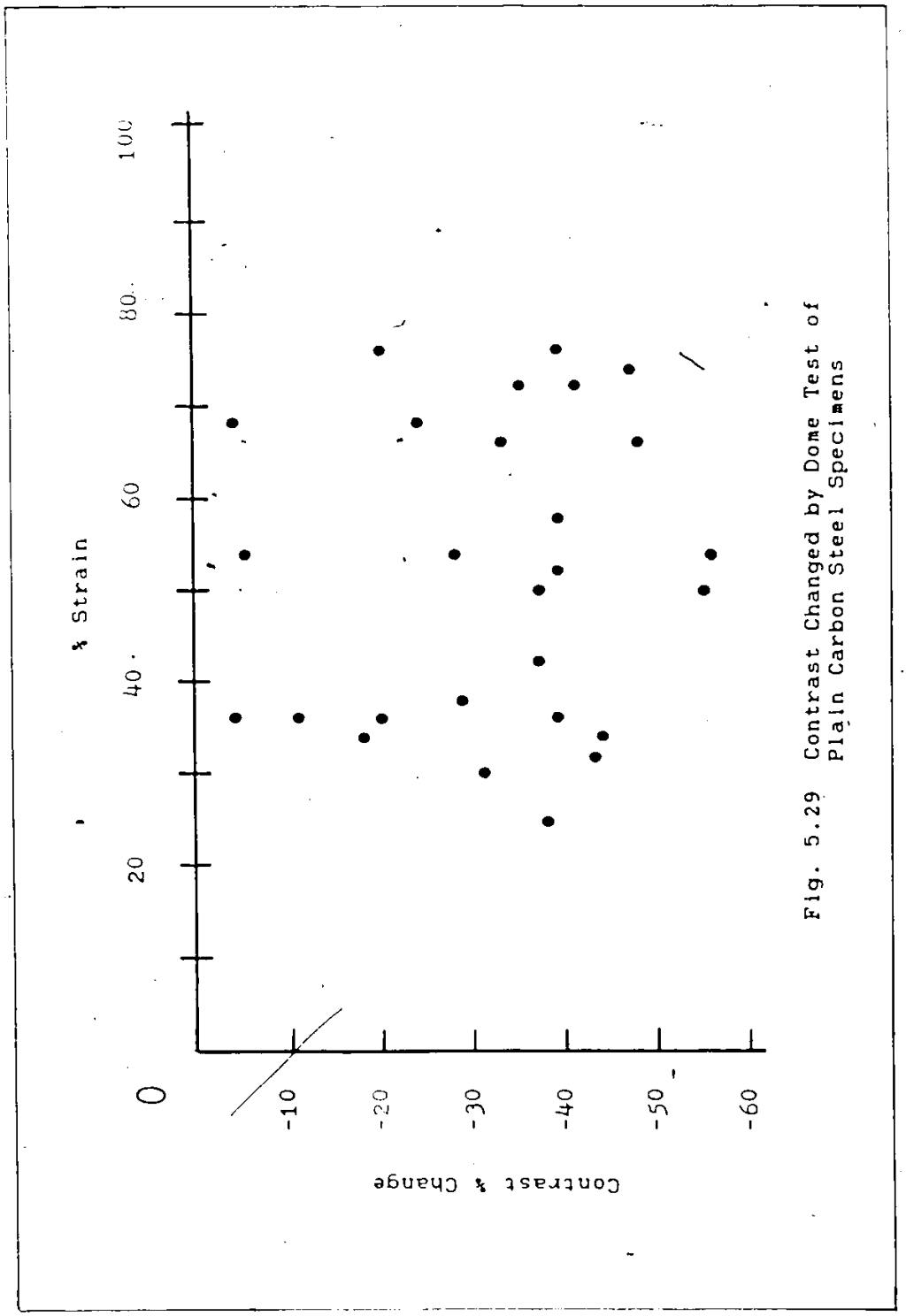

Fig. 5.29 Contrast Changed by Dome Test of Plain Carbon Steel Specimens

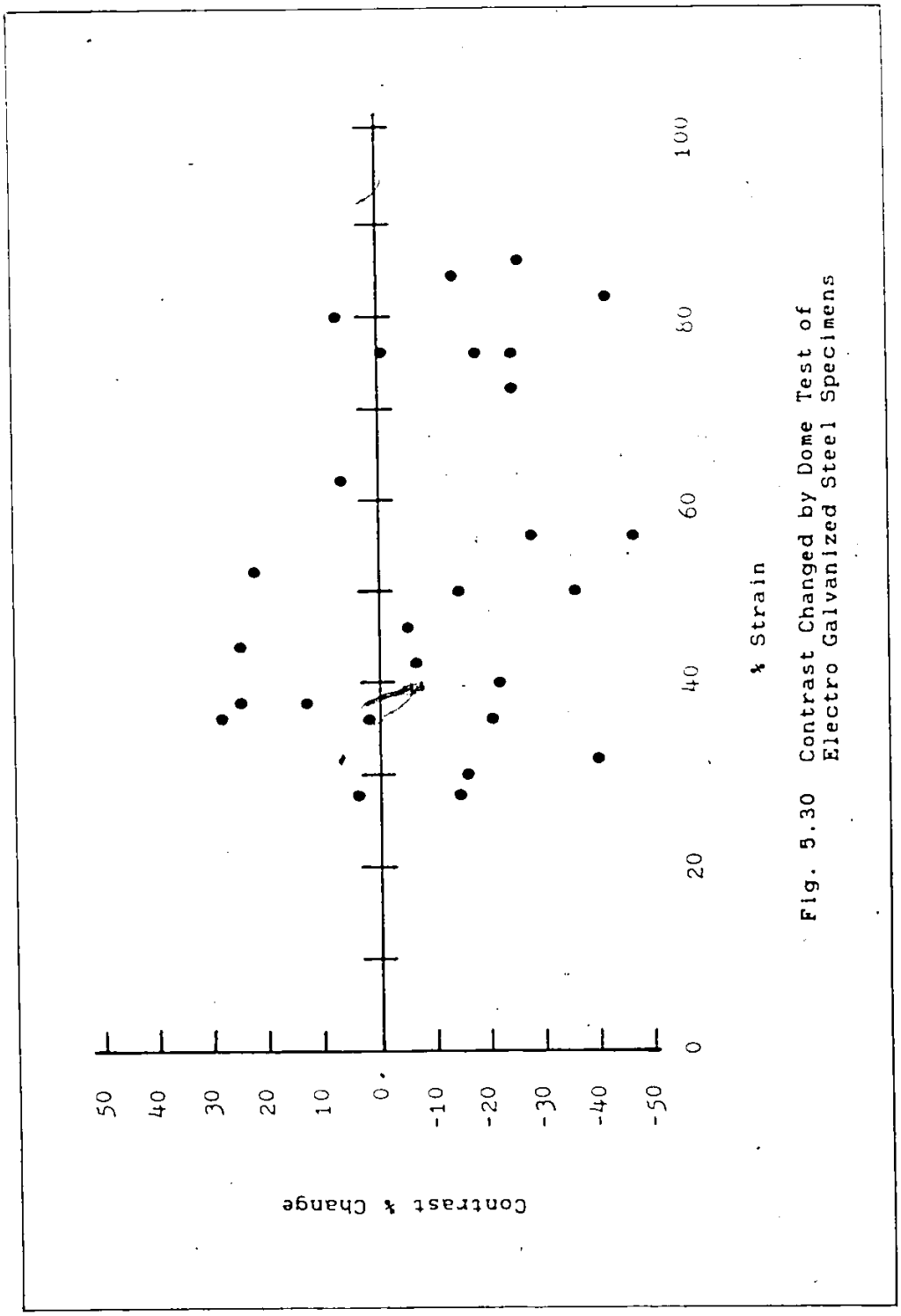

Fig. 5.30 Contrast Changed by Dome Test of Electro Galvanized Steel Specimens

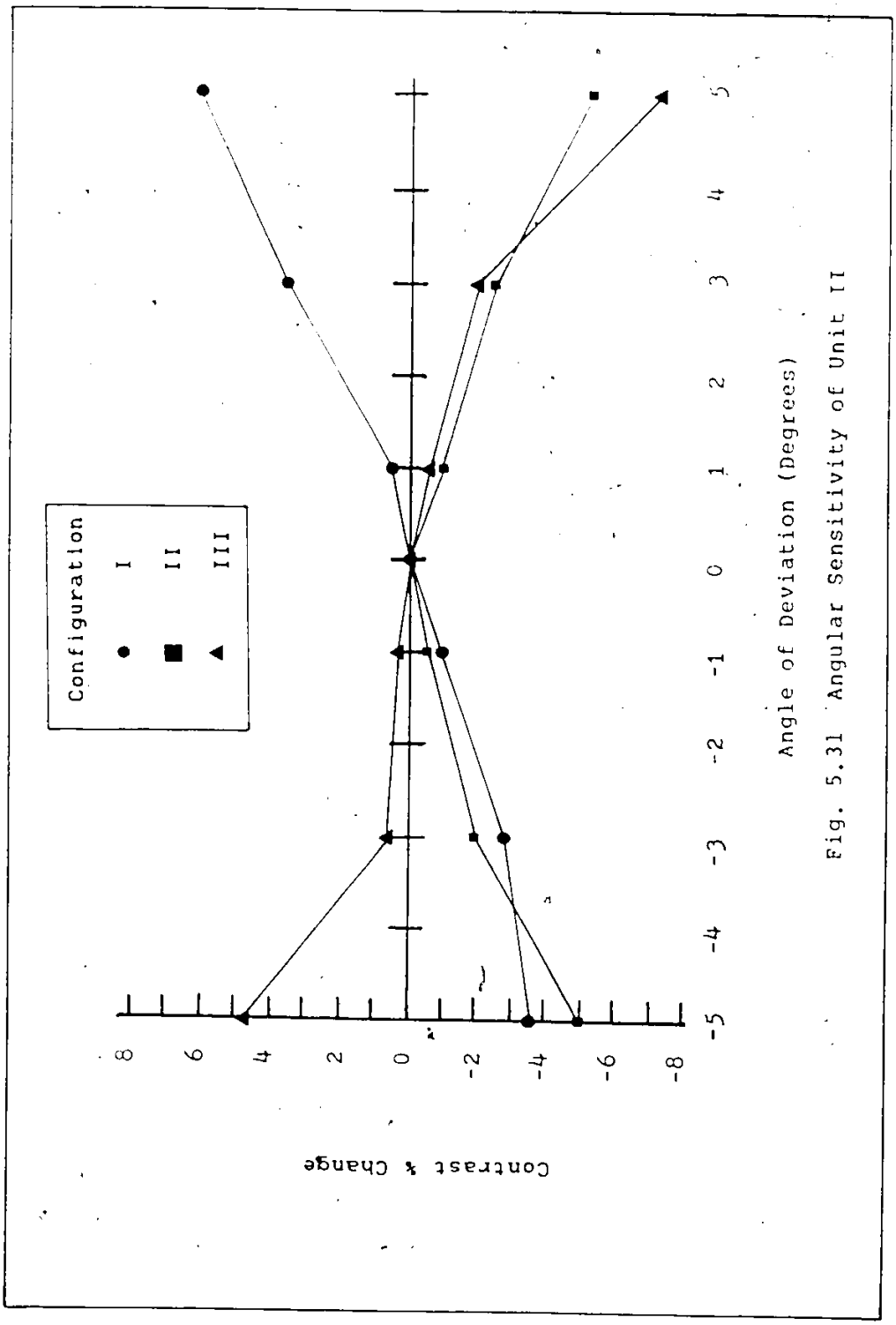

Fig. 5.31 Angular Sensitivity of Unit II

CHAPTER VI

EXPERIMENTAL PROCEDURES, RESULTS AND DISCUSSION OF SURFACE ROUGHNESS MEASUREMENT

The specimens used in this part of the study were prepared in the university's Central Research Shop by surface grinding operations. The materials under investigation were tool steel, stainless steel, copper, brass and aluminum. The chemical composition and mechanical properties of these materials are listed in Appendix C. The various roughnesses were produced by the combination of different grades of grinding wheel and feed rates.

6.1 Direction of Incident Light Path

Observations of the light scattered pattern were made by shining a He-Ne laser on a copper surface roughness sample with the light path direction first perpendicular and then parallel to the lay. The light scattered regardless the light path directions. However, each light path formed a distinct light scattering pattern and these patterns are depicted in Figure 6.1.

In order to decide which light pattern should be used in this study, the measurement of the intensity ratio of the two light paths were made. Figure 6.2 shows the schematic diagram of

the experimental set-up. A white light was used to illuminate the roughness surface. Two detectors, detector 1 at the specular angle (45 degrees) and detector 2 at the normal angle, were used to pick up the reflected specular and scattered light respectively. The intensity ratio was calculated by dividing the output voltage of the detector 2 by the output voltage of detector 1. The results are shown in Figure 6.3. The variation of the intensity ratio was much higher when the light path direction was perpendicular to the lay. This result suggested that the light path of the incident light for the surface roughness measurement should be in the direction of perpendicular to the lay of the machine marks.

6.2 Polarization Test

This test was used to determine the correlation between surface roughness and the polarization. The white light from the light source passed through a polarizing filter at an arbitrary angle before it reached the roughness sample with a incident angle of 45 degrees. The specular reflected light passed through a second polarizing filter and then to the detector. The second polarizing filter was rotated to obtain the maximum and minimum output voltage from the detector. Table 6.1 lists these results. The Vmax./Vmin. ratio did not correlate to the surface roughness and the surface roughness did not alter polarization.

6.3 Surface Roughness Measurement by Profilometer

The mechanical surface roughness (Ra) of all specimens were measured by a Mitutoyo Surftest III profilometer. The set-up and calibration procedures are listed in the operation manual [5]. Specimens were cleaned with soft paper in order to keep them free from oil, dust and dirt and then the Ra measurements were taken. The cut-off value was 0.8mm (0.03") or as specified otherwise and the damper was ON. The diamond stylus traveled 7mm (0.28") at the speed of 2mm (0.08") per second. The results of the measurement are listed in Table 6.2.

6.4 Cut-off Value of the Profilometer

The Ra reading of the sample would be changed by selecting other cut-off values. The recommended [5] cut-off values for a ground surface are 0.25mm (0.01"), 0.8mm (0.03") and 2.5mm (0.10"). To examine the effect of the cut-off values, selected copper samples were measured with four different cut-off values, and then compared to the respective intensity ratios by the set-up shown in Figure 6.2. The test results, which are shown in Figure 6.4, matched the Surface Roughness Test in Chapter V Section 5.4. The smaller the cut-off ratio, the more the intensity ratio curve shifted to the left. A cut-off value of 0.8mm (0.03") was selected as the standard of this study.

6.5 Incident Angle Test

From the literature survey, the existing optical methods

are valid only in a small range of surface roughness (Ra < 0.5 microns). In this test, four incident angles were examined on five types of metallic surface for the valid range of the surface roughness measurement. The selected incident angles in this study were 60, 70, 80 and 85 degrees. The materials under test were aluminum, brass, copper, stainless steel and tool steel. There was no additional cleaning on the sample surfaces after the mechanical surface roughnesses were taken.

The experimental set-up, shown in Figure 6.5, had a lens and two detectors placed on a semi-circle of 152mm (6") radius centered at the measuring point. The focal length of the lens was also 152mm (6"), and the function of this lens was to focus the white light from the Carley Lamp on to the sample surface. Detector 1 measured the specular reflection from the sample surface. Detector 2, measured the scattered light at an angle of 45 degrees from the specimen surface. The angular position of the detector 2 was fixed and the angular position of the lens and detector 1 varied with the incident light angle. The output voltage from detector 1 and 2 is designated as D1 and D2 respectively an the intensity ratio as D2 / D1.

During the test, the white light was focused on the spot which was measured by the profilometer. The illumination footprint of the white light on the surface is depicted on Figure 6.6. Table 6.3 lists the resulting intensity ratios (IR). These IRs are considered the optical surface roughnesses of the tested samples.

Although the length of the roughness measurement by the profilometer was only 7mm (0.28"), the roughness varied along this length (see Table 6.2). In general, the rougher surfaces also had a larger roughness variation. A result is shown in figure 6.7. It shows the experimental results for tool steel and its best fit curve. The third order correlation curve was obtained by the least squares method which based on the data of the mean mechanical roughness of each sample tested and its corresponding intensity ratio. The rest of the correlation curves were obtained in the same manner and are listed in Table 6.4. Figure 6.8 to 6.16 show the best fit curve through the data points, but do not show the experimental data points which are listed in Tables 6.2 and 6.3.

The results indicate that each of the five tested materials has a unique correlation curve (Figures 6.13 to 6.16). An assumption was made that the uniqueness of these curves was caused by the surface hardness of the materials since the breaking off of the surface as the result of grinding is quite different from the soft copper to the hard tool steel. However, it was found that the pattern of these curves did not correlate with the corresponding surface hardness or any other mechanical properties which are listed in Appendix C.

The higher incident light angle increased the size of the illumination footprint and also the useful range of optical surface roughness measurements. For example, the test results on copper samples indicated that the valid range of this optical

method with the incident angle of 60 degrees was less than 0.5 microns (20 micro inches) Ra, and the valid range increased to 3 microns (120 micro inches) Ra, the maximum roughness in this test, with the incident angle of 80 degrees. However, the sensitivity of the intensity ratio decreased with increasing incident angle. Generally the range and sensitivity will have to be optimized to suit a given application. While the range was deliberately extended for the purpose of this study, most manufacturing processes would control surface roughness to Ra < 0.8 microns (30 micro inches).

6.6 Oil Effect

Oil often exists in the working environment, and is often applied on metal surfaces for corrosion protection or as a lubricant.

In this test, tool steel samples were coated with a light oil film and were examined under the incident angles of 60 and 80 degrees. The oil film filled the valleys on the sample surface to create a smoother surface and then prevented the grinding marks from scattering light. Figure 6.17 shows that the sensitivity decreased and decreased more drastically as the angle of incidence increased. This can be seen better by comparing Figures 6.12 and 6.17).

Table 6.1 The Results of Polarization Test

Surface Roughness Ra(Microns)	Out Put From Detector Vmax. (V)	Vmin. (V)	Vmax./Vmin.
0.13	4.52	4.01	1.13
1.33	4.73	4.07	1.16
2.5+	4.18	3.16	1.16

Table 6.2 Mechanical Surface Roughness Ra

Sample #	Range microns (micro-inches)	Average
	Aluminum	
1	0.06 - 0.09 (2.5 - 3.5)	0.08 (3)
2	0.20 - 0.25 (8 - 10)	0.23 (9)
3	0.30 - 0.38 (12 - 15)	0.34 (13.5)
4	0.46 - 0.56 (18 - 22)	0.51 (20)
5	0.64 - 0.69 (25 - 27)	0.66 (26)
6	0.53 - 0.58 (21 - 23)	0.56 (22)
7	0.97 - 1.07 (38 - 42)	1.02 (40)
8	1.17 - 1.35 (46 - 53)	1.26 (49.5)
9	1.91 - 2.16 (75 - 85)	2.03 (80)
10	2.08 - 2.24 (82 - 88)	2.16 (85)
11	1.78 - 2.03 (70 - 80)	1.91 (75)
	Brass	
1	0.11 - 0.15 (4.5 - 6)	0.13 (5.3)
2	0.25 - 0.33 (10 - 13)	0.29 (11.5)
3	1.07 - 1.14 (42 - 45)	1.10 (43.5)
4	0.41 - 0.51 (16 - 20)	0.46 (18)
5	0.81 - 0.86 (32 - 34)	0.84 (33)
6	0.86 - 0.91 (34 - 36)	0.89 (35)
7	0.97 - 1.02 (38 - 40)	0.99 (39)
8	1.40 - 1.52 (55 - 60)	1.46 (57.5)
9	1.78 - 1.93 (70 - 76)	1.85 (73)
10	2.13 - 2.31 (84 - 91)	2.22 (87.5)
11	2.54 - 3.05 (100 - 120)	2.97 (110)
	Copper	
1	0.05 - 0.08 (2 - 3)	0.06 (2.5)
2	0.08 - 0.13 (3 - 5)	0.10 (4)
3	0.06 - 0.08 (2.5 - 3)	0.08 (3)
4	0.18 - 0.20 (7 - 8)	0.19 (7.5)
5	0.18 - 0.22 (7 - 9)	0.20 (8)
6	0.22 - 0.30 (9 - 12)	0.27 (10.5)

Table 6.2 continued

Sample #	Range microns (micro-inches)	Average
	Copper	
7	0.25 - 0.30 (10 - 12)	0.28 (11)
8	0.30 - 0.33 (12 - 13)	0.32 (12.5)
9	0.36 - 0.41 (14 - 16)	0.38 (15)
10	0.41 - 0.46 (16 - 18)	0.43 (17)
11	0.70 - 0.76 (27.5- 30)	0.74 (29)
12	0.89 - 0.95 (35 -37.5)	0.91 (36)
13	0.97 - 1.07 (38 - 42)	1.02 (40)
14	0.86 - 0.89 (30 - 35)	0.84 (33)
15	1.52 - 1.91 (60 - 75)	1.71 (67.5)
16	2.16 - 2.41 (85 - 95)	2.29 (90)
17	2.79 - 3.30 (110 - 130)	3.05 (120)
18	2.79 - 3.30 (110 - 130)	3.05 (120)
19	2.29 - 2.79 (90 - 110)	2.54 (100)
	Stainless Steel	
1	0.11 - 0.13 (4.5 - 5)	0.12 (4.8)
2	0.18 - 0.19 (7 - 7.5)	0.19 (7.3)
3	0.36 - 0.38 (14 - 15)	0.37 (14.5)
4	0.53 - 0.58 (21 - 23)	0.56 (22)
5	0.76 - 0.84 (30 - 33)	0.80 (31.5)
6	0.89 - 1.02 (35 - 40)	0.95 (37.5)
7	0.95 - 1.08 (37.5-42.5)	1.02 (40)
8	1.33 - 1.46 (52.5-57.5)	1.40 (55)
9	1.27 - 1.40 (50 - 55)	1.33 (52.5)
10	1.59 - 1.78 (62.5- 70)	1.68 (66)
11	1.83 - 2.08 (72 - 82)	1.96 (77)
12	1.98 - 2.16 (78 - 85)	2.08 (82)
13	2.29 - 2.54 (90 - 100)	2.41 (95)
14	2.16 - 2.36 (85 - 93)	2.26 (89)
	Tool Steel	
1	0.08 - 0.09 (3 - 3.5)	0.08 (3.3)
2	0.17 - 0.18 (6.5 - 7)	0.17 (6.8)
3	0.25 - 0.28 (10 - 11)	027 (10.5)
4	0.43 - 0.46 (17 - 18)	0.44 (17.5)
5	0.61 - 0.69 (24 - 27)	0.65 (25.5)
6	0.74 - 0.84 (29 - 33)	0.79 (31)
7	0.99 - 1.09 (39 - 43)	1.04 (41)
8	1.12 - 1.17 (44 - 46)	1.14 (45)
9	1.24 - 1.37 (49 - 54)	1.31 (51.5)
10	1.42 - 1.55 (56 - 61)	1.46 (58.5)
11	2.03 - 2.08 (80 - 82)	2.06 (81)
12	2.08 - 2.21 (82 - 87)	2.15 (84.5)
13	2.79 - 3.05 (110 - 120)	2.92 (115)

Table 6.3 Intensity Ratio (IR = D2 / D1)

Sample #	Ra (Microns)	Incident light angle 85	80	70	60
			Aluminum		
1	0.08	1.93E-3	2.78E-3	3.52E-3	7.24E-3
2	0.23	1.26E-2	4.37E-2	0.112	0.324
3	0.35	1.87E-2	5.98E-2	0.159	0.297
4	0.51	2.90E-2	0.121	----	----
5	0.66	2.23E-2	7.26E-2	0.214	0.387
6	0.56	2.01E-2	8.21E-2	0.214	0.448
7	1.02	3.40E-2	0.105	0.256	0.473
8	1.26	3.08E-2	0.117	0.228	0.421
9	2.03	8.11E-2	0.199	0.309	0.499
10	2.16	9.22E-2	0.272	0.375	0.578
11	1.91	6.63E-2	0.163	0.263	0.453
			Brass		
1	0.13	1.08E-2	2.49E-2	4.49E-2	0.106
2	0.29	1.47E-2	3.95E-2	7.34E-2	0.195
3	1.10	7.98E-2	0.154	0.320	0.586
4	0.46	2.03E-2	4.89E-2	9.39E-2	0.265
5	0.84	7.23E-2	0.256	0.474	0.649
6	0.89	8.98E-2	0.333	0.575	0.818
7	0.99	0.113	0.320	0.584	0.793
8	1.46	8.01E-2	0.196	0.365	0.536
9	1.85	0.229	0.708	1.18	1.00
10	2.22	0.348	1.051	1.16	1.07
11	2.79	0.359	0.923	1.28	1.07
			Copper		
1	0.06	1.30E-3	5.23E-3	8.98E-3	1.75E-2
2	0.10	1.07E-3	5.85E-3	8.83E-3	1.64E-2
3	0.08	1.15E-3	4.29E-3	8.96E-3	1.69E-2
4	0.19	6.95E-3	4.79E-2	0.132	0.348
5	0.20	9.56E-3	5.04E-2	0.155	0.427
6	0.27	1.16E-2	7.35E-2	0.341	0.677
7	0.28	1.42E-2	7.63E-2	0.296	0.774
8	0.32	2.17E-2	0.151	0.470	0.788
9	0.38	1.80E-2	8.67E-2	0.440	0.849
10	0.43	2.29E-2	0.112	0.411	0.746
11	0.74	3.74E-2	0.338	-----	1.09
12	0.91	5.42E-2	0.228	0.709	-----
13	1.02	9.23E-2	0.311	0.734	1.03
14	0.84	7.03E-2	0.316	0.736	1.01

Table 6.3 continued

Sample #	Ra (Microns)	Incident light angle 85	80	70	60
			Copper		
15	1.71	0.122	0.354	0.841	1.01
16	2.29	-----	0.638	0.893	0.941
17	3.05	0.195	0.666	0.948	1.11
18	3.05	0.180	0.555	0.924	1.06
19	2.54	0.179	0.621	0.906	1.05
			Stainless Steel		
1	0.12	2.49E-3	8.41E-3	3.06E-2	8.77E-2
2	0.19	1.02E-2	3.25E-2	0.162	0.392
3	0.37	7.17E-3	3.04E-2	0.121	0.287
4	0.56	1.47E-2	6.75E-2	0.302	0.571
5	0.80	2.91E-2	0.133	0.455	0.681
6	0.95	3.37E-2	0.187	0.546	0.736
7	1.02	5.21E-2	0.304	0.794	0.873
8	1.40	6.12E-2	0.338	0.569	0.774
9	1.33	5.72E-2	0.294	0.584	0.729
10	1.68	7.41E-2	0.395	0.808	0.845
11	1.96	0.152	0.547	0.932	1.15
12	2.08	0.180	0.733	1.12	1.09
13	2.41	0.180	0.646	1.11	1.12
14	2.26	0.209	0.815	1.03	1.07
			Tool Steel		
1	0.08	7.44E-3	1.81E-2	3.50E-2	7.67E-2
2	0.17	1.61E-2	4.55E-2	0.108	0.288
3	0.27	2.32E-2	7.73E-2	0.220	0.472
4	0.44	2.99E-2	0.107	0.322	0.554
5	0.65	5.49E-2	0.204	0.760	1.01
6	0.79	5.96E-2	0.188	0.459	0.728
7	1.04	7.82E-2	0.338	0.876	0.980
8	1.14	-----	-----	0.404	0.626
9	1.31	0.128	0.509	0.890	0.927
10	1.46	0.163	0.604	0.974	0.947
11	2.06	0.232	0.918	1.43	1.07
12	2.15	0.226	0.959	1.26	1.12
13	2.92	0.272	-----	1.10	1.18

Table 6.4 Curve Fitting Results of Incident Angle Test

Aluminum
Incident Angle = 85 degrees
0 Degree Coefficient = -2.843E-3
1 Degree Coefficient = 8.290E-2
2 Degree Coefficient = -7.767E-2
3 Degree Coefficient = 2.785E-2
Coefficient of Correlation = 0.9939
Standard Error of Estimate = 3.858E-3
Incident Angle = 80 degrees
0 Degree Coefficient = -2.619E-2
1 Degree Coefficient = 0.3865
2 Degree Coefficient = -0.3778
3 Degree Coefficient = 0.1205
Coefficient of Correlation = 0.9780
Standard Error of Estimate = 1.892E-2
Incident Angle = 70 degrees
0 Degree Coefficient = -5.076E-2
1 Degree Coefficient = 0.8317
2 Degree Coefficient = -0.7506
3 Degree Coefficient = 0.2111
Coefficient of Correlation = 0.9961
Standard Error of Estimate = 1.117E-2
Incident Angle = 60 degrees
0 Degree Coefficient = -5.016E-2
1 Degree Coefficient = 1.488
2 Degree Coefficient = -1.346
3 Degree Coefficient = 0.3674
Coefficient of Correlation = 0.9583
Standard Error of Estimate = 5.556E-2

$$IR = A0 + A1 \times Ra + A2 \times Ra^2 + A3 \times Ra^3 + \ldots$$

Where IR is Intensity Ratio;
Ra is Surface Roughness in Microns; and
A0, A1, A2...are the 0, 1st, 2nd...degree coefficient respectively.

Table 6.4 Continued

Brass
Incident Angle = 85 degrees
0 Degree Coefficient = 2.411E-2
1 Degree Coefficient = -6.154E-2
2 Degree Coefficient = 0.1456
3 Degree Coefficient = -2.815E-2
Coefficient of Correlation = 0.9646
Standard Error of Estimate = 3.978E-2
Incident Angle = 80 degrees
0 Degree Coefficient = 9.191E-2
1 Degree Coefficient = -0.3010
2 Degree Coefficient = 0.5659
3 Degree Coefficient = -0.1231
Coefficient of Correlation = 0.9316
Standard Error of Estimate = 0.1572
Incident Angle = 70 degrees
0 Degree Coefficient = 5.936E-3
1 Degree Coefficient = 0.2455
2 Degree Coefficient = 0.2702
3 Degree Coefficient = -6.839E-2
Coefficient of Correlation = 0.9269
Standard Error of Estimate = 0.2049
Incident Angle = 60 degrees
0 Degree Coefficient = 2.623E-2
1 Degree Coefficient = 0.7599
2 Degree Coefficient = -0.1391
Coefficient of Correlation = 0.9136
Standard Error of Estimate = 0.1570

Table 6.4 Continued

Copper
Incident Angle = 85 degrees
0 Degree Coefficient = -5.153E-3
1 Degree Coefficient = 6.511E-2
2 Degree Coefficient = 1.833E-2
3 Degree Coefficient = -6.210E-3
Coefficient of Correlation = 0.9935
Standard Error of Estimate = 8.446E-3
Incident Angle = 80 degrees
0 Degree Coefficient = -1.987E-2
1 Degree Coefficient = 0.3885
2 Degree Coefficient = -5.815E-2
Coefficient of Correlation = 0.9740
Standard Error of Estimate = 5.544E-2
Incident Angle = 70 degrees
0 Degree Coefficient = -7.388E-2
1 Degree Coefficient = 1.481
2 Degree Coefficient = -0.7478
3 Degree Coefficient = 0.1221
Coefficient of Correlation = 0.9881
Standard Error of Estimate = 5.859E-2
Incident Angle = 60 degrees
0 Degree Coefficient = -0.2461
1 Degree Coefficient = 4.163
2 Degree Coefficient = -4.353
3 Degree Coefficient = 1.761
4 Degree Coefficient = -0.2408
Coefficient of Correlation = 0.9785
Standard Error of Estimate = 9.152E-2

Table 6.4 Continued

Stainless Steel

Incident Angle = 85 degrees
0 Degree Coefficient = 6.193E-3
1 Degree Coefficient = -5.358E-3
2 Degree Coefficient = 3.734E-2
Coefficient of Correlation = 0.9747
Standard Error of Estimate = 1.760E-2

Incident Angle = 80 degrees
0 Degree Coefficient = -2.484E-2
1 Degree Coefficient = 0.1763
2 Degree Coefficient = 6.478E-2
Coefficient of Correlation = 0.9705
Standard Error of Estimate = 7.119E-2

Incident Angle = 70 degrees
0 Degree Coefficient = 5.255E-2
1 Degree Coefficient = 0.4572
Coefficient of Correlation = 0.9601
Standard Error of Estimate = 0.1072

Incident Angle = 60 degrees
0 Degree Coefficient = 0.1421
1 Degree Coefficient = 0.6994
2 Degree Coefficient = -0.1239
Coefficient of Correlation = 0.9501
Standard Error of Estimate = 0.1096

Table 6.4 Continued

Tool Steel

Incident Angle = 85 degrees
0 Degree Coefficient = 1.165E-2
1 Degree Coefficient = 2.194E-3
2 Degree Coefficient = 9.638E-2
3 Degree Coefficient = -2.283E-2
Coefficient of Correlation = 0.9972
Standard Error of Estimate = 8.248E-3

Incident Angle = 80 degrees
0 Degree Coefficient = 2.972E-2
1 Degree Coefficient = 2.342E-2
2 Degree Coefficient = 0.3530
3 Degree Coefficient = -7.522E-2
Coefficient of Correlation = 0.9984
Standard Error of Estimate = 2.325E-2

Incident Angle = 70 degrees
0 Degree Coefficient = -5.429E-2
1 Degree Coefficient = 0.9827
2 Degree Coefficient = -0.1881
Coefficient of Correlation = 0.9237
Standard Error of Estimate = 0.1900

Incident Angle = 60 degrees
0 Degree Coefficient = 7.830E-2
1 Degree Coefficient = 1.393
2 Degree Coefficient = -0.7187
3 Degree Coefficient = 0.1283
Coefficient of Correlation = 0.9185
Standard Error of Estimate = 0.1562

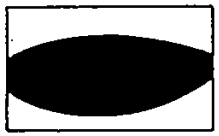

Light Path Direction Perpendicular to the Lay

Light Path Direction Parallel
to the Lay

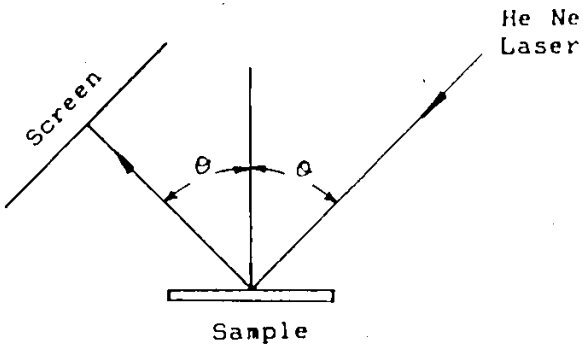

Fig. 6.1 Light Scattered Pattern

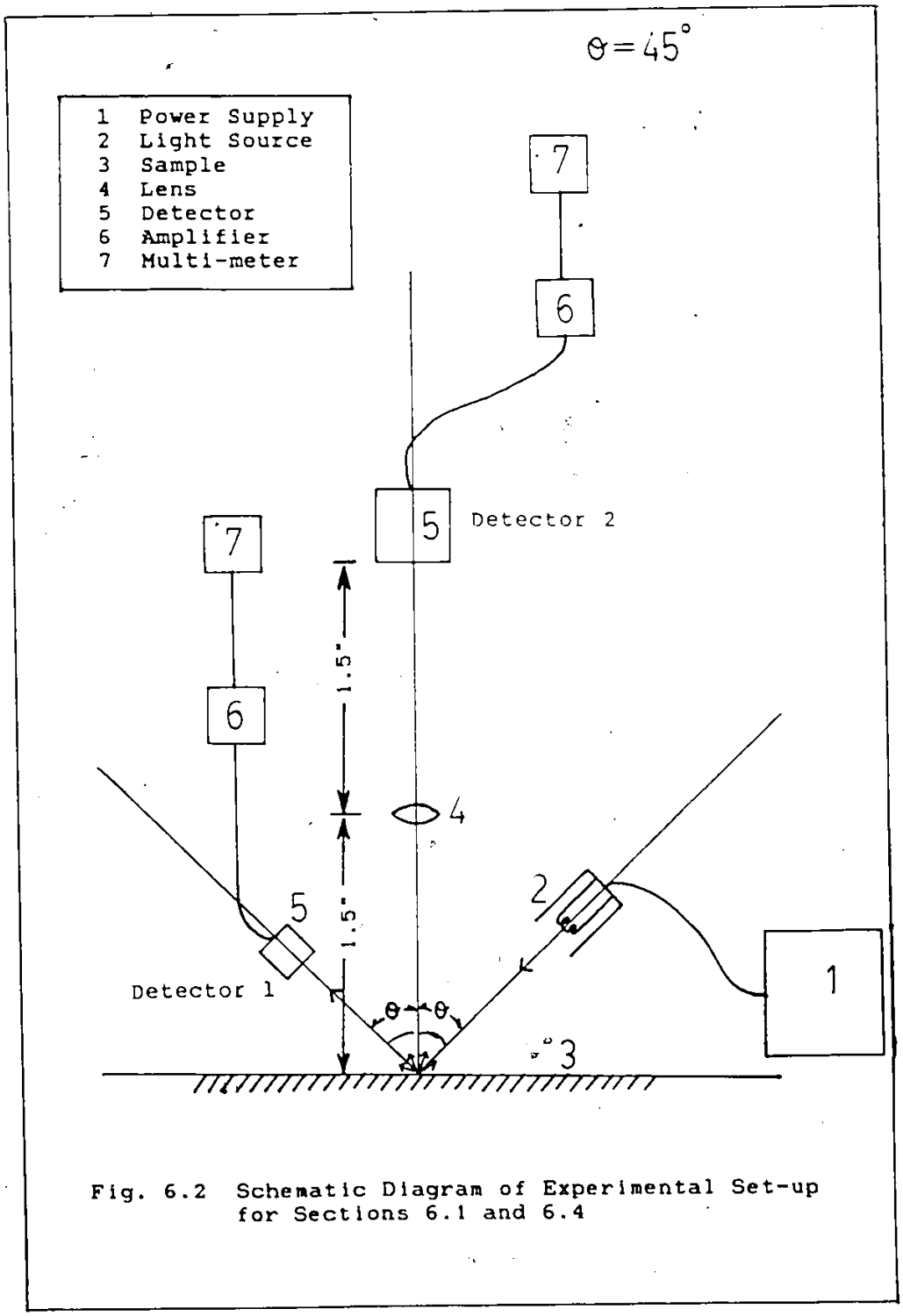

Fig. 6.2 Schematic Diagram of Experimental Set-up for Sections 6.1 and 6.4

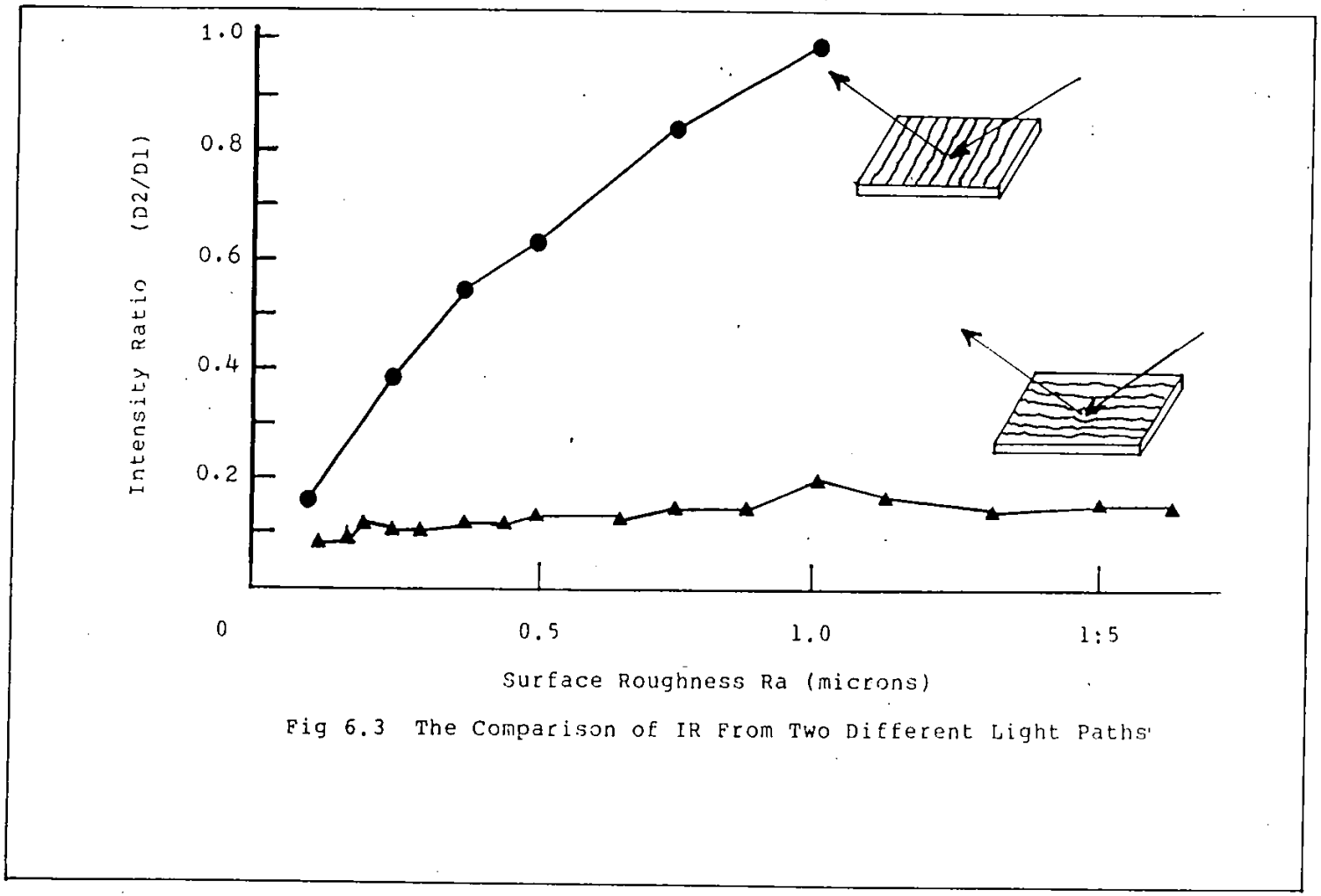

Fig 6.3 The Comparison of IR From Two Different Light Paths

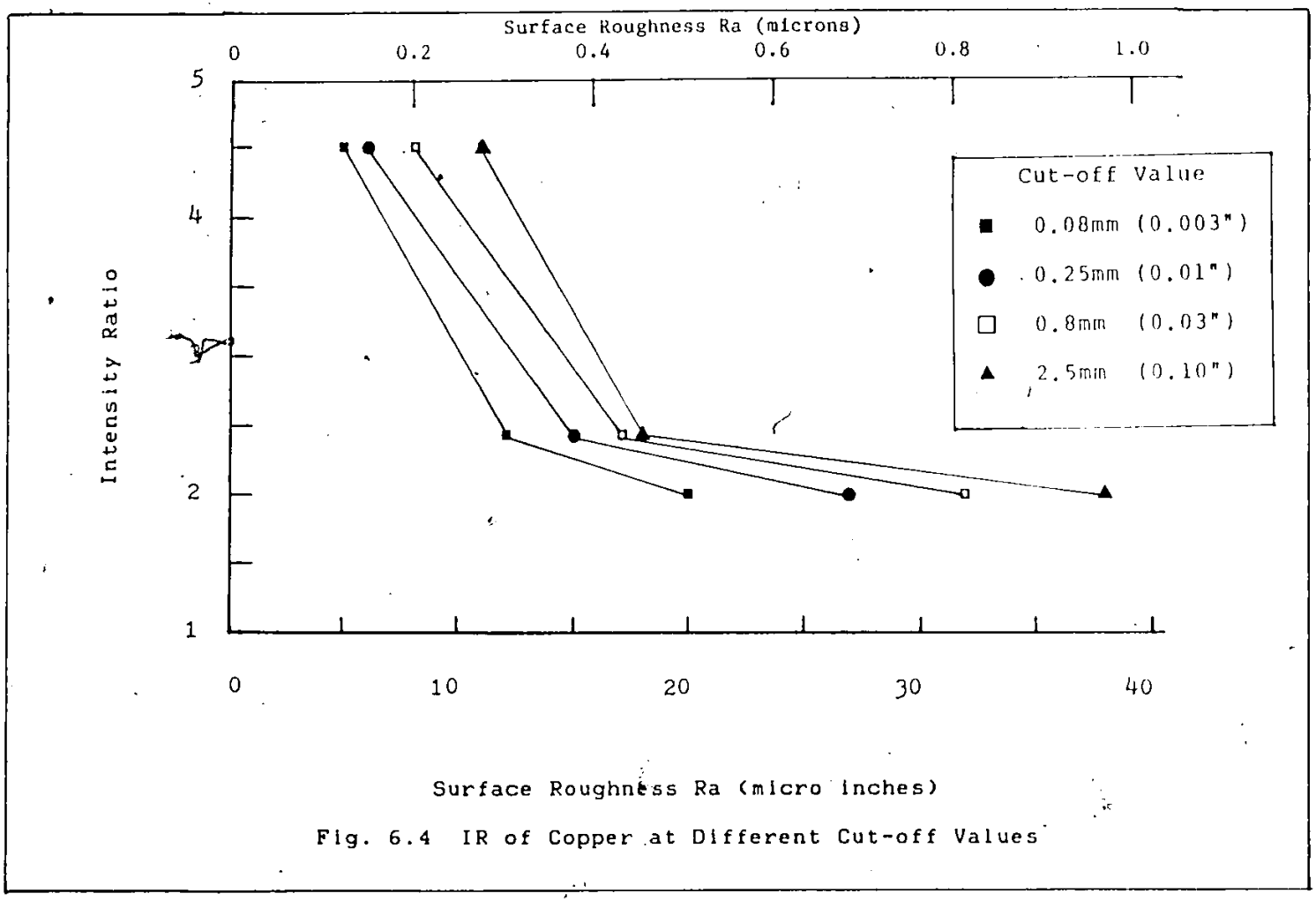

Fig. 6.4 IR of Copper at Different Cut-off Values

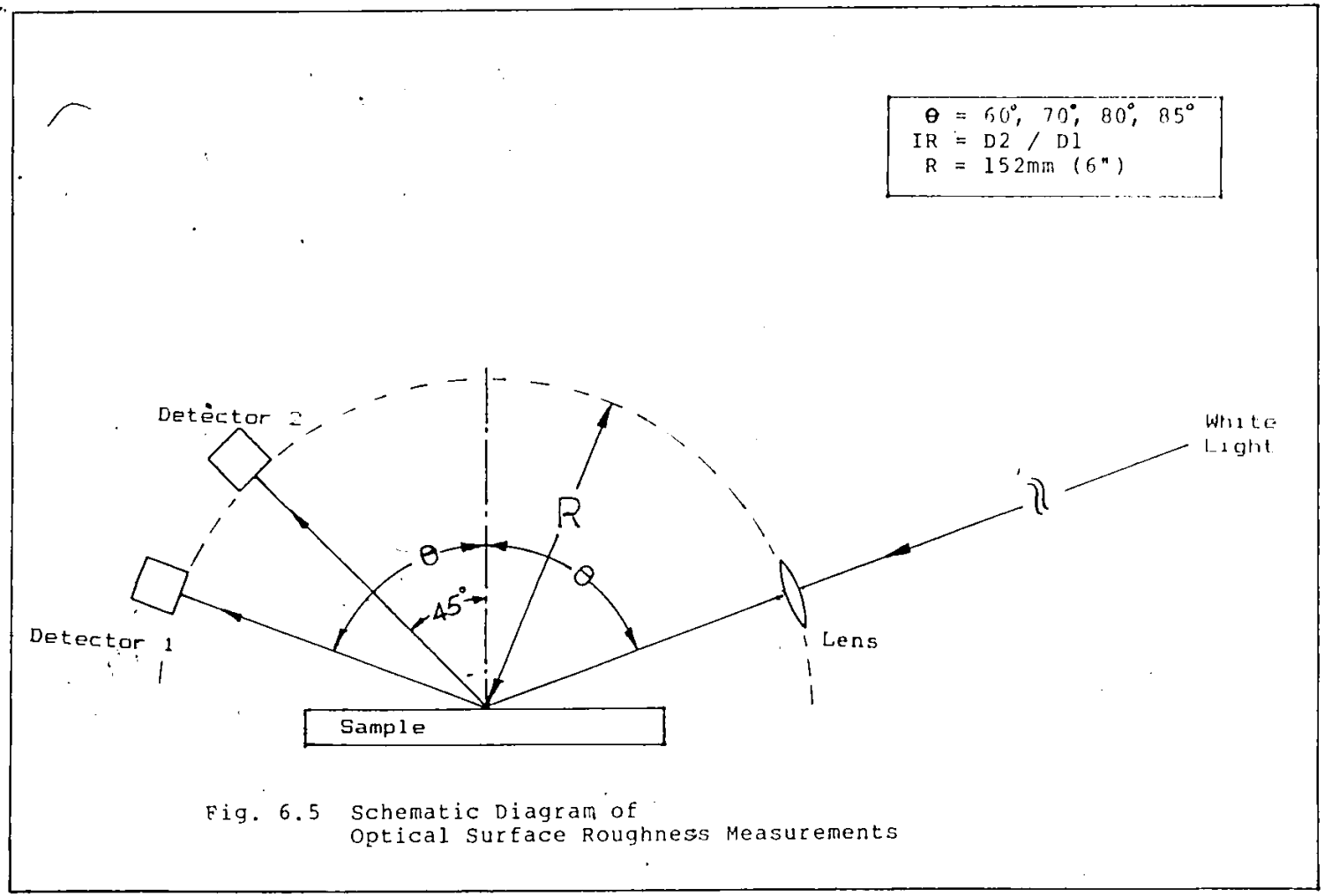

Fig. 6.5 Schematic Diagram of
Optical Surface Roughness Measurements

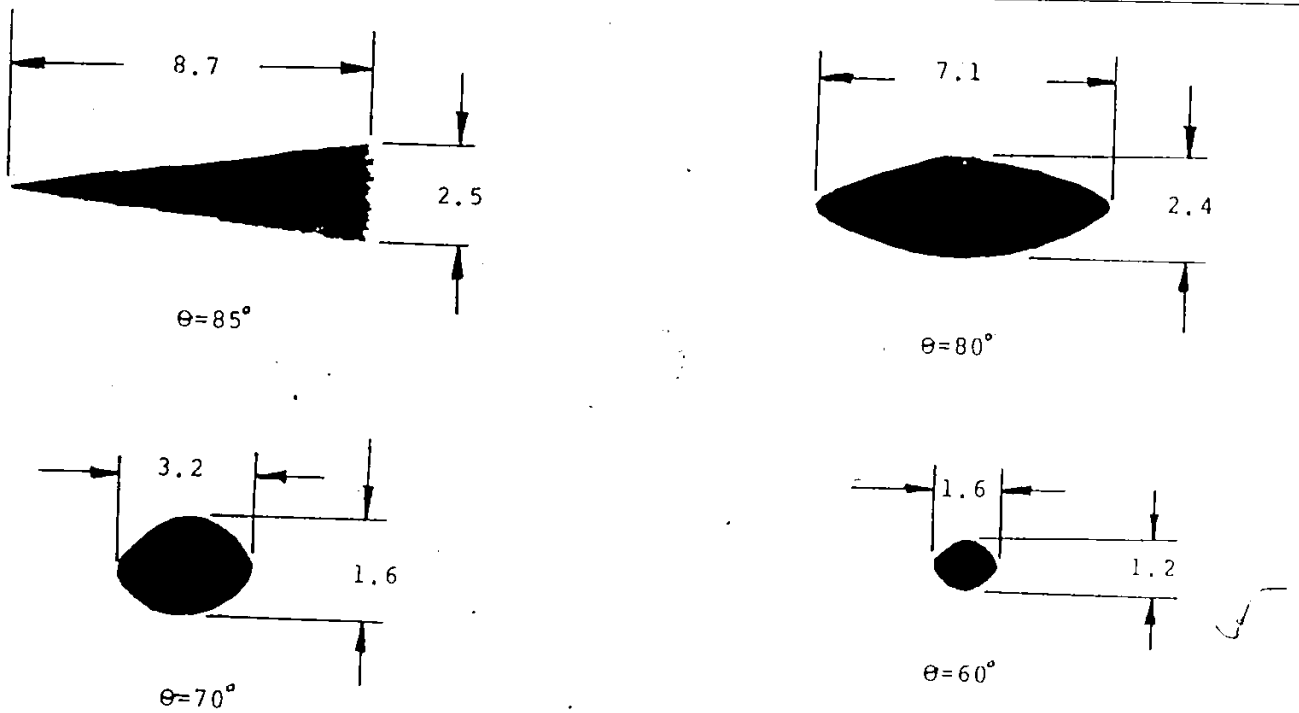

Fig. 6.6 Footprint of Illumination on Sample Surface

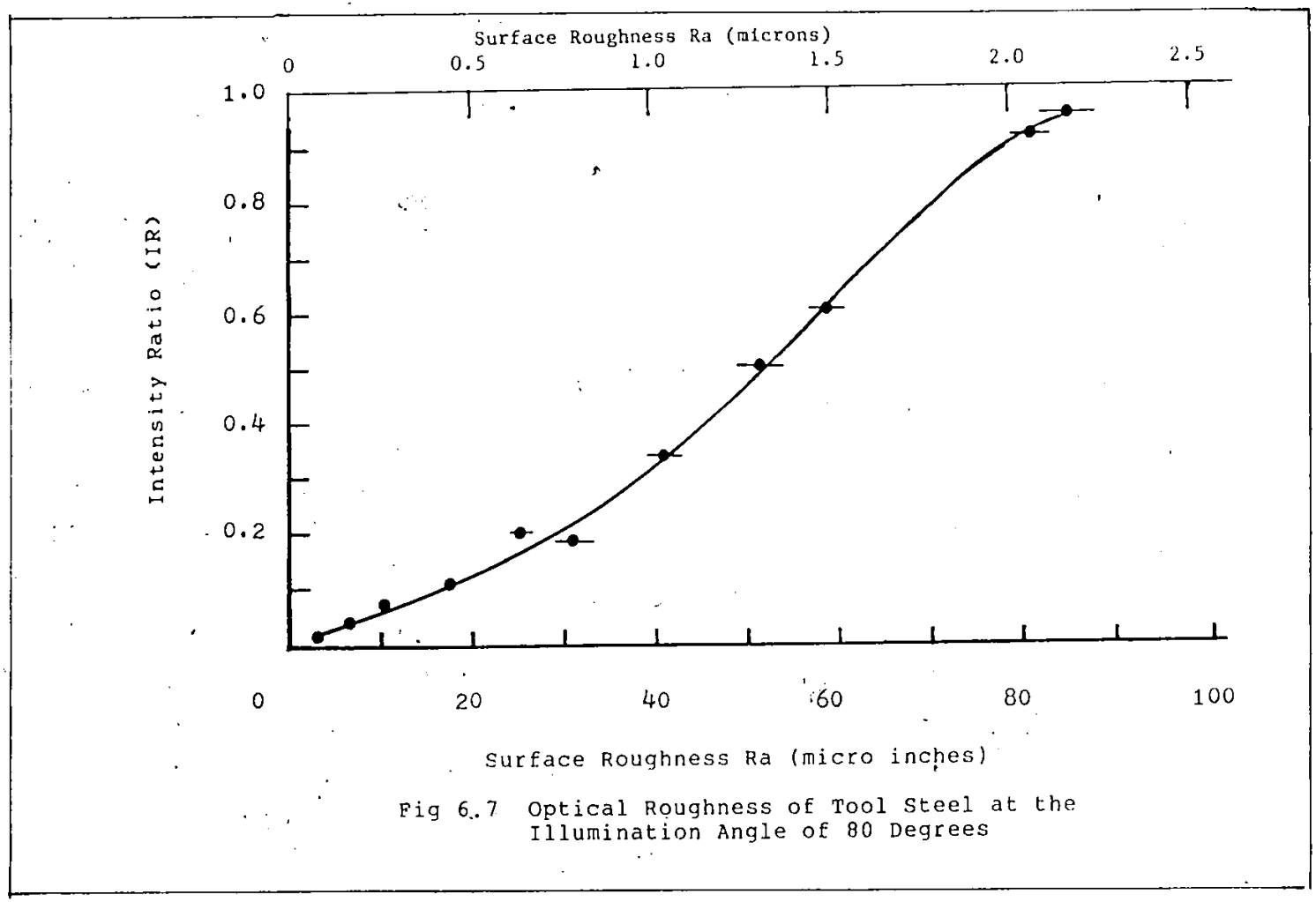

Fig 6.7 Optical Roughness of Tool Steel at the Illumination Angle of 80 Degrees

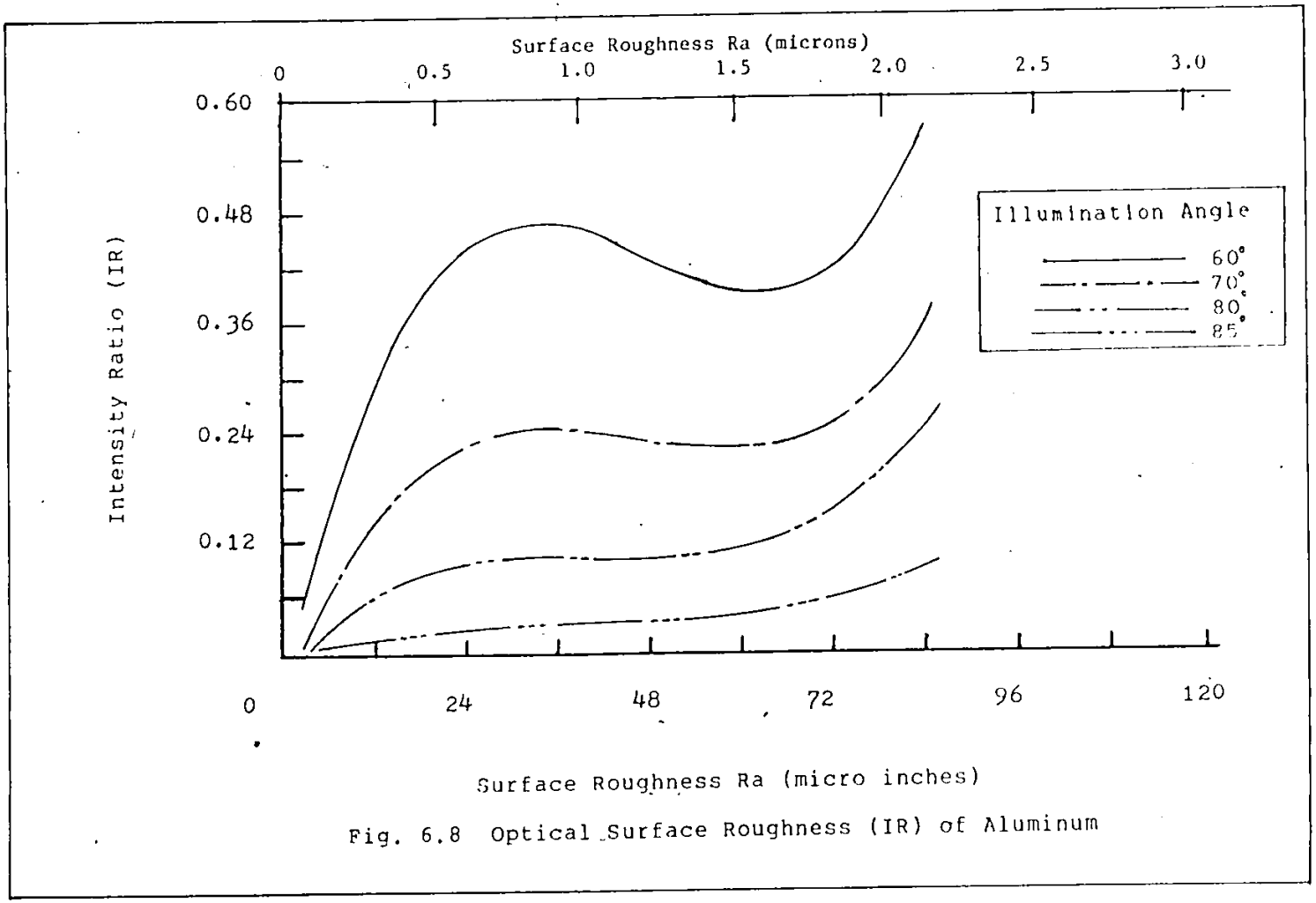

Fig. 6.8 Optical Surface Roughness (IR) of Aluminum

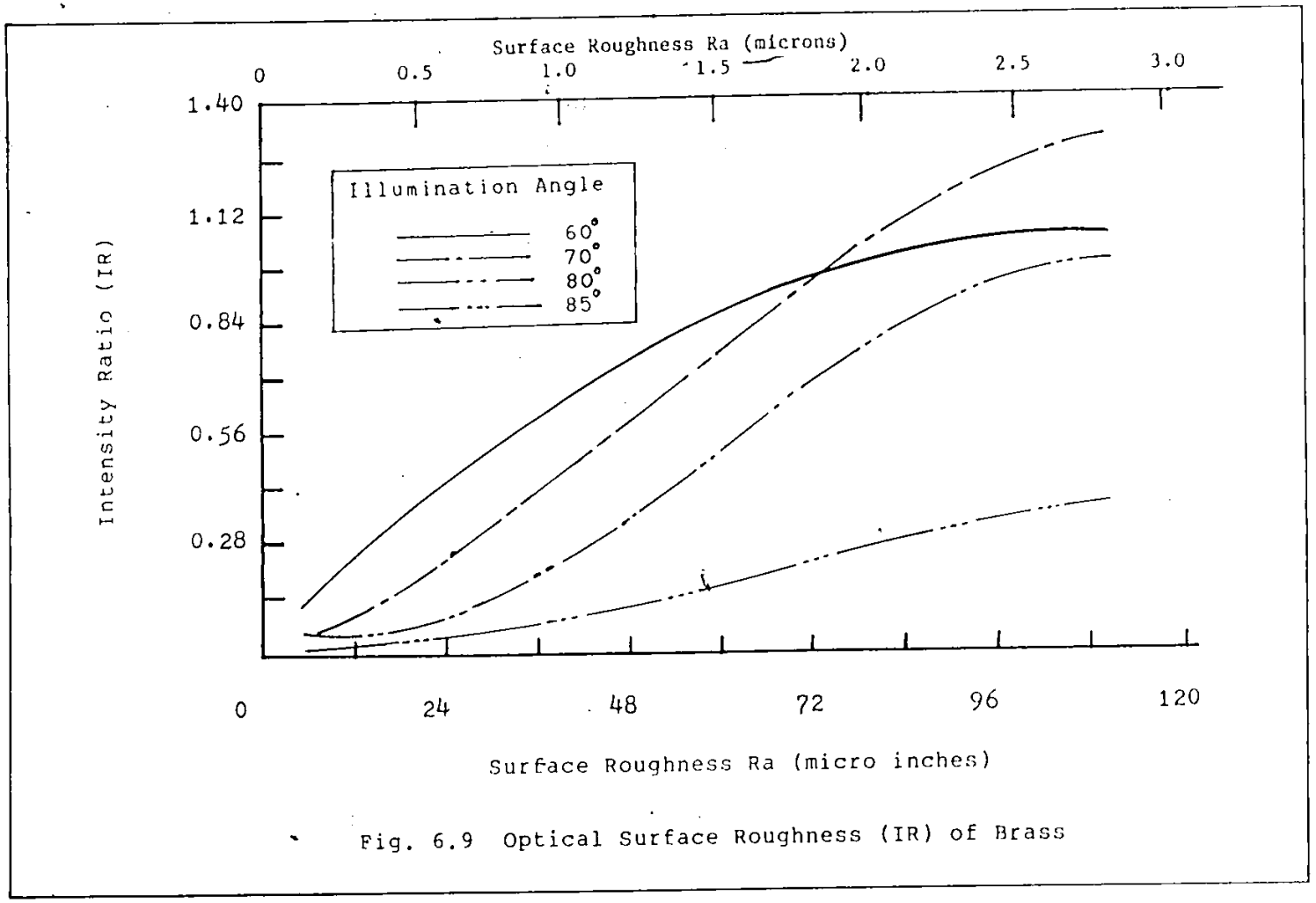

Fig. 6.9 Optical Surface Roughness (IR) of Brass

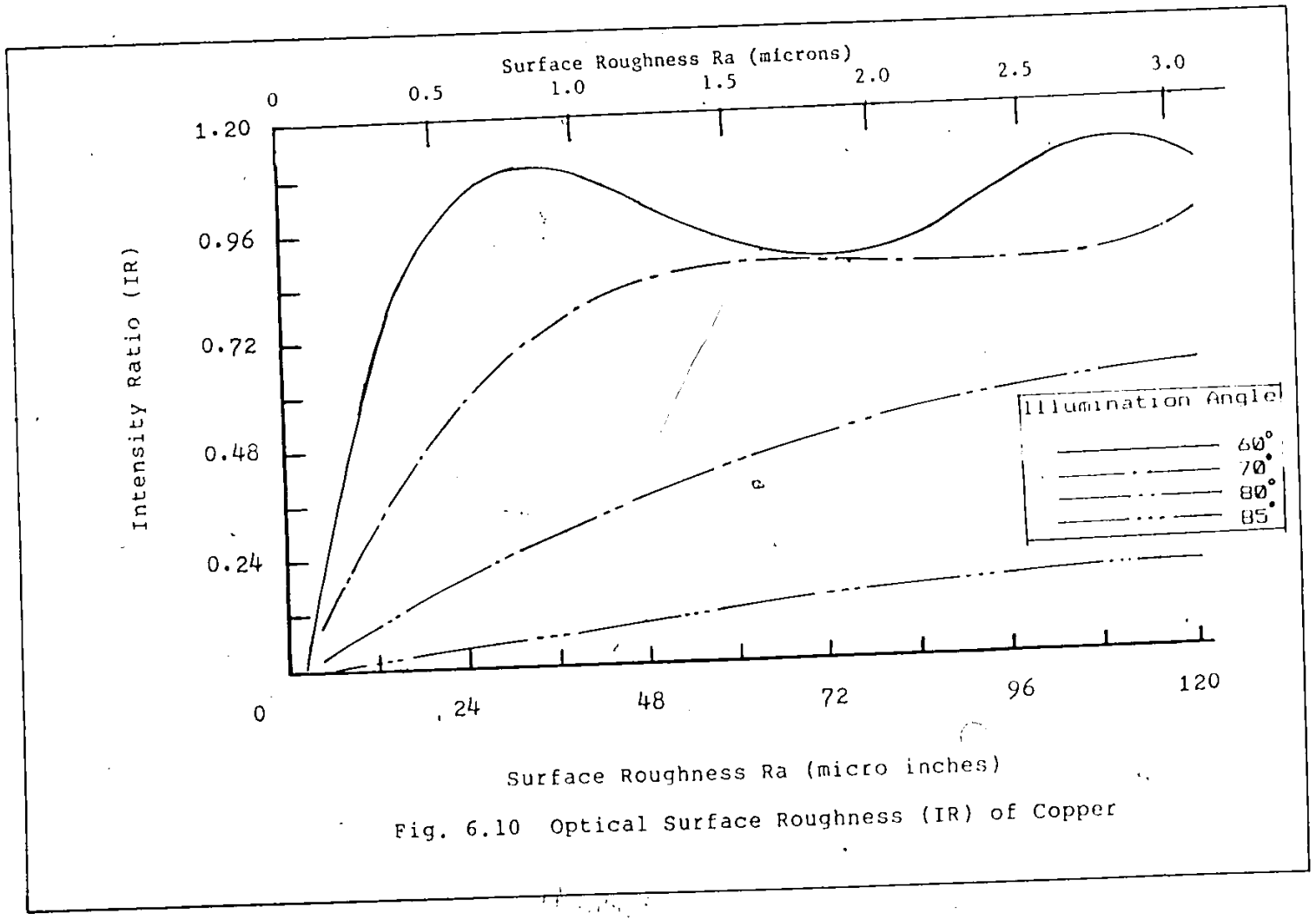

Fig. 6.10 Optical Surface Roughness (IR) of Copper

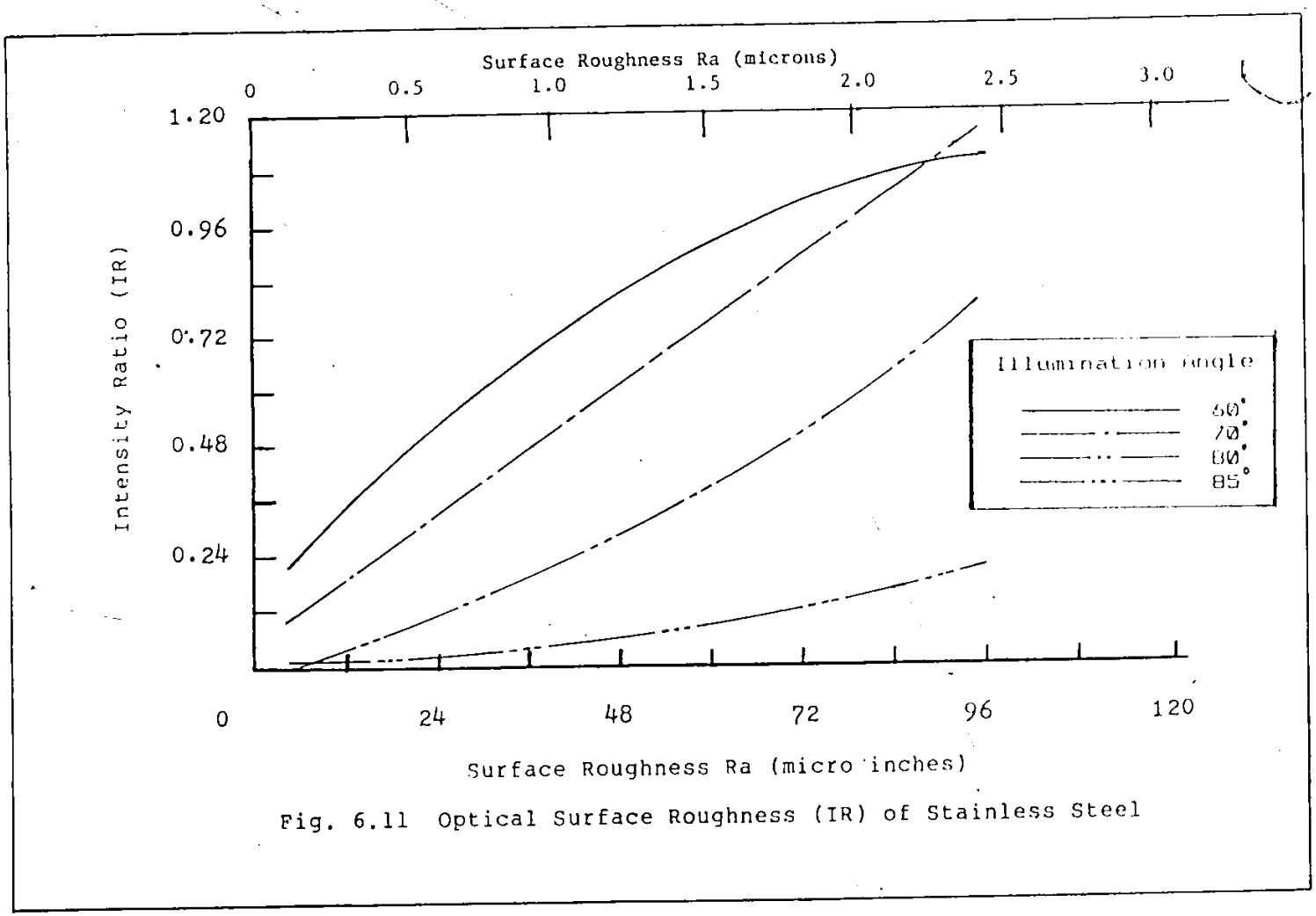

Fig. 6.11 Optical Surface Roughness (IR) of Stainless Steel

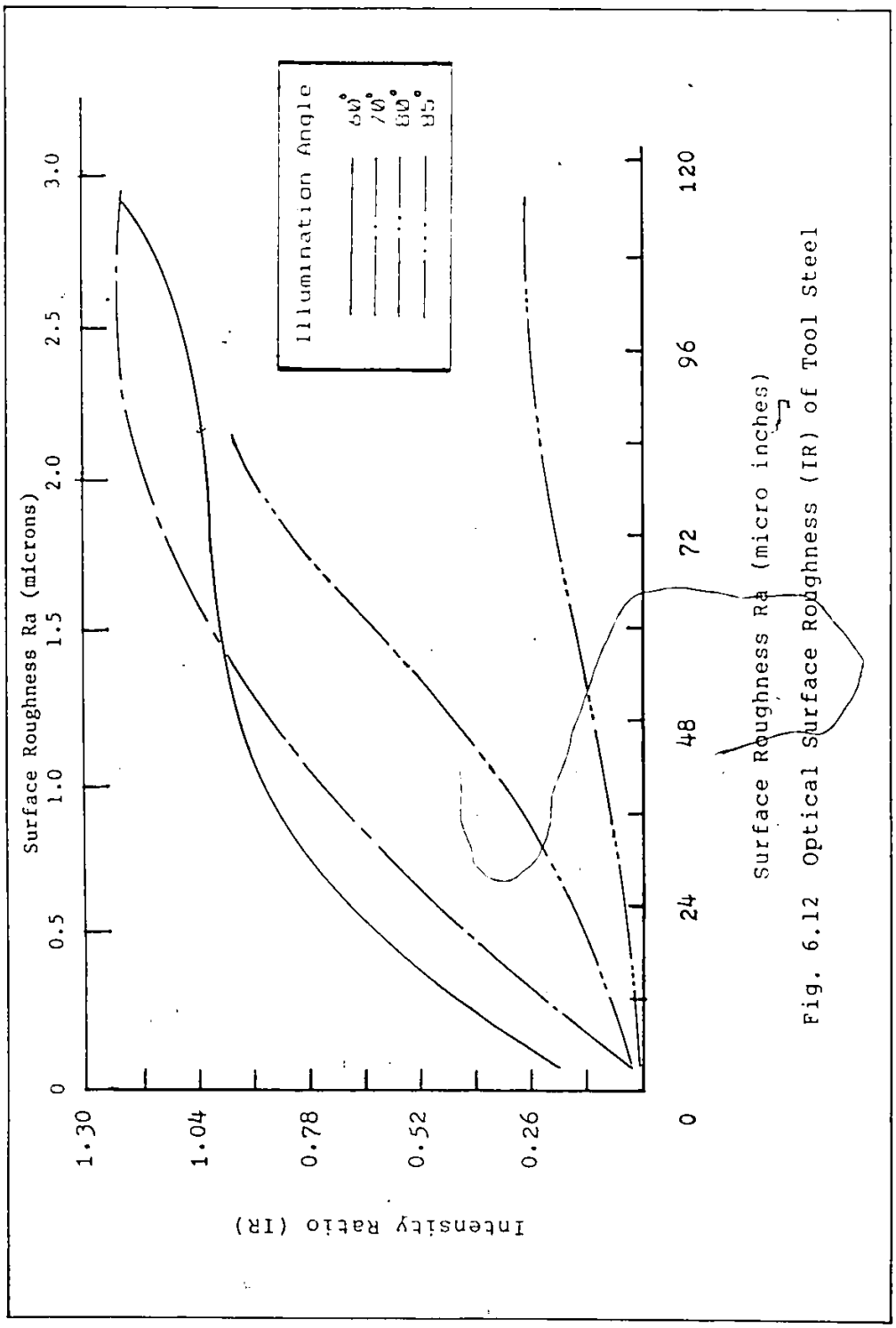

Fig. 6.12 Optical Surface Roughness (IR) of Tool Steel

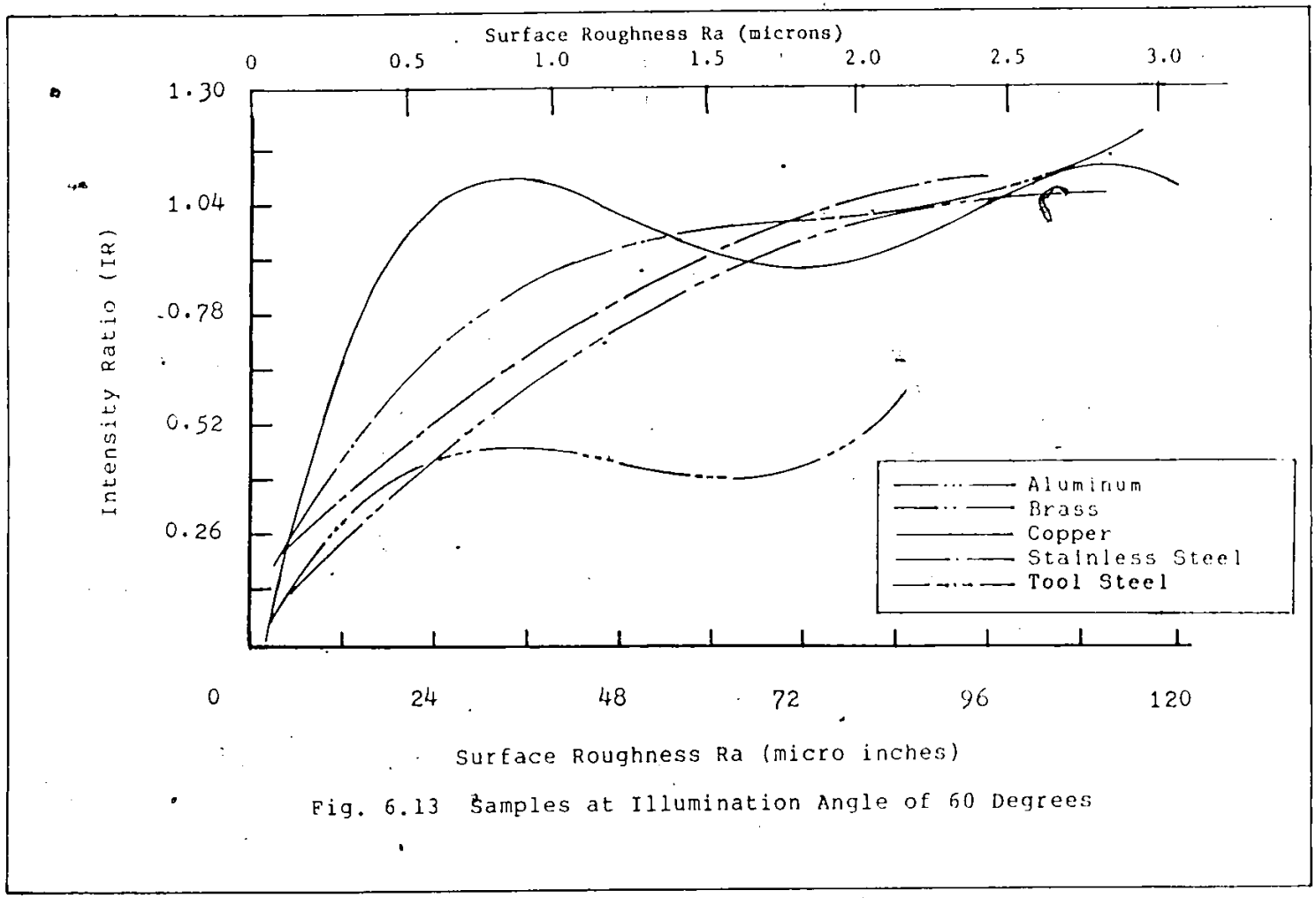

Fig. 6.13 Samples at Illumination Angle of 60 Degrees

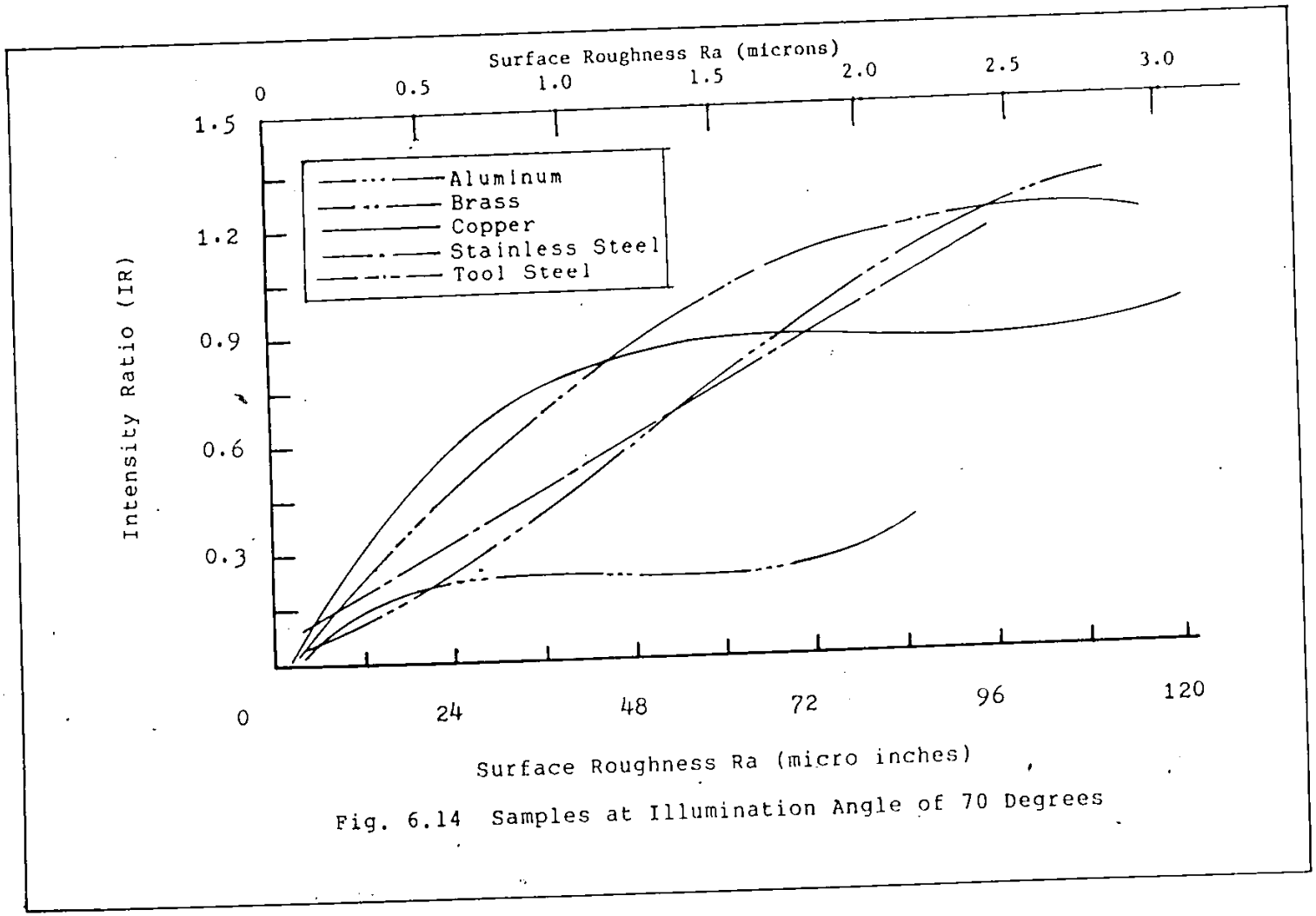

Fig. 6.14 Samples at Illumination Angle of 70 Degrees

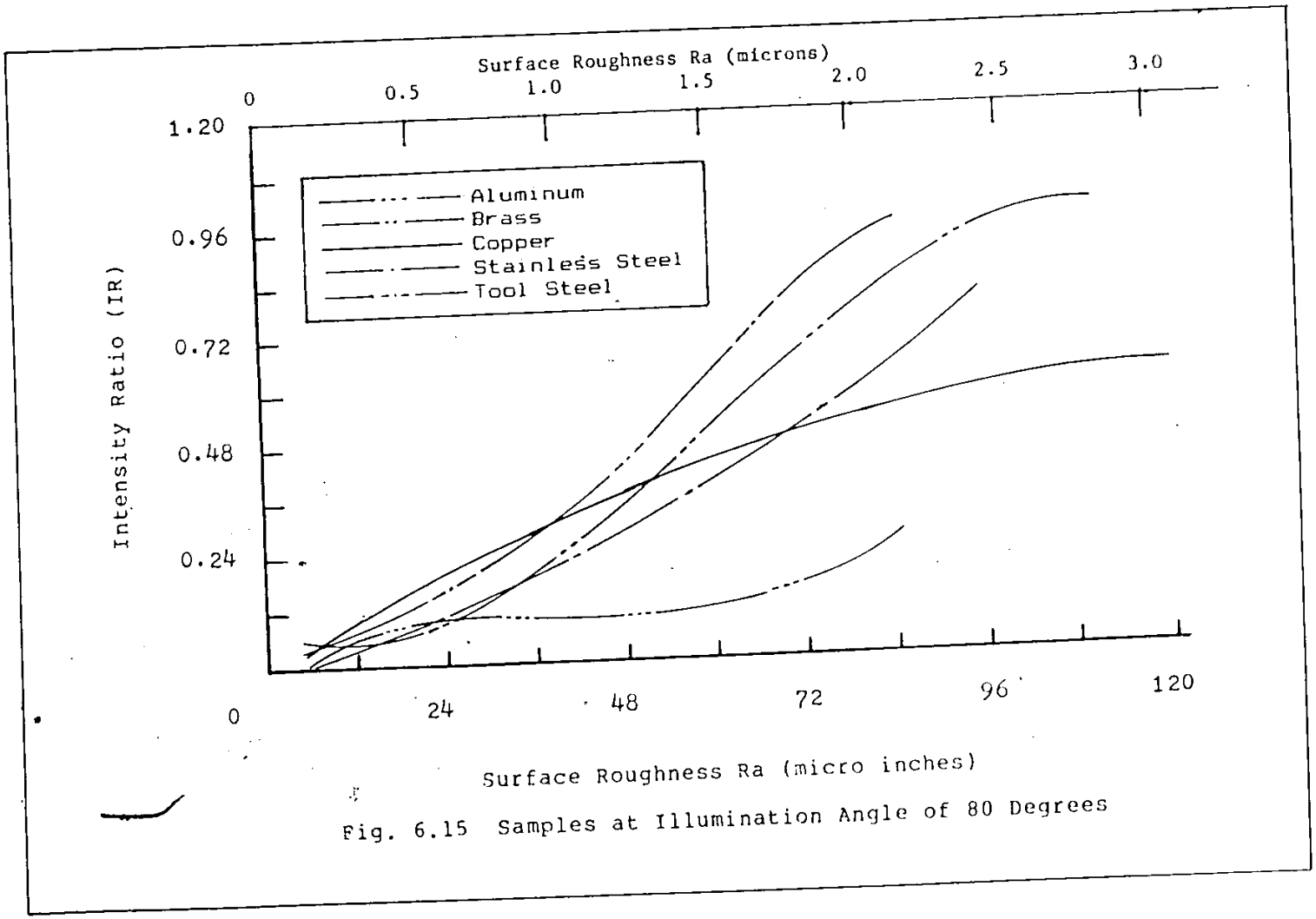

Fig. 6.15 Samples at Illumination Angle of 80 Degrees

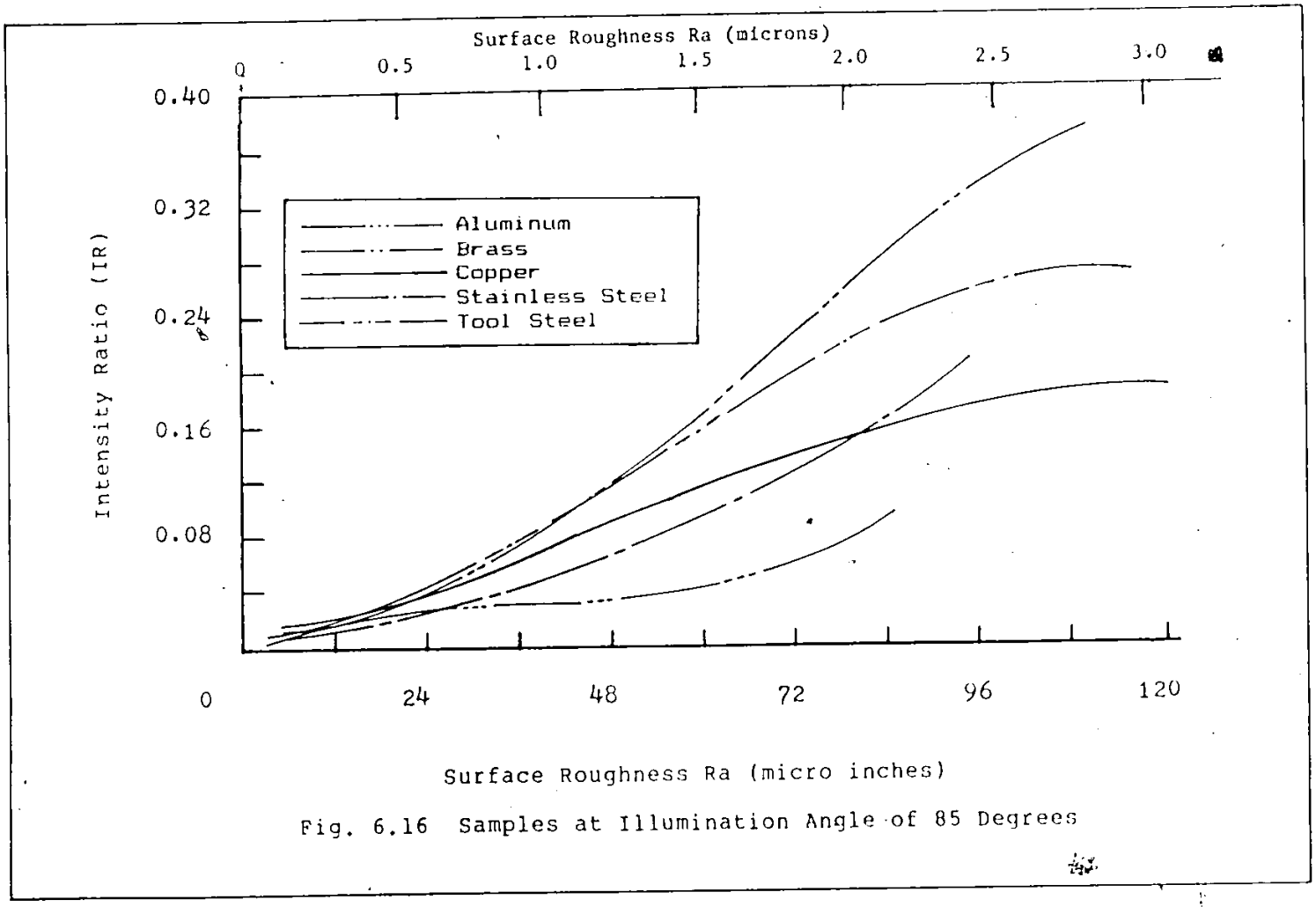

Fig. 6.16 Samples at Illumination Angle of 85 Degrees

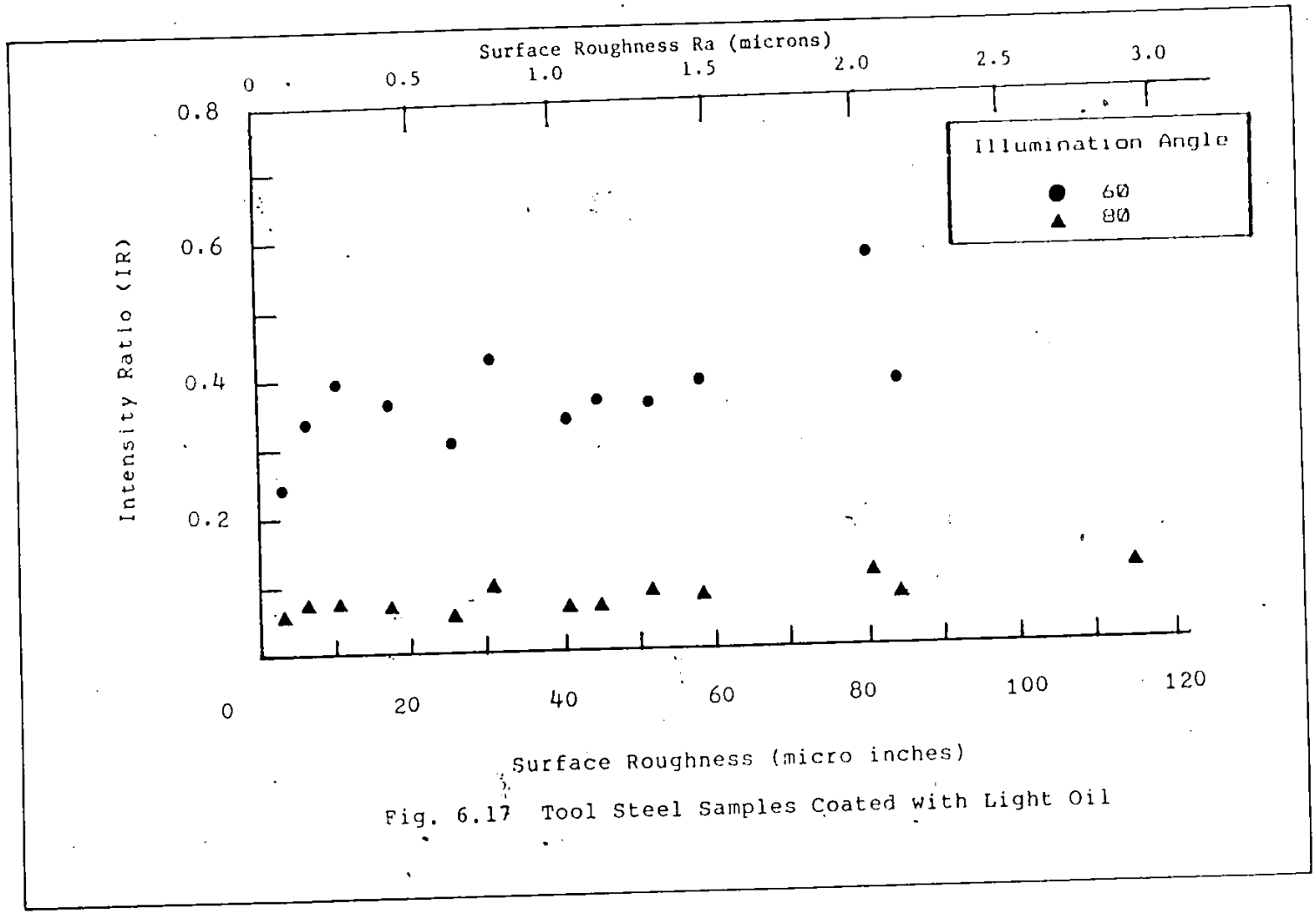

Fig. 6.17 Tool Steel Samples Coated with Light Oil

CHAPTER VII

CONCLUSIONS

This study was divided into two parts, the first part studied optical contrast measurements of etched lines on sheet metal and the second part investigated roughness measurement by optical methods. Based on the results of this study, the following conclusions were made.

A1 An electro-optical sensor to measure the contrast of etched grid lines on sheet metal was developed. Two hand held versions were built and tested and interfaced to a computer. An algorithm to extract contrast ratio measurements from an optical scan through an etched line was also developed.

A2 For optical contrast measurements, the selection of the proper size of the detector and the size of illumination field is very important. The active diameter of the detector should be approximately the same size of the width of the etched lines. In this way, excessive magnification is eliminated and hence, avoids light loss. As the illuminated field size decreases, less stray light finds its way into the detector.

A3 Besides the selection of detector and illuminated field size, the configuration of the system also affects the contrast measurement. The optical system (Hand-held-unit I) was first designed with an incident light angle of 45 degrees and the detector was located at the specular reflection angle. The results from the Configuration Test shows that this configuration yielded the highest contrast (Table 5.7). However, this configuration is also very sensitive to the variations of the metal surface, such as uneven coatings, dust and dirt. These surface variations cause variations (noise) superposed on the signals of the etched lines (Figure 5.8). In this case, the contrast may be impossible to calculate. By moving the detector away from the specular angle, these variations vanish. For this reason, configuration I employing a detector at 90 degree to the surface, is recommended for contrast measurements.

A4 The contrast can best be improved by the etching process itself. From the results of these tests, the optimal etching time for plain carbon steel was 6 to 7 minutes and for electro galvanized steel was 20 seconds. See Table 5.6.

A5 Based on the tensile test, the maximum reduction of contrast as a result of strain was 35%. The dome test indicated that the maximum contrast reduction was 56% for carbon steel and 47% for galvanized steel. The change of contrast did not correlate with strain level in both tests. The maximum change of contrast appeared at the strain level

range of 50%-60%.

A6 As the surface roughness of the sheet metal decreases, the contrast of the etched lines increases by as much as 59%, see Figure 5.6. The cost of providing this reduced surface roughness may be prohibitive.

A7 In this study, the contrast of the etched line varies from 0.263 to 0.845. Based on this experience on plain carbon steel, before deformation contrast should be 0.6 and for electro-galvanized steel, the contrast should be 0.5.

A8 Other methods which were used in an attempt to improve the contrast namely: cleaning, waxing, metal conditioners, Krylon over coat, Zyglo penetrants, variable wavelength, and polarization did not show any significant improvement on contrasts (see Appendix B).

B1 A simple technique to measure the specular and scattered reflected light from a metal surface was developed, and an optical sensor was designed and tested for this purpose.

B2 Various methods of calculating the normalized intensity ratios (IR) were made, including D2 / D1, (D1 + D2) / (D1 - D2) and so on. Where D1 and D2 are the output voltage of the detectors which measure the specular and scattered light respectively. While it is not reported here, it was found by fitting curves by the least squares method, that the best correlation with the mechanical roughness (Ra) was determined when dividing D2 by D1. Only those results are

included here.

This intensity ratio is a normalized, non-dimensional number, which did not depend on variables such as incident light intensity or gain of the amplifier.

B3 The IR variation (D2/D1) did not correlate well with any mechanical properties of the materials, such as the hardness (Brinell), tensile strength, ductility (% elongation) or modulus of toughness, hence the resulting curves are not shown.

B4 Increasing the angle of incidence θ increases the size of the illumination footprint and also the useful range of optical surface roughness measurements as shown in Figures 6.6 to 6.12. The optical surface roughness measurement decreases in sensitivity as the illumination incidence angle increases. This is shown in Figures 6.8 to 6.12. Tool steel for example is 28 times more sensitive at 60 degrees than at 80 degrees incident angle in the range 0.08 microns < Ra < 0.8 microns. However, there is 6 times more sensitive at 80 degrees than at 60 degrees incident angle in the range 1.3 microns < Ra < 1.8 microns.

Generally the range and sensitivity will have to be optimized to suit a given application. While the range was deliberately extended for the purpose of this study, most manufacturing processes would control surface roughness to Ra < 0.8 microns.

B5 The test results indicated that the intensity ratio IR

curves varied uniquely from one material to the other. Even though the mechanical stylus roughness value was the same for a copper sample and a steel sample, the optical surface roughness IR was unique as shown in Figures 6.13 to 6.16. As other reporters Tsukada and Yanagi [22], Inasaki [23] concluded that optical surface roughness IR is independent of the material, this uniqueness to the material was not expected.

In general most other reporters only varied the type of steel and/or limited their tests to Ra less than 0.6 microns hence were unable to recognize the differences which might occur between soft copper and hard tool steels. Certainly the metal removal process will be different and indeed under low magnification, these two surfaces appear quite different to the naked eye, even though the mechanical stylus readings are the same. This visual difference clearly manifests itself in a corresponding value for optical surface roughness IR.

Because the mechanical stylus measurement leaves a significant scratch on the surface, and because the hardness of copper and tool steels are significantly different, the error in correlation could well be due to errors in the mechanical stylus measurement.

B6 A film of oil on the surface of the part being measured defeats both the mechanical stylus and optical surface roughness measurements.

CHAPTER VIII

RECOMMENDATIONS

It is recommended the following studies extend this research work.

A1 This study found that the best contrast measurement was obtained when the detector was located at the specular angle. However, the signal noise makes it difficult to use in many cases. A system with two detectors to determine the contrast from specular and the normal angle simultaneously would be a better choice. The user would have to choose either output or have it selected by the computer. A study of such a system is recommended.

A2 Only the mean value of the surface signals was used as Pb (reflectance of the background) and the contrast was calculated by the computer using equation (2). The background surface signal fluctuation magnitude had no bearing on the contrast. Therefore, a second indicator is needed to compensate for this shortcoming. This second indicator should compare the signal at the etched line and the standard deviation of the average background surface signal in order to take adavantage of this information.

A3 In this study, the incident and detection angles were arbitrarily taken at normal and 45 degrees. These two angles form three combinations which were tested and reported. Other incident and detection angles should be investigated for their corresponding contrast measurements.

B1 The sensitivity (the slope of the intensity ratio and the surface roughness correlation curve) of the intensity ratio curve depends on the incident angle and the roughness range. The IR correlation curve tends to bend downwards for the smallest incident angle and upwards with the largest incident angle.

However, for stainless steel with the incident angle of 70 degrees, the correlation curve was in the form of a straight line. This is more convenient to use and may also exist in other materials.

Further investigation is recommended on the existence of the straight line correlation curve on the other four materials used in this study.

B2 The 45 degrees angular position of detector 2, which represented the scattered light, was selected after a few preliminary tests. This might not be the best angular location for the reference detector. Some studies [21] recommend that the angular position for the reference detector be 10 degrees higher than the specular reflection angle. A more detailed study on the best angular location

for the reference detector is recommended.

B3 The travelling stylus of profilometer and the light path of optical methods are all in the direction perpendicular to the lay. In some practical cases, this condition can not be satisfied. Therefore measurements of surface roughness in the direction parallel to the lay are desperately needed and this research should be carried out.

B4 This study examined ground surfaces of 5 different materials. Other surfaces produced by different machine finishing methods such as turning, milling, electrochemical machining, honing, lapping, buffing etc. should also be investigated.

B5 A feasibility study on combining the contrast and surface roughness measurement into one single unit is also recommended.

LIST OF REFERENCES

1 Sharp, H.M. "Introduction to Lighting" Prentic-Hall Inc., New York, 1951

2 Weber, R.L., Manning, K.V., White, M.W. "College Physics" McGraw-Hill Book Company, New York, 1965

3 Busch, T. "Fundamentals of Dimensional Metrology" Delmar Publishers, New York, 1966

4 Roberts, A.D. and Lapidge, S.C. "Manufacturing Processes" McGraw-Hill Inc., New York, 1977

5 "Surftest III Operation Manual" Manual No. 4016 Mitutoyo Mfg. Co., Ltd. Japan

6 Dove, R.C. and Adams, P.H. "Experimental Stress Analysis and Motion Measurement" Charles E. Merrill Books Inc., Columbus, Ohio, 1964

7 Box, W.A. "The Effect of Plastic Strains on Stress Concentrators" Society of Experimental Stress Analysis Vol. 8, No. 2, pp. 99-110, 1944

8 Brewer,G.A. "Measurement of Stain in the Plastic Range" Society of Experimental Stress Analysis Vol. 1, No. 2, pp. 105-115, 1943

9 O'haven, C.P. and Harding, J.F. "Studies of Plastic Flow Problems by Photo Grid Methods" Society of Experimental Stress Analysis Vol. 2, No. 2, PP. 59-70, 1944

10 MacLaren, E.D.D. "The Photo-Grid Process for Measuring Strain Caused by Underwater Explosions" Society of Experimental Stress Analysis Vol. 5, No. 2, pp. 115-124, 1948

11 Miller, J.A. "Improved Photo Grid Techniques for Determination of Stain Over Short Gage Lengths" Society of Experimental Stress Analysis Vol. 10, No. 1, pp. 29-34, 1952

12 Sevenhuijsen, P.J. "Two simple methods for deformation demonstration and measurement" Strain Vol. 17, No. 1, pp. 20-24, Feb. 1981.

13 Davies, H. "The Reflection of Electromagnetic Waves from a Rough Surface" Proc. Instn. Electrical Engineers, Vol. 101, pp. 209-214, 1954

14 Beckmann, P. and Spizzichino, A. "The Scattering of Electromagnetic Waves from Rough Surfaces" Macmillan, New York, 1963

15 Bennett, H.E. and Porteus, J.O. "Relation Between Surface Roughness and Specular Reflectance at Normal Incidence" Journal of the Optical Society of America, Vol. 51, No. 2, PP. 123-129, 1961

16 Houchens, A.F. and Hering, R.G. Progr. Astronautics Aeronautics Vol. 20, pp. 65-89, 1967

17 Depew, C.A. and Weir R.D. "Surface Roughness Determination by the Measurement of Reflectance" Applied Optics, Vol. 10, No. 4, pp. 969-970, 1971

18 Birkebak, R.C. "Monochromatic Directional Distribution of Reflected Thermal Radiation from Rough Surfaces" PH.D. Dissertation, University of Minnesota, 1962

19 North, W.P.T. and Agarwal, A.K. "Surface Roughness Measurement with Fiber-optics" Journal of Dynamic System, Measurement and Control, Vol. 105, pp. 295-297, 1983

20 Stout, K.J. "Optical Assessment of Surface Roughness" Precision Engineering Vol. 6, No. 1, pp. 35-39, 1984

21 Jansson, D.G., Rourke, J.M. and Bell, A.C; "High Speed Surface Roughness Measurement" Journal of Engineering for Industry (Transaction of ASME) Vol. 106, pp. 34-39, 1984

22 Tsukada, T. and Yanagi, K. "An Application of CCD Image Sensor to a Measurement of Surface Roughness" Bull. Japan Society of Precision Engineering, Vol. 17, No. 3, pp. 209-210, 1983

23 Inasaki,I. "In-process Measurement of Surface Roughness During Cylindrical Grinding Process" Precision Engineering, Vol. 7, No. 2, pp 73-76, 1985

24 Sonde, B.S "Data Converters" McGraw-Hill Publishing Ltd., New Delhi, PP. 6-61, 1979

25 Susskind, A.K. "Notes on Analog-Digital Conversion Techniques" The Technology Press of Massachusetts Institute of Technology and John Wiley & Sons, Inc., New York, PP. 2.1-2.58, 1957

26 Warme, P.K. "Adalab Interface Card Hardware Manual" Interactive Microware Inc., State College (Pennsylvania), PP. 18-21, 1984

27 De Barr, A. E. and Oliver, D. A. "Electrochemical Machining" American Elevier Publishing Company, Inc., New York, 1968

28 Pletcher, D. "Industrial Electrochemistry" Chapman and Hall London New York, PP. 172-216, 1982

29 "Electrochemical Marking Manual" The Lectroetch Company, Cleveland, Ohio.

30 "DiffractoGage Analog Operation and System 7A" Diffracto Ltd., Windsor, Ontario

31 "Planar Diffused Silicon Pin Photodiodes" United Detector Technology Inc., Data Sheet 9F002, Santa Monica, California

32 "The UDT 101A Amplifier" United Detector Technology Inc., Data Sheet S-008-1276, Santa Monica, California

33 Miller, I. and Freund, J.E. "Probability and Statistics for Engineers" Prentics-Hall, Inc., New Jersey, 1977

34 Snedecor, G.W. and Cochran, W.G. "Statistical Methods" The Iowa State University Press, 1967

35 Durelli, A.J., Phillips, E.A. and Tsao, C.H. "Introduction to the Theoretical and Experimental Analysis of Stress and Strain" McGraw-Hill Book Company, pp. 311-326, 1958

Appendix A

Linear Response Curves of System 7A

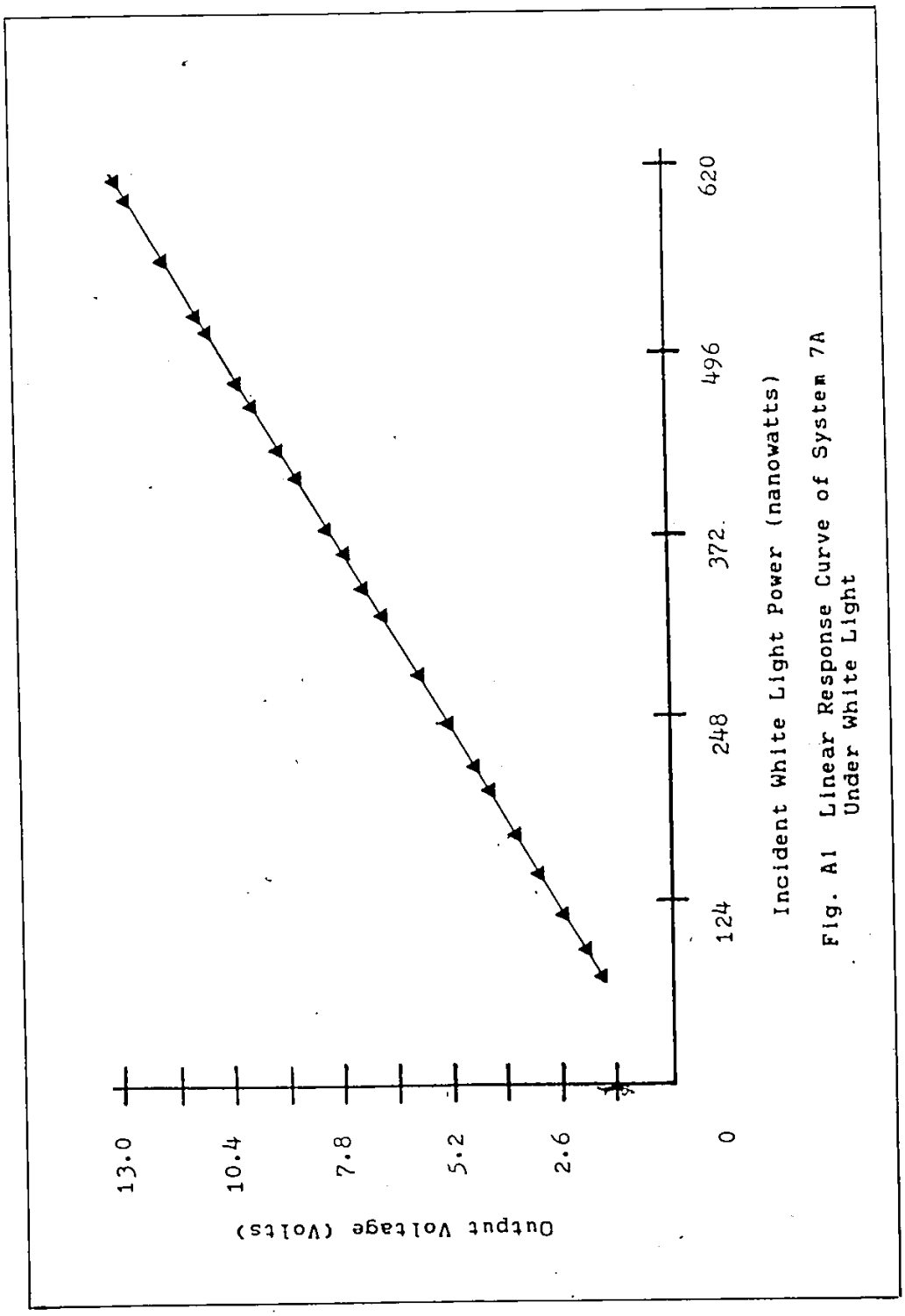

Fig. A1 Linear Response Curve of System 7A
Under White Light

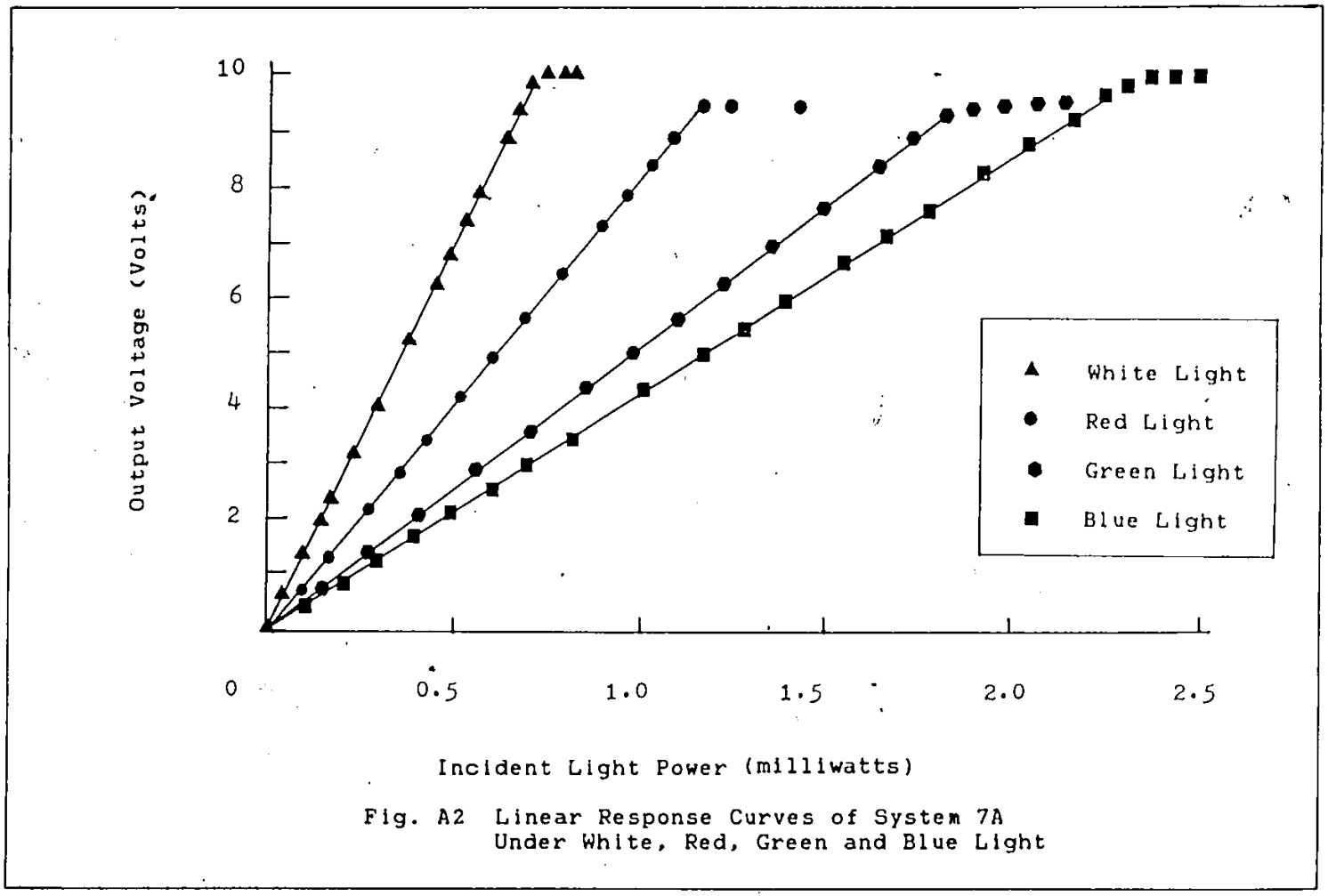

Fig. A2 Linear Response Curves of System 7A
Under White, Red, Green and Blue Light

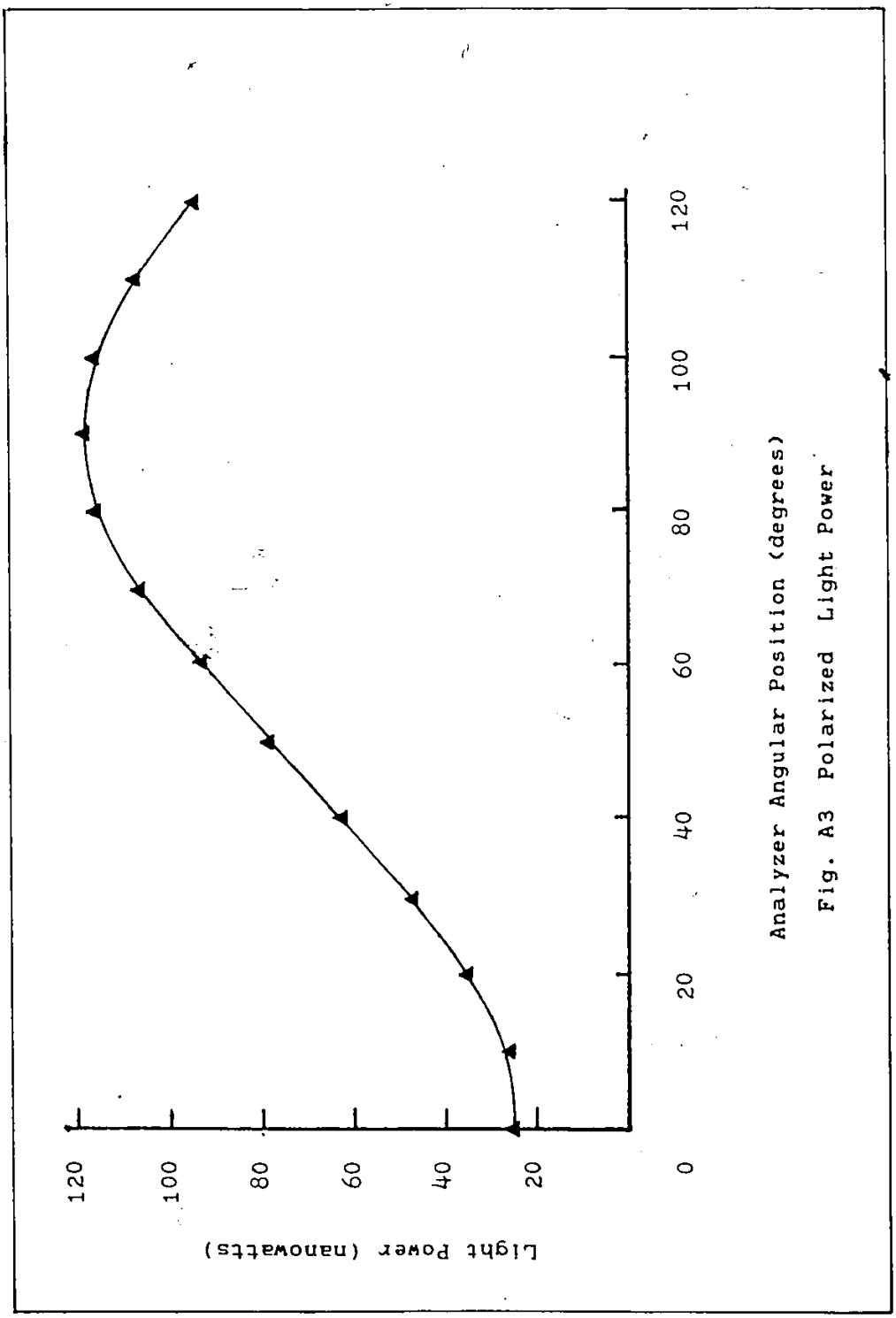

Fig. A3 Polarized Light Power

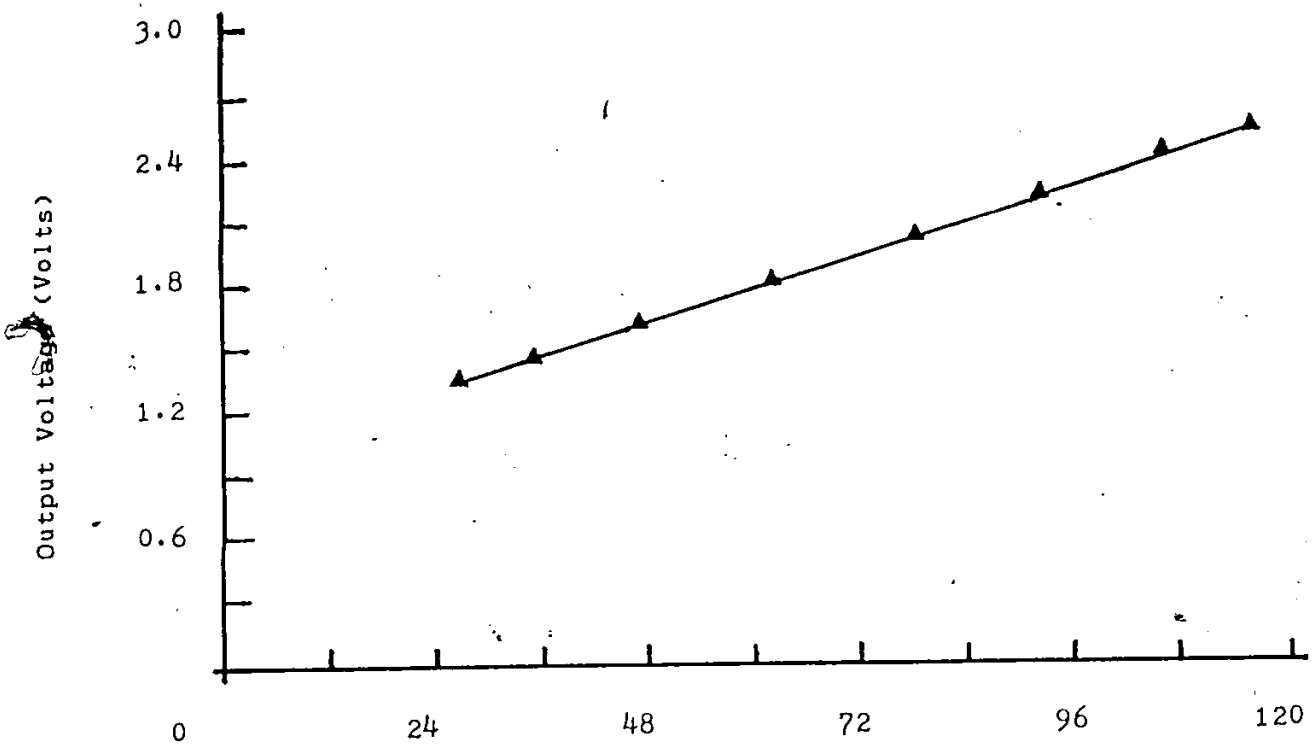

Fig A4 Linear Response Curve of System 7A
Under Polarized Light

Appendix B

Contrast Measurement on Modified Plain Carbon Steel Surface

Contrast could be made better by improving the appearance of the specimen to the optical system. Several kinds of coating and cleaner were applied on the specimen surfaces to examined their affects. The specimens used in these tests were 7" X 7" plain carbon steel. The lines were etched on the specimen surface by the electrochemical etching process. A general procedure was to scan the specimen surface by the Hand-held-unit I before and after the coating or cleaner was applied.

a) Acetone Wash: the sample was coated with a small amount of light oil which was applied on the surface during the etching process. It was scanned by the Unit I and then was cleaned thoroughly by an acetone wash and the scanning process was repeated. Finally, the sample was re-oiled with WD-40 oil and again was scanned. The test results are as follows:

Table B1 Test Results of Acetone Wash

Surface Condition	Number of Lines Scanned (N)	Mean Contrast (MC)	Standard Deviation (S)
As Received	24	0.483	2.16E-2
Cleaned by an Acetone Wash	24	0.473	4.74E-2
Added WD-40 oil	24	0.474	3.98E-2

The results suggest that the acetone wash did not improve contrast. The WD-40 oil film on the specimen protected the bare metal surface and had little affect on the line contrast.

b) Metal Conditioner: a water based acidic surface cleaner, "M-Prep Conditioner A" was used in this test. Before the application of the conditioner, the specimens were cleaned by a chlorinated hydrocarbon (Stresscoat ST-100). The test results are listed below.

Table B2 Test Results of M-Prep Conditioner A

Sample #	As Received			Coated with Conditioner A		
	N	MC	S	N	MC	S
A3	23	0.560	2.35E-2	24	0.556	3.25E-2
C5	34	0.461	2.76E-2	28	0.393	5.22E-2
B6	36	0.196	4.37E-2	27	0.141	2.88E-2

N Number of Lines Scanned
MC Mean Contrast
S Standard Deviation

The results suggest that the "M-Prep Conditioner A" did not improve the etched line contrast. As a matter of fact, it deteriorated the contrast and especially aggravated the low contrast specimen. (see B6)

c) Wax: From the surface finish test, smooth shiny surfaces improved contrast. Wax was applied on the specimens and then they were polished. The test results are listed in Table B3. The waxed surfaces appeared bright and shiny to the naked eye, but it did not improve contrast.

Table B3 Wax Test Results

Sample #	As Received N	MC	S	Waxed N	MC	S
A1	28	0.594	2.84E-2	31	0.545	4.24E-2
B4	29	0.496	3.50E-2	30	0.485	4.57E-2
A5	36	0.403	3.82E-2	24	0.236	4.19E-2

N Number of Lines Scanned
MC Mean Contrast
S Standard Deviation

d) Krylon Test: Krylon 41303 Crystal Clear and Krylon 1311 Matte Finish are spray coatings which are used to protect photographs, paintings, displays etc. from dust and dirt. The Crystal Clear is merely a clear coating. Matte Finish forms a non-gloss finish to eliminate glossy sheen and light reflection.

The specimens were wiped clean by a soft paper. The Krylon coatings were applied and then allowed 50 minutes to dry. The tests results of these coatings are listed in Table B4.

Table B4 Krylon Tests Results

Sample #	As received N	MC	S	Coated with Krylon Spray N	MC	S
Krylon 41301 Crystal Clear						
C4	30	0.552	2.45E-2	27	4.87	2.16E-2
B5	36	0.429	5.09E-2	30	3.52	3.96E-2
A6	33	0.204	3.55E-2	30	1.54	3.78E-2
Krylon 1311 Matte Finish						
C2	28	0.688	3.56E-2	21	0.671	1.88E-2
A2	30	0.686	3.24E-2	20	0.630	3.02E-2

N Number of Lines Read
MC Mean Contrast
S Standard Deviation

The results showed that there were no improvement on the

contrast by using Krylon coatings.

e) Zyglo Test: Zyglo is a penetrant commonly used to locate cracks. If the etched lines on the specimen surface were formed by many minute cracks, this would be a promising method to improve contrast. The testing procedures are listed below.

1. Spray specimen with ZC-70 cleaner and then wiped the surface clean with soft paper several minutes later.
2. Spray ZL-22 penetrant on the surfaces. This spray penetrates the cracks by capillary attraction.
3. Allow the specimen to dry for 30 minutes.
4. Clean the surface again with ZC-70 cleaner.
5. Apply a thin layer of ZP-9 developer and allowed it to dry on the surface.
6. Wipe the surface clean.
7. Use the Zyglo black light to replace the white light in the Hand-held-unit I to scan the samples.

The Zyglo black light contains a mercury vapor bulb and an absorber which absorbs any shortwave ultraviolet radiation and transmits only the longwave or near ultraviolet radiation. The penetrant is a material which glows when illuminated by this black light. Therefore, the video signal of the specimen under this black light should be the reverse signal of using white light. These tests were inconclusive, therefore the results are not show here.

f) Filtered white light: The System 7A exhibited a very linear response when under white, blue, red and green light. In this test, Yellow and green microscope filters were individually used to filter the white light. The test results are listed below.

Table B5 Results of Contrast Under Different Lights

Sample #	White Light	White light Green Filter	White light Yellow Filter
C2	N=9 MC=0.676 S=2.59E-2	N=9 MC=0.676 S=3.19E-2	N=9 MC=0.672 S=2.85E-2
C3	N=6 MC=0.718 S=2.98E-2	N=6 MC=0.720 S=2.40E-2	N-6 MC=0.715 S=3.07E-2

N Number of Lines Scanned
MC Mean Contrast
S Standard Deviation

Again, the filters did not improve the contrast.

Appendix C

Chemical Composition and Mechanical Properties of Surface Roughness Samples

ALUMINUM 2024-T4

Chemical Composition:	
Copper	4.5%
Manganese	0.6%
Magnesium	1.5%
Aluminum	Balance
Mechanical Properties:	
Tensile Strength, psi	68,000
Yield Strength, psi	47,000
Elongation, % in 2"	19
Shear Strength, psi	37,000
Brinell Hardness 10/500	120

BRASS

Chemical Composition:	
Copper	61.5%
Zinc	35.5%
Lead	3.0%
Mechanical Properties:	
Tensile Strength, psi	58,000
Yield Strength, psi	45,000
Elongation, % in 2"	25
Shear Strength, psi	34,000
Rockwell Hardness, B Scale	78

Copper

Chemical Composition:	
Copper	99.9% minimum
Mechanical Properties:	
Tensile Strength, Psi	48,000
Yield Strength, psi	44,000
Elongation, % in 2"	16
Shear Strength, psi	27,000
Rockwell Hardness, F Scale	87

STAINLESS STEEL TYPE 304

Chemical composition:	
Carbon	0.08% max.
Manganese	2.00% max.
Phosphorus	0.045% max.
Sulphur	0.030% max.
Silicon	1.00% max.
Chromium	18.00% to 20.00%
Nickel	8.00% to 12.00%
Mechanical Properties (Annealed):	
Tensile Strength, psi	85,000
Yield Strength, psi	35,000
Elongation, % in 2"	50
Rockwell Hardness, B Scale	80

TOOL STEEL

K.E.672/Newhall oil hardening alloy tool steel
A.I.S.I. type 01. BS 4659 B01
Werkstoff 1.2510

Chemical Composition:	
Carbon	0.95%
Manganese	1.20%
Chromium	0.55%
Tungsten	0.55%
Vanadium	0.20%
Mechanical Property (as hardened):	
Rockwell Hardness, C Scale	63/64

Appendix D

Computer Flow Chart and Memory Map

COMPUTER MEMORY MAP

DEC.		HEX.
0		0
	Computer work space, not available to user	
768		300
	Sound Program	
800		320
	Space	
1023		3FF
	Text Screen	
2048		800
	Main Program	
4225		1081
	Variables use in Main Program	
8192		2000
	Graphic	
16383		3FFF
	Digitized Data Points	
36096		8D00
	Quick I/O Program	
38400		9600
	DOS	
49152		C000
	Hardware I/O addresses	
53248		D000
	ROM	
65535		8AD0

COMPUTER FLOW CHART

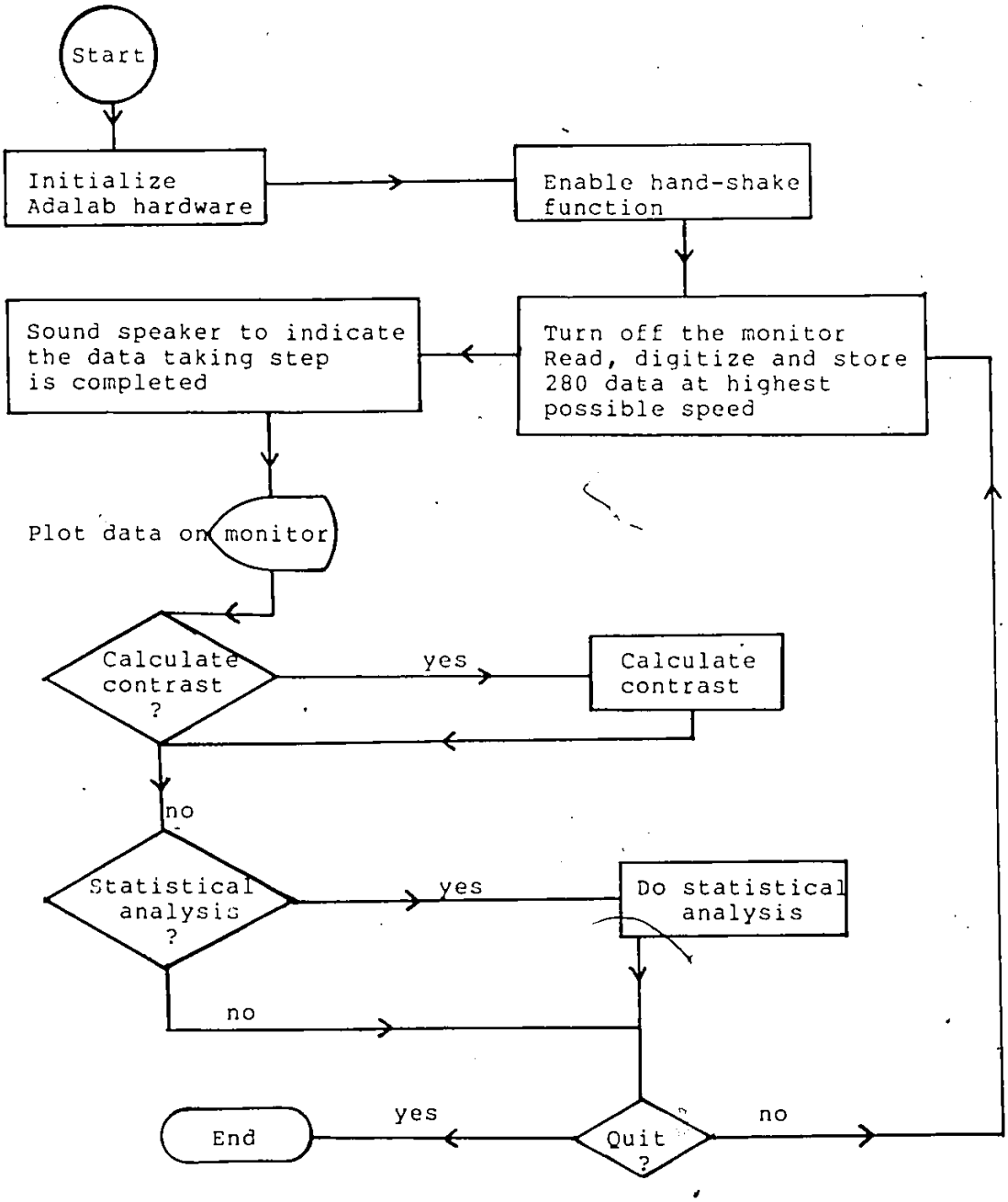

VITA AUCTORIS

1954 Born in Canton, China

1972 Received High School Education Certificate

1977 Received the diploma of Technology from the Department of Radio & Television Engineering Technology, South East College, Hong Kong.

1980 Received the diploma of Technology from the Department of Mechanical Engineering Technology, St. Clair College, Windsor, Ontario, Canada.

1983 Received the degree of Bachelor of Applied Science from the Department of Mechanical Engineering, University of Windsor, Windsor, Ontario, Canada.

1986 Currently, a candidate for the degree of Master of Applied Science in Mechanical Engineering at the University of Windsor.